Politecnico di Torino

Department of Environment, Land and Infrastructure Engineering

---

Assessment and Optimization of the Mine Ventilation System for Fan Selection and Design Improvement

Case study: Rodoretto Mine, Imerys Talc Italy S.p.A.

Master's Degree Thesis in Georesources and Geoenergy Engineering

Career Track: Sustainable Mining

Academic Supervisor
Prof. Daniele Martinelli

Candidate
Sahel Homayounfar

Company Supervisors
Sara Eremita
Thibaud Kegels

July 13, 2026

Abstract

This thesis evaluates the underground ventilation system of the Rodoretto talc mine operated by Imerys Talc Italy S.p.A. and develops a technical-economic basis for replacing its aging main exhaust fans. At the time of assessment, the mine had received three commercial proposals from CFT, Aero/Systemair, and Howden suppliers. Since these proposals differ in both fan characteristics and installation configuration, the selection task was framed as a system-level engineering decision integrating ventilation requirements, field evidence, mine development, fan-network interaction, and economic performance.

Regulatory and company criteria were translated into airflow and velocity KPIs. The existing Ventsim model, previously calibrated for the primary circuit, was corrected and updated to represent existing workings and planned short-term developments. Field air velocity measurements collected with a thermal anemometer supported assessment of the auxiliary network. Auxiliary-fan definitions, topology, and installation losses and leakage were examined against the measurements. The commercial proposals were then simulated in the existing pre-2028 and planned post-2028 layouts. Technical screening preceded economic comparison.

The mandatory whole-mine airflow requirement was 47.97 m^3/s. Among the three proposals, the CFT and Aero/Systemair cases were represented as parallel main-fan installations, whereas the Howden case was represented as a two-stage series installation. The CFT and Aero/Systemair options satisfied the whole-mine requirement in both layouts, delivering approximately 69 and 83 m^3/s, respectively, at stable operating points. The Howden configuration delivered approximately 33 m^3/s and failed the requirement by 31%, so it was excluded from the economic comparison. Although Aero/Systemair provided greater whole-mine capacity, CFT and Aero/Systemair produced similar local performance, and neither satisfied every local and regional KPI with the represented auxiliary network. An improvement sensitivity substantially increased face delivery, but regional compliance remained incomplete. The controlling constraint was therefore identified as auxiliary-air distribution, influenced by duct resistance, leakage, duct condition, and fan installation, rather than insufficient main-fan capacity.

The retained options were ranked using a lexicographic economic model over a 12-year horizon. CFT achieved an incremental NPV approximately EUR 24,200 higher than Aero/Systemair and also produced the lower present-value OPEX, life-cycle cost,

and discounted payback. The CFT parallel arrangement is therefore recommended among the assessed main-fan options. A dedicated assessment of the auxiliary network is required to achieve airflow compliance across all active areas.

Keywords: mine ventilation; Ventsim; ventilation-network calibration; auxiliary ventilation; fan performance; technical-economic assessment; airflow modelling; scenario assessment.

Acknowledgements

I would like to express my deepest gratitude to my family and loved ones, whose unwavering support in every possible way made this journey possible.

I am especially grateful to my academic supervisor, Prof. Daniele Martinelli, for his guidance, encouragement, and constant belief in me throughout my academic journey. I would also like to extend my sincere thanks to my company supervisors for their continuous support and valuable guidance.

This experience has been both a privilege and an important opportunity for growth. Throughout my studies and the development of this thesis, I have grown significantly, both academically and personally, and I deeply value the knowledge, experience, and perspective I have gained along the way.

Contents

Abstract i

Acknowledgements iii

List of Figures viii

List of Tables x

List of Abbreviations and Symbols xiii

1 Introduction 1

1.1 Background and Motivation 1
1.2 Industrial Problem Definition 2
1.3 Aim and Objectives 3
1.4 Research Questions 4
1.5 Scope and Delimitations 5
1.6 Research Approach Overview 5
1.7 Contribution 6
1.8 Structure of the Thesis 7

2 Literature Review 8

2.1 Underground Mine Ventilation as a Safety and Design Problem 8
2.2 Ventilation Network Behavior, Resistance, and Duty Point 9
2.3 Main Fan Selection, Fan Arrangements, and System-Level Efficiency . . . 10
2.4 Auxiliary Ventilation, Leakage, and Face Air Delivery 11
2.5 Ventilation Network Modelling, Validation, and Calibration 12
2.6 Energy Efficiency, Control, and Technical-Economic Optimization 13
2.7 Synthesis of the Literature and Research Gap 14

3 Study Context 16

3.1 Rodoretto Mine and Industrial Setting 16
3.2 Production Transition and Planning Horizon 17

3.3 Existing Ventilation System 18
3.4 Available Data and Modelling Basis 19
3.5 Implications for the Present Thesis 20

4 Methodology **22**
4.1 Overall Methodological Logic 22
4.2 KPI Framework and Regulatory Basis 23
4.2.1 Selection logic for the KPIs 23
4.2.2 Regulatory thresholds 25
4.2.3 Translation of the regulations into design quantities 25
4.2.4 Traffic cases adopted from the company sizing logic 26
4.3 Decision Variables, Pressure-Flow Reasoning, and Objective-Function Formulation 28
4.3.1 Lexicographic Model as the Decision Rule 31
4.4 Baseline Model, Model Updates, and Observed System Issues 32
4.4.1 Auxiliary-fan placement near branch intersections 34
4.5 Field Survey Design for the Auxiliary System 35
4.5.1 Reason for a dedicated auxiliary survey 35
4.5.2 Prepared survey criteria 35
4.5.3 Executed field procedure 37
4.5.4 Processing of the measured velocities 38
4.6 Calibration of the Auxiliary Network in Ventsim 39
4.6.1 Calibration boundary and comparison dataset 39
4.6.2 Stage 1: geometry-consistency correction of comparison sections . 43
4.6.3 Stage 2: topology verification and auxiliary fan definition setup . 45
4.6.4 Stage 3: baseline run and fan-side diagnosis 46
4.6.5 Stage 4: local installed-loss calibration by shock-loss representation 47
4.6.6 Stage 5: delivered-flow calibration and representation of branch losses 48
4.6.7 Branch-specific calibration logic 48
4.6.8 Acceptance criteria and methodological limits 49
4.7 Scenario Construction and Offer Evaluation 50
4.8 Economic Assessment Procedure 51
4.8.1 Implemented discounted-cash-flow procedure 52
4.9 Methodological Boundaries 53

5 Results **55**
5.1 Implemented Ventsim model updates 55
5.1.1 Objective and working approach 55
5.1.2 Implemented changes 56
5.1.3 Updated layout and representative geometry revisions 56

5.2 Auxiliary-ventilation measurement campaign 58
5.2.1 Purpose and relation to the model 58
5.2.2 Survey coverage and adaptive measurement strategy 58
5.2.3 Executed measurement procedure 58
5.2.4 Observed physical condition of the auxiliary installations 59
5.2.5 Immediate outcome of the campaign 61
5.3 Initial baseline comparison before auxiliary calibration 62
5.3.1 Geometry-consistency correction of diameters and comparison sections 64
5.3.2 Topology verification and auxiliary fan definition setup 68
5.4 Auxiliary-network loss calibration 72
5.4.1 Calibration basis and evaluation logic 72
5.4.2 Accepted fan-by-fan shock-loss scenarios 73
5.4.3 Main-network gate and transition to downstream calibration . . . 73
5.4.4 Downstream branch-loss and leakage calibration 75
5.4.5 Final calibrated auxiliary-network state 75
5.5 Comparative technical assessment of the offered main-fan arrangements . 76
5.5.1 Representation and operating points of the offered fans 77
5.5.2 Whole-mine capacity gate 79
5.5.3 Local and regional performance of the retained offers 85
5.5.4 Auxiliary-network improvement sensitivity 91
5.5.5 Stress-scenario and variable-speed decision 92
5.5.6 Technical screening outcome 92
5.6 Economic evaluation of the retained main-fan offers 92
5.6.1 Economic inputs and operating basis 93
5.6.2 Annual energy use and operating cost 95
5.6.3 Discounted cash-flow results 95
5.6.4 Lexicographic economic ranking 96
5.6.5 Sensitivity and robustness 96
5.6.6 Economic recommendation 97

6 Discussion **98**
6.1 Future research on auxiliary-network improvement 98

7 Conclusions **100**
7.1 Principal findings 100
7.2 Final recommendation 101
7.3 Further work 102

References **103**

A Supplementary Calculations and Supporting Material **107**
A.1 Auxiliary-Ventilation Measurement-Comparison Records 107
A.2 Final Auxiliary-Calibration Records 111
A.3 Detailed Offer KPI Records 114
A.3.1 CFT Local and Regional KPI Records 114
A.3.2 Aero Local and Regional KPI Records 117
A.3.3 Auxiliary-Network Improvement Sensitivity Records 120
A.4 Year-by-year discounted cash-flow record 124

List of Figures

1.1 Simplified two-dimensional ventilation scheme of the Rodoretto mine as presented in the annual technical report. 3

3.1 Ventsim duty panels for the two existing Woods 48J2 main exhaust fans. 19
3.2 Company-provided Rodoretto Ventsim model used as the modelling basis. 20

4.1 Sampling pattern for auxiliary-fan inlet and duct-outlet velocity measurements 37
4.2 Auxiliary-ventilation measurement stations; numbered labels correspond to the calibration and results tables 42

5.1 Representative Rodoretto model geometry revision 57
5.2 Far North upper-level ramp added to the updated Ventsim model. 57
5.3 South Intermediate ramp and drift additions in the updated Ventsim model 57
5.7 Zetal VH1004.4 catalogue curves used for the baseline auxiliary-fan definitions [30, 31] 70
5.8 XS–XN Zetal VH1004.4, 2 x 45 kW fan definition entered in Ventsim . . 71
5.9 N–S Zetal VH1004.4, 2 x 30 kW fan definition entered in Ventsim 71
5.10 CFT pre-2028 duty panels at 100% fan speed. 80
5.11 CFT post-2028 duty panels at 100% fan speed. 81
5.12 Aero pre-2028 duty panels at 100% fan speed. 82
5.13 Aero post-2028 duty panels at 100% fan speed. 83
5.14 Modelled duty panels for the offered Howden series arrangement at 100% speed. Both cases remain near 34 m^3/s and operate at the low-pressure edge of the represented curve 84
5.15 CFT airflow distribution at 100% speed in the pre-2028 layout (top) and post-2028 layout (bottom) 87
5.16 CFT velocity distribution at 100% speed in the pre-2028 layout (top) and post-2028 layout (bottom) 88
5.17 Aero airflow distribution at 100% speed in the pre-2028 layout (top) and post-2028 layout (bottom) 89

5.18 Aero velocity distribution at 100% speed in the pre-2028 layout (top) and post-2028 layout (bottom) 90

List of Tables

4.1 Performance indicators used in the thesis and the basis for their selection 24
4.2 Case 1: main-gallery "very high traffic" sizing case adapted from the company report [1] . . . 27
4.3 Case 2: extraction-area "high traffic" sizing case adapted from the company report [1] . . . 27
4.4 Activity-specific auxiliary airflow requirements adopted from the company report [1] . . . 28
4.5 Observed auxiliary-ventilation issues and methodological implications . . 33
4.6 Prepared survey criteria used to structure the auxiliary-ventilation visit . 36
4.7 Practical survey rules adopted for the auxiliary-ventilation visit 36
4.8 CV confidence classes for auxiliary-measurement repeatability 39
4.9 First-version measurement-comparison workbook used before auxiliary-model correction . . . 41
4.10 Measured auxiliary branches and their calibration roles 41
4.11 Classification bands used in Stage 1 to interpret the magnitude of area-consistency error, $|e_A^*|$ . . . 44
4.12 Classification bands used in Stage 1 to interpret the magnitude of diameter-consistency error, $|e_D^*|$ . . . 44
4.13 Economic information structure required for the offer comparison 52

5.1 Representative first-pass baseline mismatches before auxiliary calibration 63
5.2 First-pass examples showing denominator effects in raw quantity-error interpretation . . . 64
5.3 First-pass model-implied-area checks used to identify section-representation mismatches . . . 65
5.4 Station-by-station geometry-consistency diagnosis before correction . . . 67
5.5 Station-by-station geometry-consistency diagnosis after correction 67
5.6 Auxiliary-fan definitions assigned during the fan-definition stage 69
5.7 Representative duty-point values reported by Ventsim for the entered XS–XN Zetal VH1004.4, 2 x 45 kW fan definition . . . 69

5.8 Representative duty-point values reported by Ventsim for the entered Nord–Sud Zetal VH1004.4, 2 x 30 kW fan definition 69
5.9 Accepted auxiliary-fan installed-loss scenarios selected from the local shock-loss calibration stage.
Airflow quantities are in m^3/s 74
5.10 Stage-gate main-network check applied after each accepted local shock-loss scenario 74
5.11 Downstream airflow-delivery comparison before and after branch-level downstream calibration. Airflow quantities are in m^3/s; delivery percentage is $100Q_{out}/Q_{in}$ 75
5.12 Equivalent downstream airflow-control resistance used in the final auxiliary calibration 76
5.13 Main-fan definitions and arrangements represented in the comparative Ventsim models 77
5.14 Modelled duty points of the offered arrangements at 100% fan speed . . . 79
5.15 Whole-mine capacity screening at the designated exhaust 80
5.16 Comparative KPI results for the retained CFT and Aero arrangements before auxiliary-network improvement 85
5.17 Colour-map interpretation used for the offer-assessment airflow and velocity figures 86
5.18 Effect of the idealized auxiliary-network improvement on the principal KPI outcomes 91
5.19 Candidate CAPEX used in the economic comparison. All values are in EUR; Softime and Microl are common to both alternatives 93
5.20 Mine-provided electricity consumption, tariff, and fan OPEX values used to define the baseline electricity cost 93
5.21 Modelled electrical-power inputs used in the economic calculation 94
5.22 Financial assumptions applied consistently to the retained offers 94
5.23 Annual candidate energy use, electricity OPEX, and saving relative to the existing-fan baseline 95
5.24 Economic results over the 2026–2037 analysis horizon 95
5.25 Sequential lexicographic comparison of the retained offers 96
5.26 Sensitivity to annualized January–May 2026 baseline consumption 97

A.1 First-version auxiliary-ventilation measurement-comparison record for the 30 March 2026 campaign, Part I-A: field, repeatability, and measured-airflow columns for Stations 1–8 108

A.2 First-version auxiliary-ventilation measurement-comparison record for the 30 March 2026 campaign, Part I-B: field, repeatability, and measured-airflow columns for Stations 9–15 109
A.3 First-version auxiliary-ventilation measurement-comparison record for the 30 March 2026 campaign, Part II: model-comparison and reserved post-calibration columns 110
A.4 Final calibrated station-level velocity comparison used to assess the auxiliary-ventilation calibration for the 30 March 2026 campaign 112
A.5 Final calibrated station-level airflow comparison used to assess the auxiliary-ventilation calibration for the 30 March 2026 campaign 112
A.6 Final calibrated duct leakage porosity assignments used in the downstream auxiliary calibration 113
A.7 Detailed CFT active-face control results at 100% fan speed in the pre-2028 and post-2028 layouts 115
A.8 Detailed CFT regional-boundary results at 100% fan speed in the pre-2028 and post-2028 layouts 116
A.9 Detailed Aero active-face control results at 100% fan speed in the pre-2028 and post-2028 layouts 118
A.10 Detailed Aero regional-boundary results at 100% fan speed in the pre-2028 and post-2028 layouts 119
A.11 CFT improved-network active-face control records for the auxiliary-network sensitivity 121
A.12 Aero improved-network active-face control records for the auxiliary-network sensitivity 122
A.13 Improved-network regional-boundary records for the auxiliary-network sensitivity 123
A.14 CFT discounted savings relative to the existing-fan baseline 125
A.15 Aero discounted savings relative to the existing-fan baseline 125

List of Abbreviations and Symbols

Abbreviations and Project Labels

Term	Meaning in this thesis
AMCA	Air Movement and Control Association International
Aero/Systemair	Aero S.r.l. offer using Systemair AXC main-fan data
ASHRAE	American Society of Heating, Refrigerating and Air-Conditioning Engineers
CAPEX	Capital expenditure
CFD	Computational fluid dynamics
CFT	CFT GmbH main-fan offer assessed in the thesis
CV	Coefficient of variation
DPP	Discounted payback period
DPR	*Decreto del Presidente della Repubblica*; Italian Presidential Decree
FEL	Front-end loader
FSP	Fan static pressure
FTP	Fan total pressure
Howden	Previous ventilation-survey provider and supplier of one assessed main-fan offer
KPI	Key performance indicator
MCC	Motor control centre
Nord	North area auxiliary-ventilation fan or branch label
NPV	Net present value
OPEX	Operating expenditure
PV	Present value
SCADA	Supervisory control and data acquisition
SIA	Swiss Society of Engineers and Architects
Sud	South area auxiliary-ventilation fan or branch label
UGL	Underground loader
VFD	Variable-frequency drive
VSD	Variable-speed drive
XN	North Extension auxiliary-ventilation branch or model label
XS	South Extension auxiliary-ventilation branch or model label

Symbols

Symbol	Meaning in this thesis
A	Cross-sectional area
D	Duct or airway diameter used for measurement-area calculation
K_s	Safety factor used in the ventilation-sizing calculation
Q	Airflow quantity
Q_{req}	Required airflow quantity for the relevant activity or assessment location
R	Airway or duct resistance in the quadratic pressure–flow relation
X	Shock-loss coefficient used to represent local installation losses
v	Air velocity
ΔP, Δp	Pressure difference, pressure rise, or pressure loss, depending on context
η	Fan or overall efficiency
ρ	Air density
$\bar{v}$	Mean measured air velocity
$\bar{Q}$	Mean measured airflow quantity
σ_{pop}	Population standard deviation of repeated velocity measurements
e_v, e_Q	Percentage error in velocity and airflow quantity
Q_{sim}, Q_{meas}	Simulated and measured airflow quantities
Q_{in}, Q_{out}	Inlet and outlet airflow quantities used for delivery comparison
P_{elec}	Electrical power input
E_y	Annual electricity use in year y
c_e	Electricity tariff
r	Annual discount rate

Chapter 1

Introduction

This thesis addresses the technical-economic assessment of the mine ventilation system at the Rodoretto underground talc mine operated by Imerys Talc Italy S.p.A. in support of main-fan replacement. The work originates from a practical industrial need. The mine currently relies on aging main fans whose spare components are no longer readily available, while the mine itself is entering a period of operational transition in which ventilation management is becoming increasingly important [1, 2]. As a result, the fan replacement problem cannot be treated as a simple equipment procurement decision. It must instead be approached as an engineering evaluation problem that links worker safety, airflow adequacy, mine development, model reliability, and economic performance.

1.1 Background and Motivation

Ventilation is one of the core systems of any underground mine. It provides fresh air to working areas, dilutes and removes diesel exhaust and airborne contaminants, contributes to acceptable thermal conditions, and supports safe and continuous operation. At the same time, mine ventilation is a major energy consumer. For that reason, ventilation design is not only a safety problem but also a strategic operational and economic issue. A poorly performing ventilation system may create unsafe or uncomfortable conditions underground, while an oversized or inefficient system may result in unnecessary energy use and operating cost.

These general challenges are highly relevant at Rodoretto. The mine report shows that Rodoretto has a strategic role within the Italian talc sector and that mining is currently distributed across historical areas and extension areas. The operation is in a transition period. The North and South areas are approaching exhaustion, while the South Extension and North Extension areas are being ramped up. The transition also includes the planned development of South Intermediate and of the Far North sector on two levels, adding further ventilation demand and network complexity as the active mine

layout evolves. The same report notes that mining work may occur across several areas in the same year, although only part of them can be active at the same time due to technical, logistical, and safety constraints [1]. Within this context, ventilation management becomes progressively more important because production flexibility, development sequencing, and workplace conditions depend on how effectively air can be distributed through a changing underground network.

The company's need that motivated this thesis is therefore both immediate and forward-looking. The existing main fans are old, the availability of replacement components is limited, and the mine has received commercial offers for replacement fans [3, 4, 5]. The role of the thesis is not to screen a broad range of hypothetical alternatives, but to evaluate the solutions that have actually been offered to the company. These offers differ not only in equipment choice but also in the proposed arrangement of the main fans, including configurations such as parallel and series operation. For that reason, the thesis evaluates the offered solutions under the real resistance, airflow distribution, leakage conditions, and short-term layout changes of the mine.

1.2 Industrial Problem Definition

The industrial problem was initially expressed in practical terms. The task was to identify the most suitable replacement strategy among the commercial offers received for the main fans and to assess the technical and economic consequences of the available options. As the thesis progressed, this practical request was reformulated as a technical-economic decision problem in which the offered fan solutions, their arrangements, and the behavior of the ventilation network are evaluated together.

The existing representation of the Rodoretto ventilation system was not fully adequate for such a decision. Among the materials provided by the company, a 2D ventilation scheme appears in the annual technical report and is represented in Figure 1.1 [1], while a 3D Ventsim model was also supplied for simulation work. The 3D model was developed by Howden as part of the 2025 ventilation survey and calibrated against measured pressure and airflow data for the primary ventilation network, while the auxiliary network remained uncalibrated [2].

The ventilation survey report provided by Howden reinforced the importance of this modelling step. It describes the two double-stage main fans as installed in parallel and exhausting air from the entire mine, and it notes that the primary fans appear to operate in a low-pressure region, which can lead to reduced system performance and insufficient airflow [2]. The thesis therefore builds on the Howden model by extending the validation and calibration work to the auxiliary fans and branches, processing field measurements collected for that purpose, correcting points that were modelled wrongly, and updating the network to include already excavated drifts and relevant future developments. At

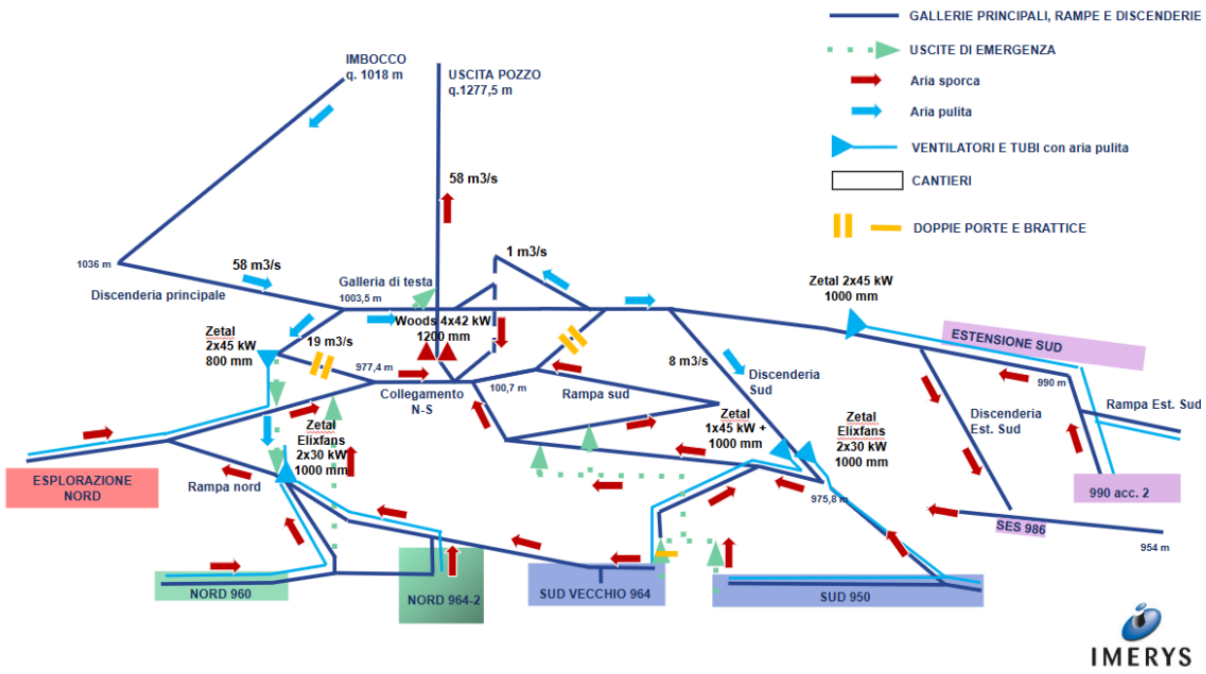

Figure 1.1: Simplified two-dimensional ventilation scheme of the Rodoretto mine as presented in the annual technical report.

the same time, observations made during site work identified weaknesses in the auxiliary ventilation, especially in relation to duct condition, leakage, and the need to verify auxiliary-fan behavior. These points show that the ventilation problem is not limited to the nominal rating of the main fans; it is a system-level problem involving network behavior, installation conditions, leakage, model credibility, and the evaluation of the offered fan arrangements.

From the thesis perspective, the industrial problem can therefore be restated in the following way. How can the current and near-future Rodoretto ventilation system be assessed with sufficient reliability to support the selection of technically adequate and economically justified fan replacement options?

1.3 Aim and Objectives

The main aim of this thesis is to assess the Rodoretto mine ventilation system and support selection of a technically adequate and economically justified main-fan replacement under realistic operating conditions, while identifying the auxiliary-network constraints that affect airflow delivery.

To achieve this aim, the work is structured around the following objectives.

1. Establish the ventilation requirements that the system must satisfy, with particular attention to airflow demand (Q), air-velocity limits (v), and operational safety constraints.

2. Review the current ventilation arrangement and improve the representation of the mine network using a simulation model that is suitable for scenario analysis, including corrections to wrongly modelled points and updates to existing and planned drifts.

3. Use site measurements and available survey data to assess the model representation and interpret mismatches associated with airflow distribution, leakage, auxiliary-fan behavior, and fan duty points.

4. Extend the existing primary-network calibration work to the auxiliary fans and ventilation branches, establishing a traceable basis for offer assessment while retaining unresolved distribution deficiencies.

5. Evaluate the commercial fan offers in the pre-2028 and post-2028 layouts through a stage-gate framework and apply the defined 15% resistance stress scenario only to configurations that satisfy the mandatory baseline KPIs.

6. Compare feasible offered solutions from both technical and economic perspectives, including capital cost, operating cost, and payback-oriented indicators.

7. Formulate a recommendation that is grounded in model results, operational constraints, and the decision needs of the mine.

An important conceptual feature of the thesis is that the preferred replacement solution is not treated as a qualitative statement. Instead, the thesis translates it into two linked evaluation dimensions, namely performance adequacy and economic optimality. Performance assessment is staged. Each offered arrangement is first screened for mandatory whole-mine capacity and stable fan operation. The retained main-fan arrangements are then assessed against local and regional KPIs so that main-fan feasibility can be distinguished from complete ventilation-system adequacy. Economic comparison is applied only to the arrangements that pass the main-fan screening gate, using CAPEX, OPEX, discounted payback, and life-cycle indicators including NPV.

1.4 Research Questions

The thesis is guided by one central question.

> How can the Rodoretto mine ventilation system be evaluated to support the selection of an appropriate replacement strategy for the main fans?

This main question can be decomposed into the following operational sub-questions.

- What airflow and ventilation conditions must be guaranteed in the mine under the relevant operational scenarios?
- How accurately does the current ventilation model represent actual underground conditions?
- Which mismatches between modelled and real behavior are caused by resistance assumptions, leakage, or fan operating conditions?
- How does short-term mine development affect ventilation performance, and when can the 15% resistance stress scenario be applied as a robustness test?
- Which offered arrangements satisfy the whole-mine capacity and fan-operating requirements, and what local or regional constraints remain?
- Among those feasible options, which alternative provides the most convincing economic justification for the company?

1.5 Scope and Delimitations

This thesis is focused on the Rodoretto underground mine as a case study and is primarily concerned with the main exhaust fan replacement problem. Auxiliary ventilation is treated in detail where it affects model calibration, airflow delivery, and local performance constraints, but the thesis does not define or cost the construction-level redesign of every auxiliary duct, fan position, and local control measure. The study focuses on evaluating the commercial offers received by the company, including the different main-fan arrangements proposed in those offers, such as parallel and series operation.

The time horizon of the assessment is intentionally practical rather than speculative. The pre-2028 case represents the existing operating layout, while the post-2028 case represents the planned short-term developments available for assessment. A 15% resistance stress scenario is defined as a conditional robustness test for a configuration that first satisfies the mandatory baseline KPIs. This choice reflects the reality that mine planning is iterative and periodically updated; therefore, the goal is not to predict a fixed long-term final state but to make a justified decision using the best validated information currently available.

1.6 Research Approach Overview

The workflow of the thesis follows a staged engineering logic. The first stage defines the ventilation requirements and the evaluation framework for the later comparison of the offered solutions. In this stage, the minimum required ventilation performance is derived

from operational needs and the standards used by the mine, notably SIA 196/98 together with the Italian regulatory framework referenced in the company material, including DPR 128/59 and DPR 320/56 [6, 7, 8]. The current mine ventilation network is then analysed through a simulation model supplied by the company and calibrated by Howden for the primary ventilation circuit, and further updated within this thesis so that it can represent the geometry and performance of the system more reliably.

The next stage concerns validation and calibration. This is a central part of the work because a fan recommendation is only as credible as the model on which it is based. For this reason, field measurements for the auxiliary network calibration became necessary. Airflow measurements, available pressure-drop information, and observations of ducting condition are used to interpret mismatches between the model and the actual mine. Particular attention is given to leakage treatment, auxiliary-fan calibration, and fan duty point. This stage also includes correcting wrongly modelled points and updating the network to represent already excavated drifts and relevant future developments.

After the model updates and auxiliary-network assessment establish a traceable basis, the study shifts from describing the current state to testing the commercial offers received by the company. These solutions are evaluated in the pre-2028 and post-2028 layouts using the staged performance criteria. The 15% resistance stress scenario is reserved for a configuration that satisfies the mandatory baseline KPIs, since additional resistance cannot convert an already deficient baseline into an acceptable case. The candidate set is defined by real supplier proposals, including parallel and series main-fan arrangements. Only arrangements that satisfy the mandatory whole-mine capacity gate and operate stably proceed to economic comparison, while their local and regional performance is retained as a separate system-adequacy assessment. The economic analysis is therefore linked directly to the ventilation assessment rather than being treated as an independent comparison of purchase prices.

1.7 Contribution

The contribution of this thesis is twofold. At the practical level, it provides Imerys with a defensible basis for selecting and justifying a main-fan replacement strategy. At the engineering level, it demonstrates a workflow in which industrial ventilation decisions are supported by regulation-based requirements, field measurements, network modelling, staged performance assessment, and economic comparison.

The thesis converts a general replacement need into an evidence-based recommendation while distinguishing main-fan capacity from complete ventilation-system adequacy. This distinction is especially important in a mine where ventilation conditions are influenced by changing layouts, production transitions, leakage, and local installation effects.

1.8 Structure of the Thesis

The remainder of this manuscript is organized as follows.

- Chapter 2 presents the literature review and background on mine ventilation, fan selection, ventilation network modelling, and economic evaluation.
- Chapter 3 introduces the Rodoretto mine context and the operational setting of the case study.
- Chapter 4 describes the methodology, including requirement definition, modelling strategy, measurement logic, calibration approach, and economic evaluation framework.
- Chapter 5 presents the model outputs, calibration results, technical screening of the commercial offers, and economic comparison.
- Chapter 6 interprets the implications of the technical and economic results and identifies the need for a separate auxiliary-network improvement study.
- Chapter 7 summarizes the principal findings, provides the final main-fan recommendation, and defines the required further work.

Chapter 2

Literature Review

This chapter reviews the scientific and technical literature that underpins the present thesis. It concentrates on themes that are directly relevant to the Rodoretto case. The review examines underground mine ventilation as both a safety system and a production system, explains how pressure and airflow behave in mine networks, considers the selection and arrangement of main and auxiliary fans, and discusses how leakage, resistance, numerical modelling, calibration, scenario testing, and energy-aware optimization influence engineering decisions. Rather than treating these themes as separate topics, the literature is read here as a connected body of knowledge for supporting a real fan-selection decision in an operating mine.

2.1 Underground Mine Ventilation as a Safety and Design Problem

Underground mine ventilation is one of the core engineering systems that enables safe and productive mining. Its basic functions are well established in the literature. It must provide sufficient fresh air to personnel and equipment, dilute or remove harmful gases and dust, manage thermal conditions, and maintain acceptable working environments throughout a changing underground network [9, 10]. In practice, ventilation is not only a safety requirement but also a design and planning problem, because the air distribution that is acceptable at one stage of mine development may become inadequate after new workings are opened, resistances change, or production fronts move.

Classical mine ventilation literature emphasizes that ventilation design is governed by a combination of regulatory limits, operational needs, and the physical behavior of the network [9]. Modern practice adds a further dimension. Ventilation has become a major operating-cost driver, and therefore engineers are increasingly required to achieve adequate airflow with lower energy consumption and better controllability [10, 11]. This means that a contemporary ventilation study cannot stop at checking whether air reaches

the mine. It must also examine whether the system reaches the required operating points efficiently, robustly, and in a way that remains valid as the mine evolves.

This broader understanding is especially important for mines that already have installed infrastructure and are evaluating replacement or upgrade decisions. In such cases, the engineering task is not the design of an idealized new network from zero, but the assessment of real options under real constraints. The literature therefore supports an approach in which ventilation is treated simultaneously as a safety system, a fluid network, and an economic system [10, 11].

2.2 Ventilation Network Behavior, Resistance, and Duty Point

The theoretical basis of mine ventilation analysis is the representation of the mine as a network of branches and nodes, where airflow distribution is governed by mass conservation at junctions and pressure balance around closed circuits [9, 12]. In this framework, airway geometry, roughness, local losses, regulators, and leakage collectively determine network resistance, while fans provide the pressure rise required to move air through the system. This view remains foundational because it allows the engineer to connect measurable underground features to system-level behavior.

An essential concept in this literature is the relationship between airflow quantity, Q, and pressure loss. For a given network, the required pressure generally increases strongly with increasing Q, and the operating condition of a fan is determined by the intersection between the fan characteristic curve and the system curve [9, 10]. The operating point, or duty point, is therefore not a fixed property of the fan alone. It emerges from the interaction between fan performance and network resistance. This has two important consequences for engineering practice. First, a fan cannot be selected on nominal motor power alone. Second, changes in the network, such as added drifts, changed leakage paths, or alternative fan arrangements, can shift the duty point even when the fan itself is unchanged.

The literature also shows that the interpretation becomes more complex in multiple-fan networks. El-Nagdy [13] showed that in systems with more than one fan, each fan effectively interacts with a subsystem characteristic rather than with a single fixed mine curve. This means that the behavior of one fan depends on the operating state of the others, and that stability cannot be assumed in advance. The issue is particularly relevant where alternative arrangements, such as parallel and series operation, are being considered. Parallel arrangements generally favor increased quantity at lower pressure rise, whereas series arrangements can increase available pressure but may alter subsystem interaction, stability, and control behavior. The literature therefore supports treating

fan arrangement as a system decision, not as a secondary installation detail [13].

From a decision-making perspective, fan selection is inherently multi-criteria. Kursunoglu and Onder [14] showed that appropriate fan selection in underground mines depends on simultaneously considering flow requirement, pressure, efficiency, economics, and practical operating constraints. Their work is valuable because it frames fan choice not as a single-parameter comparison, but as an engineering trade-off problem. This logic is directly relevant to real industrial cases, where technically feasible alternatives may still differ substantially in efficiency, controllability, maintainability, and economic performance.

2.3 Main Fan Selection, Fan Arrangements, and System-Level Efficiency

Literature on mine fan performance increasingly distinguishes between the efficiency of an individual fan and the efficiency of the fan assemblage as installed in the mine. This distinction is important. A fan may have a favorable catalog efficiency and still operate inefficiently once inlet conditions, outlet conditions, transitions, diffusers, silencers, or poor installation geometry are taken into account. De Souza [11] argues that substantial energy losses in mine ventilation systems arise not only from the fan itself but from the way the full assemblage is designed and integrated into the network. From a thesis perspective, this is a critical point because it shifts attention from nameplate power to system performance.

The literature also makes clear that oversizing and undersizing have different but equally important consequences. An undersized fan may fail to maintain the required airflow or pressure margin as the network develops, while an oversized fan may satisfy the airflow target only at the cost of avoidable energy use, poor operating efficiency, or excessive throttling [9, 11]. In mines where variable-speed operation is available, some of the oversizing risk can be mitigated through control. However, the literature still recommends matching the selected fan and arrangement as closely as possible to the expected operating envelope instead of relying on control to compensate for poor initial selection [11, 15].

For operating mines, this means that the evaluation of fan alternatives should include at least four linked questions. These concern whether the offered fan can meet the airflow and pressure requirements, whether it operates in a stable and efficient range, how its behavior changes when the network is updated, and what energy and operating cost consequences follow from the selected arrangement. These questions recur throughout the literature and motivate the integrated technical-economic assessment adopted in the present thesis [14, 11].

2.4 Auxiliary Ventilation, Leakage, and Face Air Delivery

While main ventilation provides the global airflow structure of a mine, auxiliary ventilation determines whether fresh air is actually delivered to development headings and other dead-end workings. The literature consistently treats auxiliary ventilation as an essential part of the overall mine ventilation system rather than as a secondary detail [16, 17]. In development and production settings where the main airways do not directly ventilate the face, the performance of ducted auxiliary systems can control the real Q available at the workplace.

The design of auxiliary ventilation systems is influenced by duct diameter, duct length, fan selection, shock losses, fan spacing where multiple units are used, and especially leakage [16]. Duckworth and Lowndes [16] showed that the design of auxiliary systems becomes rapidly non-trivial as headings become longer and system losses accumulate. Their work demonstrates that a useful model of auxiliary ventilation must go beyond a nominal fan specification and represent the duct system and its losses explicitly.

Leakage is one of the most important themes in this part of the literature. Millar et al. [18] showed that leakage in auxiliary ventilation ducts does not merely reduce the quantity delivered to the face. It also changes the operating point of the fan, influences power demand, and can distort the interpretation of observed friction factors if it is not explicitly represented. Their work is particularly relevant for field-based calibration because it explains why apparent disagreement between measured and modeled behavior may arise from duct leakage rather than from a simple error in airway friction. More recent work by Menendez et al. [17] further develops this theme by combining analytical and CFD approaches to predict leakage, pressure loss, and energy consequences in auxiliary duct systems. Their results show that duct quality, diameter, and leakage class have large effects on both airflow delivery and energy consumption.

Taken together, these studies show that auxiliary ventilation cannot be handled as a fixed boundary condition when the objective is to evaluate the overall behavior of a mine ventilation network. If auxiliary fans or ducts are not properly represented, the total model may reproduce the main air circuit reasonably well while still misrepresenting the actual air delivered to active headings. For a thesis concerned with model credibility and with the selection of main fan options, this is a major point. Uncertainty in auxiliary ventilation can propagate into the interpretation of total resistance, leakage, and future ventilation adequacy [16, 18, 17].

The literature also shows that auxiliary-fan *placement* is itself an engineering variable and should not be reduced to a purely geometric drafting choice. General mine-ventilation guidance reported by ASHRAE indicates that, in a blowing system, the auxiliary fan is commonly installed in a fresh-air base at the start of the drift, from where the ducting

extends toward the face [19]. More detailed work by Morla et al. [20] examined the optimum location of auxiliary fans with respect to recirculation control in dead-end workings. Their results showed that no single universal setback distance can be applied in every case: when the intake airflow was sufficiently greater than the fan quantity, setbacks of about 5 m for a smaller fan and about 10 m for a larger fan were effective in the cases studied, whereas if the intake quantity only matched fan capacity, recirculation could persist even at the larger setback distance [20]. This is an important result for practical modelling, because it means that fan position near a branch entrance must be interpreted together with available intake quantity and not as an isolated rule.

In parallel, broader fan-installation guidance on system effect emphasizes that non-uniform inlet conditions, nearby elbows, and abrupt geometry changes close to the fan can reduce actual performance compared with catalog expectations [21]. For auxiliary ventilation in development headings, this means that a technically credible design should consider not only the nominal fan duty and duct length, but also whether the fan is installed parallel to the airflow, whether the approach flow is reasonably unobstructed, and whether bends or poor fan–duct coupling introduce additional losses. Therefore, the literature supports treating auxiliary-fan setback, alignment, and local installation quality as part of auxiliary-ventilation design rather than as secondary detailing.

2.5 Ventilation Network Modelling, Validation, and Calibration

Numerical modelling has become a standard tool in underground ventilation engineering because mine networks are too complex and too dynamic to assess reliably through hand calculations alone [10, 12]. Modern software environments such as Ventsim and related network solvers make it possible to represent the mine in three dimensions, attach airway properties and fan curves to specific branches, and test the effect of planned developments, altered resistances, regulator settings, or new equipment. However, the literature is clear that a usable model is not simply a digital drawing of the mine. It is a predictive engineering model whose credibility depends on calibration and validation against field data.

Xu et al. [22] explicitly addressed the calibration problem in mine ventilation network models and showed that non-linear optimization can be used to reduce mismatch between model outputs and field measurements by adjusting uncertain parameters in a structured way. Their work is important because it formalizes what is often treated informally in practice. If branch resistances, leakage behavior, or fan characteristics are not consistent with measured conditions, then scenario studies based on the model may be misleading. Calibration is therefore not a superficial step added after modelling; it is what allows the

model to function as a decision tool.

Case-study literature reinforces this conclusion. Karagianni and Benardos [23] developed a detailed Ventsim model of an underground bauxite mine and calibrated it against measured airflow data before using it to support future mine expansion. Similarly, Maleki et al. [24] combined VENTSIM 3D with mathematical programming to analyze and optimize an underground mine ventilation network, demonstrating that model-based evaluation is most powerful when the network representation is sufficiently detailed and tied to operational constraints. Dziurzynski et al. [12] added a further perspective by showing that sensitivity analysis can identify which resistance changes are most influential in a network, helping engineers understand where updates or disturbances are likely to matter most.

The cumulative message of these studies is clear. A ventilation model suitable for decision support needs a realistic representation of geometry, an explicit definition of fans, ducts, and regulators, defensible resistance and leakage parameters, comparison with field measurements, and structured updating when mine development changes the network. This literature strongly supports the use of measured airflow and pressure data to refine a model before comparing candidate fan solutions. It also supports the idea that a partially calibrated model should be completed and updated rather than discarded, particularly when a reliable primary structure already exists [22, 23, 12].

2.6 Energy Efficiency, Control, and Technical-Economic Optimization

Mine ventilation is widely recognized as one of the major energy consumers in underground mining, which is why energy efficiency has become a central literature theme rather than a peripheral consideration [11, 15]. In many operations, the installed ventilation power is large, the duty cycle is nearly continuous, and even modest improvements in fan efficiency or operating strategy can produce meaningful reductions in yearly cost. This is one reason why the literature increasingly links ventilation engineering with optimization and economic assessment.

One important branch of this literature examines the energy performance of fan installations. De Souza [11] showed that large efficiency gains can be achieved by improving the design of main fan assemblages, reducing unnecessary losses, and moving the operating point toward a better efficiency region. Another branch focuses on control strategies. Chatterjee et al. [15] formulated the optimization of main-fan speeds under ventilation-on-demand and time-of-use tariff conditions, showing that variable-speed operation and production-aware control can reduce both energy use and cost. Their study is important because it links fan laws, airflow constraints, and electricity tariffs in a single framework.

Further development of this trend is visible in supervisory and model-based control studies. Sjostrom et al. [25] reported the implementation of optimized model-based control in an operating underground mine and showed that coordinated control of main and booster fans can significantly reduce energy use while still respecting airflow and pressure constraints. More recent mathematical optimization work continues to push in the same direction. Wen et al. [26] proposed a mixed-integer non-linear programming approach for ventilation network regulation, while Saleem [27] combined network modelling with machine-learning-based optimization to reduce energy consumption in an underground ventilation system.

These studies show that the state of the art is moving from static adequacy checks toward intelligent and energy-aware ventilation management. At the same time, the literature also indicates an important practical limitation. Many advanced optimization studies assume that the underlying network representation, instrumentation, and control architecture are already reliable. In industrial decision-making, however, the first challenge is often more basic and more difficult, namely to obtain a trustworthy model of the actual mine and then use that model to assess realistic equipment choices. For this reason, the literature on optimization does not replace the need for calibration, scenario testing, and economic comparison at the case-study level. Instead, it provides the methodological background for why energy consumption, annual operating cost, and controllability should be part of a modern fan evaluation.

2.7 Synthesis of the Literature and Research Gap

The literature reviewed in this chapter provides a coherent foundation for the present thesis. First, classical ventilation texts and modern practice papers show that mine ventilation must be treated as a coupled safety, design, and operating-cost problem [9, 10]. Second, research on network behavior and multi-fan systems shows that fan performance cannot be interpreted independently of network resistance, leakage, and arrangement [13, 14]. Third, auxiliary ventilation studies demonstrate that duct leakage, local losses, and fan placement strongly affect face air delivery and can materially influence the interpretation of the wider network [16, 18, 17, 20, 21]. Fourth, model-calibration literature shows that measured data are indispensable if a ventilation model is to be used credibly for future scenarios and equipment comparisons [22, 23, 12]. Finally, optimization studies show that technical adequacy and energy performance must increasingly be assessed together rather than sequentially or independently [11, 15, 25, 26, 27].

At the same time, a specific applied gap remains between the literature and the needs of the Rodoretto case. Much of the published work focuses on general design theory, auxiliary ventilation in isolation, advanced optimization methods, or case studies in which the model and measurement infrastructure are already mature. Fewer studies address the

practical situation in which an operating mine already has commercial replacement offers on the table, a three-dimensional network model exists but is only partially calibrated, parts of the geometry and development status still need updating, and the decision must compare offered fan arrangements on both technical and economic grounds.

The present thesis addresses that gap by integrating several tasks that are often treated separately in the literature. It starts from a company-provided 3D Ventsim model previously calibrated only for the primary ventilation circuit, completes the credibility of the network by processing recent measurements and extending calibration to the auxiliary system, updates the network by correcting wrongly modeled points and by adding already excavated drifts and relevant near-term developments, and then uses the updated model to evaluate the commercial offers received by the mine, including alternative arrangements such as parallel and series operation. The contribution of the thesis is therefore not only the comparison of offered fans, but the creation of a defensible technical-economic decision basis grounded in calibrated network behavior. That framing follows directly from the literature reviewed above and defines the role of the methodology presented in the next chapter.

Chapter 3

Study Context

This chapter presents the industrial and technical context of the Rodoretto case study. The purpose is not to repeat the general motivation already introduced in Chapter 1, but to describe the specific mine setting in which the ventilation assessment is carried out. The chapter therefore focuses on the mine location and organization, the ventilation-relevant features of the mining setting, the current production transition toward extension areas, the ventilation system presently in operation, and the data and modelling basis available for the thesis. Together, these elements explain why fan selection at Rodoretto must be treated as a case-specific engineering problem rather than as a simple catalogue comparison.

3.1 Rodoretto Mine and Industrial Setting

Rodoretto is an underground talc mine operated by Imerys Talc Italy in the Germanasca Valley, in the Piedmont region of the northern Italian Alps. According to the technical report provided by the company, the operation has particular strategic relevance within the national context of talc production [1]. The site is located in mountainous terrain at roughly 1000 m elevation, and the underground workings form part of a longer mining history in the valley.

From an operational perspective, Rodoretto functions as a regularly operating underground mine with organized production, haulage, and maintenance activities distributed across defined shifts. The company annual technical report states that the production team operates five days per week over three shifts per day, with eleven workers plus one foreman underground per shift, while haulage and maintenance activities support the mining cycle through dedicated crews and shift patterns [1]. This matters for the present thesis because ventilation demand is tied not only to geometry and equipment, but also to the actual organization of underground work. The requirements used later in the thesis therefore have to remain consistent with the real personnel and equipment exposure that

the mine expects during normal operation.

The regulatory and administrative setting is also important for framing the study. The Rodoretto workings and infrastructures lie within the Nuova Fontane mining concession, whose current authorization extends to June 2032 according to the company documentation [1]. This does not mean that the mine ends in 2032, but it does mean that near-term engineering decisions should be grounded in the currently validated development horizon rather than in an overly speculative long-term layout. For this reason, the thesis places greater emphasis on the short-term operating horizon of the mine and on a later stress-scenario check than on a fully open-ended life-of-mine optimization.

From a ventilation perspective, the most important physical features of the mine are the access layout, the distribution of active headings, and the mining method. The deposit is reached through an adit and decline system, and the workings extend across historical northern and southern sectors as well as newer extension zones [1]. Mining is carried out by underhand cut-and-fill with cemented backfilling and selective extraction, with a combination of remotely controlled electrical scalers and drill-and-blast depending on the heading conditions [1]. For the present thesis, the key consequence is that the mine contains work areas with different geometries, support conditions, and local operating needs, so the ventilation system must serve both the main network and more localized areas where auxiliary air delivery becomes decisive.

3.2 Production Transition and Planning Horizon

One of the central reasons this case is interesting from a ventilation-engineering standpoint is that Rodoretto is transitioning from historical mining areas toward extension areas. The older North and South sectors are close to exhaustion, although some limited deeper or lateral continuity may still be exploited, while the North Extension and especially the South Extension are taking on increasing importance in the future production profile [1]. The report also notes that more than half of the reported reserves are now located in the South Extension, while the North Extension has already entered production and continues to be developed under more challenging geotechnical conditions [1]. In addition to the extension areas described in the annual report, the company-provided short-term development information also includes South Intermediate and the Far North sector on two levels.

This transition matters directly for ventilation because a network that was acceptable when production was concentrated in the historical sectors may behave differently once the center of activity shifts toward newer and deeper or more distant extension areas. In addition, the annual report explicitly notes that ventilation management becomes increasingly important during the ramp-up of the extension zones because development sequencing, logistics, and production balance all interact with airflow availability and

quality [1]. In other words, the mine is changing not only in geological terms, but also in the spatial distribution of the activities that drive ventilation demand.

For the thesis, this means that the study context cannot be reduced to a snapshot of today's workings only. At the same time, it would not be methodologically sound to base the fan evaluation on a highly speculative long-range final layout. The most reasonable engineering basis is therefore the latest validated development information provided by the company, together with the short-term future additions that are sufficiently mature to be represented credibly in the model. This is consistent with the practical purpose of the thesis, which is to support an actual decision on received commercial offers using the best currently validated mine information.

3.3 Existing Ventilation System

The Rodoretto ventilation system combines a mine-wide primary circuit with localized auxiliary ventilation. According to the Howden survey report, the mine has a single main entrance acting as the fresh-air intake and two double-stage Woods 48J2 main exhaust fans installed in parallel at the exhaust side of the network [2]. These two fans exhaust air from the entire mine and therefore define the behavior of the primary ventilation circuit. The same report states that the June 2025 survey measured both airflow and pressure throughout the accessible network and used those data to calibrate the primary ventilation model in Ventsim DESIGN [2].

The survey report also indicates that the measured and simulated duty points of the current main fans lie in a low-pressure operating region of their characteristic curve, which is consistent with the results of the present thesis [2]. The corresponding Ventsim duty panels for the two existing Woods 48J2 fans are shown in Figure 3.1. From the thesis perspective, this is a key part of the study context because it shows that the current installation cannot be judged only in terms of whether it operates or not. Its operating position on the fan curve raises questions about performance margin and the suitability of future replacement arrangements. This is one reason why the thesis evaluates complete offered solutions, including fan arrangement, rather than nominal motor power alone.

The auxiliary ventilation network is also an important part of the Rodoretto context. The annual report explains that the auxiliary ventilation system is based on Zetal VH 1004.4 counter-rotating fans in several installed configurations, including $2 \times 45\,\mathrm{kW}$, $2 \times 30\,\mathrm{kW}$, and $1 \times 45\,\mathrm{kW}$, depending on the area to be ventilated [1]. The company documentation further indicates that, for a single access, the auxiliary system should be capable of providing at least $6\,\mathrm{m}^3/\mathrm{s}$ and up to approximately $9\,\mathrm{m}^3/\mathrm{s}$ when two stopes are mined simultaneously in the same access [1]. These figures are relevant because they link local auxiliary airflow directly to workplace requirements.

During the thesis work, however, direct site observation showed that the auxiliary

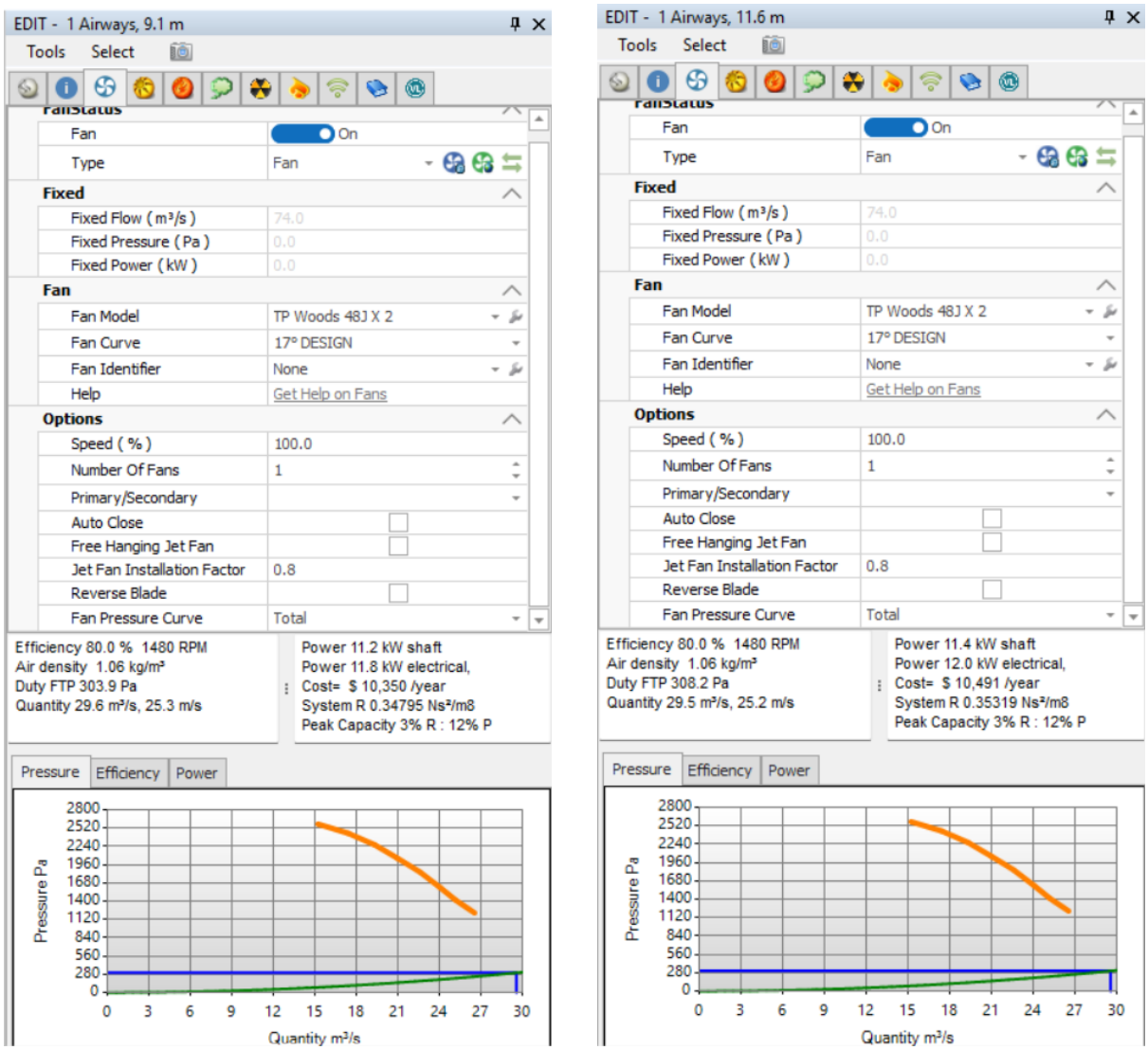

(a) Left existing main-fan airway. (b) Right existing main-fan airway.

Figure 3.1: Ventsim duty panels for the two existing Woods 48J2 main exhaust fans.

system cannot be treated as uniformly reliable. Duct condition, leakage, and installation quality vary between locations, and these issues influence how much air is actually delivered to the working faces. This matters for the present study because the apparent adequacy of the main system cannot be interpreted independently of the quality of local air delivery. A mine can have acceptable total intake and exhaust quantities while still underperforming at specific active faces if auxiliary losses are significant.

3.4 Available Data and Modelling Basis

The thesis begins from a set of company materials that together define a technical basis for analysis. At the broadest level, the *Annual Technical Report 2024*, issued in February 2025, provides the operational context of the mine, including the organization of work, the transition from historical sectors to extension areas, the mining method, the short-

term planning logic, and the existing auxiliary ventilation configurations [1]. This report is particularly useful for understanding why the mine is asking for a fan evaluation now and which parts of the operation are likely to matter most in near-term scenario testing.

At the network level, the company also provided a three-dimensional Ventsim model, shown in Figure 3.2, that had already been developed and calibrated by Howden for the primary ventilation circuit [2]. This is a major contextual advantage for the thesis because it means the work is not starting from a purely schematic drawing or from an entirely uncalibrated model. The Howden survey established a calibrated basis for the primary network by comparing field measurements with simulated airflow and pressure values and iteratively refining the model [2]. In practical terms, that previous work converts the thesis from a model-creation exercise into a model-completion and decision-support exercise.

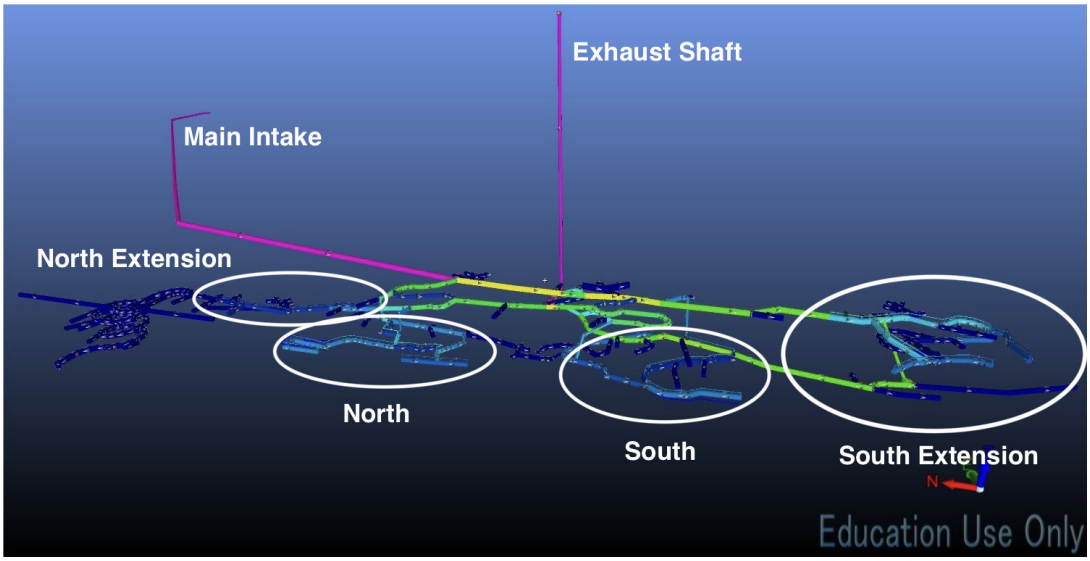

Figure 3.2: Company-provided Rodoretto Ventsim model used as the modelling basis.

Although the supplied model provided a strong starting point, it was not sufficient on its own for the final purpose of the thesis. The work therefore completed the representation and calibration of the auxiliary system, processed the measurements collected for that purpose, corrected points that were modelled incorrectly, and updated the network to include already excavated drifts and relevant near-term future developments. These completed updates established the model basis subsequently used to compare the replacement offers.

3.5 Implications for the Present Thesis

Taken together, the case-study context explains why the thesis has the structure adopted in this manuscript. The mine is an operating underground production system with aging

main exhaust fans, a non-trivial auxiliary network, and a development pattern that is moving from historical areas toward extension zones. The primary ventilation model was calibrated by Howden, and this thesis extended the measurement-based calibration to the auxiliary system before using the updated network for decision support. At the same time, the fan decision was evaluated using real commercial offers whose proposed arrangements differ and whose suitability depends on the actual behavior of the mine network.

For these reasons, the thesis is positioned between a conventional design study and industrial troubleshooting. It is not simply a new mine ventilation design, because Rodoretto already exists and is operating. It is not merely a procurement comparison either, because catalogue fan data alone cannot resolve the interaction between network resistance, leakage, future developments, and arrangement choice. The study context therefore justifies the combined approach adopted in the following chapter, namely regulation-based requirement definition, model updating, field-supported calibration, scenario analysis, and technical-economic comparison of the received fan offers.

Chapter 4

Methodology

This chapter presents the detailed methodological framework used to transform the Rodoretto fan-replacement problem into a structured technical-economic decision study. The work does not treat fan selection as a simple catalogue comparison. It starts from regulatory ventilation requirements, translates them into measurable performance criteria, uses an existing calibrated three-dimensional Ventsim model as the baseline for the primary ventilation circuit, completes the missing calibration of the auxiliary network through a staged field-supported workflow, freezes the present-day mine configuration for baseline calibration, and only then evaluates the commercial offers received by the mine under realistic current and near-term layout conditions.

The detailed treatment is necessary because the thesis problem has two strongly coupled parts. The first part is technical. The mine must receive enough air in the relevant main airways, ramps, and active areas, and the air must be delivered under conditions that remain acceptable as the layout evolves. The second part is economic. Among the solutions that are technically acceptable, the mine needs a recommendation that is also justified in terms of investment and operating cost. For that reason, the methodology is built as a stage-gate process in which technical feasibility is established first and economic ranking is applied afterward.

4.1 Overall Methodological Logic

At the methodological level, the thesis is organized into four connected phases.

1. Establish the performance framework by defining the key performance indicators, extracting their threshold values from the regulations and standards used by the mine, and formulating the fan-selection problem as a coupled technical-economic decision task.

2. Build the baseline model basis by adopting the existing Howden Ventsim model of the primary ventilation circuit, correcting the present-day mine representation, and

separating short-term development branches so that baseline calibration and later scenario testing are not mixed prematurely.

3. Calibrate the auxiliary network through field measurements, measurement-to-model comparison, and staged adjustment of fan behaviour, local installed losses, duct leakage, and effective resistance until the simulated branch behaviour becomes physically defensible against the observed underground system.

4. Use the calibrated baseline as the decision platform for reintroducing the short-term development branches, testing the received commercial offers under the selected scenarios, and ranking the technically feasible solutions by economic criteria.

The sections that follow develop these four phases in detail. This logic is consistent with calibration-oriented mine ventilation modelling practice, which requires scenario analysis and equipment comparison to be based on a model that has been confronted with field data rather than on an unverified network representation [22, 23].

4.2 KPI Framework and Regulatory Basis

4.2.1 Selection logic for the KPIs

The first methodological decision was the definition of the key performance indicators, because the thesis needed a rigorous way to answer what "adequate ventilation" means for Rodoretto. The selected KPIs reflect worker safety, pollutant dilution, and network functionality.

From the beginning, the methodology distinguished between two classes of quantities. The first class contains the performance KPIs that a replacement offer must satisfy in the final decision. The second class contains calibration variables that make the model trustworthy enough to support that decision. Air quantity, Q, and air velocity, v, belong to the first class because they express the actual ventilation duty of the system. Repeatability, inlet-versus-outlet mismatch, leakage ratio, and duty-point plausibility belong to the second class because they determine whether the simulated system reflects the physical one with sufficient credibility. The performance indicators used in the thesis and the basis for their selection are summarized in Table 4.1.

The selected KPIs have different roles in the workflow. The Q requirement (Q_{req}) and the v limits act as the main technical acceptance criteria for the offer evaluation. The worker and machine coefficients define how Q_{req} is calculated. As explained in Subsection 4.5.4, the coefficient of variation and the outlet interpretation criterion are methodological checks rather than design KPIs, because they determine how the measured auxiliary data are interpreted and used in calibration.

KPI	Target	Source	Reason for selection
Air quantity, Q	$Q \geq Q_{\text{req}}$	Company ventilation-sizing method, based on SIA 196/98 and Italian regulations [1, 8, 6]	Primary adequacy criterion for breathing air and diesel dilution.
Air velocity, v, in airways	$0.1 \leq v \leq 6.0$ m/s	DPR 128/59, Art. 261 [7]	Checks local flow acceptability beyond total quantity.
Fresh air per worker	0.05 m^3/s per person	DPR 320/56, Art. 30 [8]	Regulatory lower bound for worker-related airflow demand.
Diesel loading-machine factor	0.066 $m^3/s\,kW$	SIA 196/98, as applied in the company sizing method [1, 6]	Accounts for exhaust dilution from loading machines.
Diesel hauling or service-machine factor	0.033 $m^3/s\,kW$	SIA 196/98, as applied in the company sizing method [1, 6]	Accounts for exhaust dilution from hauling and service machines at the reduced sizing factor.
Safety factor	$K_s = 1.2$	Company ventilation-sizing method [1]	Provides design margin for operational uncertainty.
Auxiliary delivery repeatability	CV confidence class: $< 10\%$ preferred; 10–15% cautious; $> 15\%$ low-confidence	Thesis survey protocol	Prevents unstable outlet readings from being over-weighted in calibration interpretation.
Local auxiliary outlet condition	Acceptable outlet flow and interpretable local velocity; 0.25 m/s used as the practical lower field threshold	Thesis survey protocol	Identifies dead-air or near-null delivery at auxiliary-duct outlets.

Table 4.1: Performance indicators used in the thesis and the basis for their selection

The choice of Q and v as the primary decision KPIs also needs to be stated explicitly. Q is the direct variable that answers whether enough fresh air is delivered to dilute diesel emissions and supply the active areas. v is needed because a branch can carry an acceptable integrated quantity while still having locally poor or excessively fast flow. Other variables such as temperature, humidity, or contaminant concentration remain relevant in underground ventilation, but they were not selected as the primary decision KPIs in this thesis because the available decision problem is centered on main-fan replacement and network capacity, and the directly available dataset is strongest for airflow and pressure-based assessment.

4.2.2 Regulatory thresholds

The regulatory basis used by the mine combines Italian rules and the SIA approach adopted in the company ventilation calculations. The two most important Italian references are DPR 128/59 and DPR 320/56. According to DPR 128/59, the average air velocity in the narrowest section of an underground passageway must not exceed 6 m/s and, except in the specific situations exempted by the decree, it must not be lower than 0.1 m/s [7]. DPR 320/56 requires a minimum fresh-air provision of 3 m^3/min per worker, which corresponds to 0.05 m^3/s per person underground [8]. The company report also states that the diesel-dilution coefficients used in the mine are taken from SIA 196/98, namely 0.066 m^3/s kW for loading equipment and 0.033 m^3/s kW for hauling or service equipment [1].

The same regulatory material also supports the measurement campaign itself. DPR 128/59 requires periodic investigation of airflow, temperature, and humidity in the main, branch, and auxiliary ventilation circuits, while DPR 320/56 contains the related provisions on breathable atmosphere and temperature limitations [7, 8]. In the present thesis, these provisions are not treated merely as legal background, but as part of the methodological justification for considering field measurements and model updating as core components of the study rather than optional supplements.

4.2.3 Translation of the regulations into design quantities

For Rodoretto, the minimum airflow requirement is derived from the number of exposed workers, the diesel power active in the relevant area, and the safety factor used in the ventilation-sizing method documented in the company's *Annual Technical Report 2024* [1]. The calculation is separated into a people component and machine components so that the contribution of each driver remains explicit. The individual terms are

$$Q_{\mathrm{pers}} = 0.05\, N_{\mathrm{p}} \tag{4.1}$$

$$Q_{\text{load}} = 0.066 \sum P_{\text{load}} \tag{4.2}$$

$$Q_{\text{haul}} = 0.033 \sum P_{\text{haul}} \tag{4.3}$$

The company method applies the safety factor to the diesel-equipment contribution, while the prescribed personnel contribution remains unmodified. The resulting requirement is written as

$$Q_{\text{req}} = K_s \left(0.05\, N_{\text{p}} + 0.066 \sum P_{\text{load}} + 0.033 \sum P_{\text{haul}}\right) \tag{4.4}$$

where Q_{pers}, Q_{load}, and Q_{haul} are the airflow requirements for personnel, loading equipment, and hauling or service equipment, respectively, N_{p} is the number of persons simultaneously present, $\sum P_{\text{load}}$ is the sum of diesel loading-machine power in kW, $\sum P_{\text{haul}}$ is the sum of diesel hauling or service-machine power in kW, and $K_s = 1.2$ is the safety factor used in the ventilation-sizing method documented in the company's *Annual Technical Report 2024*. The report states that this method is based on SIA 196/98 [1, 6]. Equation 4.4 is the equation used throughout the thesis to convert operational activity into a ventilation requirement. It is also the point where the operational description of the mine is translated into model inputs. Once the personnel and equipment configuration of a case is defined, the required Q becomes calculable and can be compared directly with the simulated quantity at the relevant main or local branches.

The company report distinguishes between whole-mine traffic conditions in the main gallery and local peak activity in an extraction area or access. That distinction is important and was retained in this thesis. A whole-mine traffic case is appropriate for checking the adequacy of the main ventilation circuit. A local or per-area case is appropriate for checking service ramps, accesses, and auxiliary delivery. The methodology therefore does not multiply one local peak case by the number of potentially active areas unless the intention is explicitly to build a separate whole-mine simultaneous-demand aggregation. This avoids overstating the demand in one airflow direction by assuming that several locally defined peaks occur together in exactly the same way and at the same time.

4.2.4 Traffic cases adopted from the company sizing logic

The annual report already contains two high-traffic sizing cases that are directly useful for the thesis. They are reproduced here as they define the minimum airflow basis used later for screening the offered solutions.

The total of 47.97 m^3/s in Table 4.2 is the basis on which the main ventilation circuit was originally sized in the company report. The same report states that the main ventilation survey measured about 58 m^3/s in the main adit as a preliminary verification,

which means that the methodology can compare both the designed minimum and the measured available quantity [1]. To avoid adding a false precision to a planning-based case, the thesis uses the report value as the required whole-mine benchmark rather than recomputing a new fleet-wide case from the entire equipment inventory.

Diesel equipment	**Power (kW)**	**Persons**	Q_{req} **contribution** (m^3/s)
FEL (CAT 926M)	106	1	8.45
Contractor 4 axles	330	1	13.25
Scania 4 axles	330	1	13.25
UGL (Atlas Copco ST2G)	81	1	6.47
Dumper T1601C	164	1	6.55
Total			**47.97**

Table 4.2: Case 1: main-gallery "very high traffic" sizing case adapted from the company report [1]

Diesel equipment	**Power (kW)**	**Persons**	Q_{req} **contribution** (m^3/s)
Piattaforma Lorenzana 1	54	2	2.26
UGL (Atlas Copco ST2G)	81	1	6.47
Piattaforma Lorenzana 2	54	2	2.26
Jumbo Sandvik DD12	60	1	2.376
Total			**13.366**

Table 4.3: Case 2: extraction-area "high traffic" sizing case adapted from the company report [1]

Table 4.3 is important because it links the whole-mine ventilation problem to the local demand at the areas that are actually served by auxiliary ventilation. It shows that a peak local area demand of about 13.37 m^3/s is consistent with the report statement that about 15 m^3/s was available in each of the North, North Extension, South, and South Extension service ramps [1].

The company report also defines three activity-specific cases for a single level served by auxiliary ventilation. Supporting work assumes a two-person crew using a Lorenzana SL33 scissor lift, whereas mucking assumes a two-person crew using an Atlas ST2G underground loader. The simultaneous case represents both activities occurring within the same level.

The published values in Table 4.4 are retained as the activity-classification thresholds used in the offer assessment. They account for personnel demand and diesel-exhaust dilution with the safety factor applied according to the company method. Retaining the reported values also avoids introducing false precision from recalculating quantities using coefficients presented in the source with limited decimal precision. The resulting

Activity case	**Diesel equipment**	**Power (kW)**	**People**	Q_{req} (m^3/s)
Supporting only	Lorenzana SL33 scissor lift	54	2	2.26
Mucking only	Atlas ST2G underground loader	81	2	6.52
Simultaneous supporting and mucking	Lorenzana SL33 scissor lift and Atlas ST2G underground loader	$54 + 81$	$2 + 2$	8.78

Table 4.4: Activity-specific auxiliary airflow requirements adopted from the company report [1]

operational range is consistent with the report specification of at least 6 m^3/s for one active workface and up to approximately 9 m^3/s when supporting and mucking occur simultaneously within one access [1].

4.3 Decision Variables, Pressure-Flow Reasoning, and Objective-Function Formulation

Before the formal optimisation logic can be defined, the physical quantities that govern fan performance in the network must be stated explicitly. The fan does not determine airflow independently. The operating point is established by the interaction between the fan characteristic and the resistance of the network [9, 10]. The total pressure is interpreted as

$$P_{\text{t}} = P_{\text{s}} + P_{\text{v}} \tag{4.5}$$

where P_{s} is the static pressure and P_{v} is the velocity pressure. At network level, the pressure drop of an airway or duct branch is represented by

$$\Delta P = RQ^2 \tag{4.6}$$

where R is the resistance. For auxiliary duct sections and idealized airway segments, the resistance can be written in Atkinson form as

$$R = \frac{kPL}{A^3} \tag{4.7}$$

where k is the friction factor, P is the perimeter, L is the length, and A is the cross-sectional area [9]. This relation is important in the methodology because it explains why geometry updates, duct deterioration, and leakage-related effects can all shift the duty point of the fan. In practice, the airway size and friction factor are assigned and the software calculates the resulting resistance, while calibration adjusts the assumptions

whenever field evidence shows that the default behaviour is not representative enough.

In methodological terms, the main-fan replacement problem is treated as a discrete decision problem. The candidate set is not an open catalogue of abstract fan sizes, but the set of commercial offers actually received by the mine, together with the arrangements proposed in those offers, including parallel and series operation. The task is therefore to define how those real alternatives are screened for technical feasibility and then ranked economically.

The overall decision problem is expressed through two linked objectives, consistent with the multi-criteria character of underground-fan selection discussed in the literature [14].

- **Objective 1, performance feasibility**. Each offered solution must satisfy the selected ventilation KPIs in the evaluated mine scenarios.
- **Objective 2, economic optimality**. Among the technically feasible solutions, the preferred option should provide the strongest economic justification.

This two-part formulation was selected deliberately. In mine ventilation, technical infeasibility cannot be compensated for by lower cost. A cheaper solution is not acceptable if it fails to deliver the required Q, violates the v limits, or leaves critical working areas under-ventilated. The economic objective therefore operates only on the subset of technically feasible solutions. This is why the thesis does not merge every term into one unconstrained score from the start. The technical criteria define admissibility. The economic criteria define preference inside the admissible set.

In logical form, the thesis interprets the best option as

$$\text{Best option} \equiv \text{Performance-feasible} \wedge \text{Economically preferred} \tag{4.8}$$

Let $p \in \mathcal{P}_{\text{offer}}$ denote an offered fan package and arrangement, let $s \in \mathcal{S}$ denote one of the analysed mine scenarios, and let j denote a critical location in the network such as the main adit, a service ramp, or a branch serving an active area. The main technical constraints are written as

$$Q_j(p, s) \geq Q_{\text{req},j}(s) \tag{4.9}$$

$$v_{\min,j} \leq v_j(p, s) \leq v_{\max,j} \tag{4.10}$$

where $Q_j(p, s)$ is the airflow predicted by the model for option p in scenario s at location j, $Q_{\text{req},j}(s)$ is the required airflow derived from the selected traffic case, and $v_j(p, s)$ is the corresponding air velocity. The feasible set is

$$\mathcal{F} = \{p \in \mathcal{P}_{\text{offer}} \mid Q_j(p,s) \geq Q_{\text{req},j}(s),\ v_{\min,j} \leq v_j(p,s) \leq v_{\max,j}\ \forall j, s\} \tag{4.11}$$

For interpretation purposes, the methodology also uses the local airflow margin

$$M_{Q,j}(p,s) = \frac{Q_j(p,s) - Q_{\text{req},j}(s)}{Q_{\text{req},j}(s)} \tag{4.12}$$

because an option that only barely meets the requirement in the current layout may become fragile once leakage, resistance increases, or short-term geometry updates are taken into account. The same logic applies to velocity. A solution that stays comfortably inside the acceptable range is more robust than one that touches the limit under the baseline scenario.

The stage-gate decision rule can therefore be stated more explicitly. First, the feasible set $\mathcal{F}$ is determined from the KPI constraints. Second, the preferred option is selected from that feasible set by lexicographic comparison of the economic criteria, as explained in Subsection 4.3.1. In words, the methodology first removes all options that fail the ventilation duty and only then compares the surviving options economically.

For each technically feasible option, the economic evaluation is built from the following components.

$$C_{\text{CAPEX}} = C_{\text{eq}} + C_{\text{inst}} + C_{\text{elec}} + C_{\text{civil}} + C_{\text{ctrl}} + C_{\text{int}} + C_{\text{decom}} + C_{\text{cont}} \tag{4.13}$$

Equation 4.13 defines the complete potential CAPEX structure. In the implemented comparison, CAPEX included the supplier fan-package price, the cost of the VSD software supplied by Softime, and the cost of the electrical package and VSD installation supplied by Microl. These were the traceable cost components available on a consistent basis for all alternatives. Hence, for option p, the evaluated CAPEX is

$$C_{\text{CAPEX},p} = C_{\text{fan},p} + C_{\text{Softime}} + C_{\text{Microl}}, \tag{4.14}$$

Other potential CAPEX components in Equation 4.13 were not assumed to be physically zero, but were excluded from the quantified comparison because no reliable and consistently defined offer-specific values were available. Softime and Microl were common to all alternatives and therefore affect the absolute NPV and payback values without affecting the relative CAPEX difference between offers.

$$C_{\text{OPEX},y} = C_{\text{energy},y} + C_{\text{maint},y} + C_{\text{other},y} \tag{4.15}$$

$$C_{\text{energy},y} = P_{\text{avg},y}\, H_y\, c_{\text{e},y} \tag{4.16}$$

When measured electrical power is not available, the average power can be estimated from the validated duty point through

$$P_{\text{elec}} = \frac{Q\,\Delta P}{\eta_{\text{overall}}} \tag{4.17}$$

where Q is airflow, ΔP is pressure rise, and η_{overall} is the combined efficiency.

The annual saving of a candidate option relative to the baseline is

$$S_y = C^{\text{base}}_{\text{OPEX},y} - C^{\text{option}}_{\text{OPEX},y} \tag{4.18}$$

and the payback can be written as

$$\text{Payback} = \frac{\Delta C_{\text{CAPEX}}}{S_{\text{annual}}} \tag{4.19}$$

The discounted metric used when the required financial inputs are available is the net present value

$$\text{NPV} = -\Delta C_{\text{CAPEX}} + \sum_{t=1}^{n} \frac{S_t - C_{\text{extra},t}}{(1+r)^t} \tag{4.20}$$

The economic objective is deliberately decomposed into CAPEX, OPEX, payback, and NPV because each metric answers a different practical question. CAPEX answers how much implementation effort is required at the beginning. OPEX answers how expensive the solution is to run. Payback answers how quickly the additional investment is recovered relative to the current installation. NPV answers the full discounted value of the replacement over the analysis horizon. Together, these metrics capture not only cost level but also timing and long-term economic efficiency.

4.3.1 Lexicographic Model as the Decision Rule

The economic ranking is carried out through a lexicographic model. This decision rule is appropriate because technical feasibility remains non-negotiable, the number of commercial offers is limited, and the mine is comparing a small set of real packages rather than optimizing over a broad abstract design space.

The lexicographic approach ranks the feasible options sequentially rather than collapsing every criterion into one score. After the technically infeasible options have been removed, the remaining offers are compared in ordered stages. In the present thesis, the ordering is

$$\mathbf{L}(p) = \left(-N\hat{P}V(p),\ D\hat{P}P(p),\ \hat{C}_{\text{CAPEX}}(p),\ \hat{C}_{\text{OPEX}}(p)\right) \tag{4.21}$$

and the selected solution is

$$p^* = \text{lexmin}_{p \in \mathcal{F}} \mathbf{L}(p) \tag{4.22}$$

where $\hat{NPV}$, $\hat{DPP}$, $\hat{C}_{\text{CAPEX}}$, and $\hat{C}_{\text{OPEX}}$ denote normalized forms of net present value, discounted payback period, capital expenditure, and operating expenditure, used only to express the lower-order comparisons on commensurate dimensionless scales. In practical terms, this means that the method first prefers the feasible option with the strongest NPV. If two options remain effectively equivalent at that level, the next comparison is made on discounted payback. If they still remain too close to separate confidently, CAPEX and then OPEX are used as lower-order tie breakers. Maintenance, controllability, and implementation practicality can then be used as qualitative supporting criteria when the remaining difference is marginal.

This sequential logic matches the actual industrial decision well. In that setting, it is more transparent to say that technical feasibility comes first, then long-term economic value, then investment recovery speed, and only after that the secondary economic differences.

The same decision logic also admits uncertainty margins. If a stress envelope is imposed on the required quantity or on network resistance, the governing expressions become

$$Q_{\text{req}}^{\text{stress}} = (1 + \alpha_Q)\, Q_{\text{req}} \tag{4.23}$$

$$R^{\text{stress}} = (1 + \alpha_R)\, R \tag{4.24}$$

where α_Q and α_R represent conservative uncertainty factors. A value of 15% is adopted as the stress envelope for uncertain simultaneous activity, leakage, and short-term resistance growth. These stress mechanisms are useful because they test whether a technically feasible solution remains acceptable when the mine moves away from the idealized baseline.

4.4 Baseline Model, Model Updates, and Observed System Issues

The modelling basis for the thesis is the three-dimensional Ventsim DESIGN model created and calibrated by Howden for the primary ventilation circuit [2]. The report states that the calibrated model was brought to a condition in which the deviation of the measured values did not exceed 12% and the total mass-flow difference between intake and exhaust sums was 3.7% [2]. This existing model is therefore used as the baseline network

representation rather than reconstructing the whole mine from zero.

At the outset of the thesis, the baseline model was not treated as complete. It provided a credible representation of the primary network, but it did not include a complete measurement-based calibration of the auxiliary system or the model corrections and short-term mine updates identified during the thesis work.

Before the offer evaluation, the model was therefore updated in three ways.

- **Geometry correction**. Points that were modelled incorrectly were corrected.
- **Current-state updating**. Already excavated drifts and changes in the mine geometry were represented.
- **Near-term development inclusion**. Future developments sufficiently defined for the study horizon were added to the scenario model.

For calibration purposes, however, these three update tasks were not applied in one undifferentiated model state. The existing mine was first isolated and used as the calibration boundary for the auxiliary system. The short-term development branches were defined separately as scenario geometry and were reintroduced only after the present-day model had reproduced the measured auxiliary behaviour with sufficient credibility. This sequence was methodologically important, since current-system mismatch could otherwise have been attributed incorrectly to future branches whose geometry was necessarily more provisional.

Field observation	**Ventilation effect**	**Modelling implication**
Visible tears or perforations in duct sections	Distributed or local air loss before the face	Leakage must be calibrated explicitly and cannot be ignored
Poor couplings or damaged fan-duct joints	Local leakage and pressure loss near the fan or branch entrance	Inlet and outlet measurements must both be used
Unfavourable fan positioning or inlet obstruction	System effect and reduced effective fan performance	Nominal fan data alone are insufficient for duty-point interpretation
Non-uniform duct geometry, bends, or installation defects	Additional resistance and reduced delivery to the branch end	Friction and local losses must be adjusted during calibration
Very weak delivered air at some outlets	Local under-ventilation despite nominal installed equipment	Branch-level checks are required in addition to whole-mine checks

Table 4.5: Observed auxiliary-ventilation issues and methodological implications

During the thesis work and the site visits, several recurring issues were also observed in the current ventilation system, especially in the auxiliary installations. Auxiliary fans were not always placed in positions that favour clean inlet conditions. Some installations showed inlet obstructions or poor positioning relative to the airway. Duct condition was not uniform and visible tears or damage were present in some sections. Bad couplings and local installation defects were also observed at some fan-duct connections. These observations are important as they explain why auxiliary calibration could not be treated as a secondary detail. They imply that local delivered air cannot be inferred reliably from nominal fan data alone. The Howden report documents the same types of issues and also reports that the primary fans operate in a low-pressure region and that some auxiliary fans run in stalled or unfavourable conditions [2]. In the present thesis, however, the visual duct and installation issues are treated as direct site observations that motivated the field campaign, while the low-pressure interpretation of the primary fans is treated as an inherited model-based finding from the Howden baseline. These observations and their methodological implications are summarized in Table 4.5.

4.4.1 Auxiliary-fan placement near branch intersections

During the model-update work, several possible auxiliary-fan locations were tested near the entrance of a branch connected to the main adit. The tested positions differed in their distance from the branch intersection, while the remainder of the branch geometry remained unchanged. In the Ventsim model, these positional changes did not significantly alter the airflow quantity, Q, obtained at the end of the branch, even though the branch itself was relatively long and included bends.

This outcome was interpreted as limited model sensitivity to a small positional shift under otherwise unchanged branch conditions. In the tested cases, the total branch resistance, duct length, leakage condition, and fan duty remained essentially the same, so moving the fan by a short distance near the branch entrance produced little change in the calculated delivered quantity. The result was therefore not treated as evidence that auxiliary-fan location is unimportant in practice.

For this reason, auxiliary-fan placement was treated as both a model-geometry choice and a practical installation constraint. The Rodoretto survey report prepared by Howden states that auxiliary fans should generally be installed parallel to the airflow and in the centre of the airway where possible, and that obstructions close to the inlet create additional and unnecessary pressure losses [2]. This is consistent with broader guidance. ASHRAE describes a blowing auxiliary fan as commonly installed in a fresh-air base at the start of the drift [19], while Morla et al. showed that recirculation control depends on both setback distance and available intake quantity, with effective setbacks of about 5 m for a smaller fan and about 10 m for a larger fan where intake quantity was sufficiently

greater than fan quantity [20]. AMCA guidance similarly emphasizes that non-uniform inlet conditions, nearby elbows, and abrupt geometry changes can reduce fan performance [21].

The practical guidance adopted for the updated branch layout was therefore to place auxiliary fans slightly inside the new branch rather than directly at the branch intersection. A setback of approximately 5–10 m from the connection with the main tunnel was considered appropriate, with about 10 m preferable where space and operational constraints allow. The fan should be centred in the airway, aligned parallel to the airflow, and connected to the duct system with inlet and outlet conditions kept as straight and unobstructed as possible. If the company-requested position is retained, it should be understood as geometrically compatible with the tested layout, while the setback recommendation represents better engineering practice where site constraints permit it.

4.5 Field Survey Design for the Auxiliary System

4.5.1 Reason for a dedicated auxiliary survey

A measurement campaign was designed and conducted on 30 March 2026 to quantify how much air each auxiliary fan system actually draws and how much of that air is delivered to the downstream branches in the South, South Extension, North, and North Extension areas. These data were used to estimate leakage, identify local system effects, and complete the calibration of the full ventilation network [16, 18, 17, 22].

4.5.2 Prepared survey criteria

A formal survey protocol was established before the site visit using the applicable regulations, the Howden report, auxiliary-ventilation design guidance from the literature, and the thesis calibration requirements (see Tables 4.6 and 4.7) [2, 16, 17]. The protocol defined the measurement locations, the variables to be recorded, and the intended role of each observation in the later calibration workflow. Its methodological purpose was to ensure that the field data could be translated directly into airflow calculations, leakage interpretation, duty-point assessment, and model inputs without ambiguity.

The prepared survey sheet also included the identifiers and repeatability descriptors required for later processing, including date, time, station, repetition number, instrument reading, mean velocity, standard deviation, coefficient of variation, and airflow. During execution, some raw-entry fields were not needed because the survey instrument provides the time-averaged velocity directly over the selected interval. The survey structure nevertheless remained valid, since it preserved a consistent basis for repeatable measurement and later processing of the dataset.

Survey item	Location	Purpose	Calibration use
Auxiliary fan inlet velocity	At each auxiliary fan inlet	Determine actual inlet airflow and infer real operating behaviour	Check fan-side quantity and duty-point plausibility
Outlet or branch velocity	At each outlet branch supplied by the measured fan	Determine delivered airflow to the active area	Compare delivered versus inlet quantity and estimate losses
Duct diameter	At the measured duct sections	Calculate cross-sectional area	Convert velocity into volumetric flow
Repeatability check	Three repetitions per station	Ensure measurement stability	Assign confidence to a point for calibration interpretation
Photographic documentation	Fans, ducts, couplings, bends, tears, outlet conditions	Record physical causes of leakage or system effect	Support the choice of leakage and resistance representation

Table 4.6: Prepared survey criteria used to structure the auxiliary-ventilation visit

Prepared field rule	Reason for inclusion in the methodology
Three repetitions per station	Enables calculation of the coefficient of variation and assignment of a confidence class to each point
One-minute measurement duration	Gives the instrument enough time to return a stable mean velocity while remaining practical underground
Anemometer motion kept slow and controlled	Reduces operator-induced disturbance and improves repeatability
Operator positioned outside the main jet where possible	Avoids disturbing the measured flow with the body of the surveyor
Measurement taken close to the fan inlet or duct mouth, not far away in the drift	Captures the actual delivered or drawn flow instead of a dispersed downstream field
Photographic documentation at every measured system	Preserves evidence for leakage, obstruction, or installation defects that help explain mismatches

Table 4.7: Practical survey rules adopted for the auxiliary-ventilation visit

4.5.3 Executed field procedure

The executed survey covered the four auxiliary-fan systems and their accessible outlet branches in the South, South Extension, North, and North Extension sectors. Two outlet branches were inaccessible during the survey. At each selected fan inlet and duct outlet, the probe was moved across the opening according to the sampling pattern illustrated in Figure 4.1 to obtain a representative cross-sectional mean velocity. The procedure was repeated three times, with each measurement lasting one minute, and the mean value displayed by the Testo 425 was recorded for each repetition. The diameter of the duct was also recorded so that the cross-sectional area could be calculated. Photographs were taken of the fans, ducts, outlet conditions, and visible defects such as tears or poor couplings.

Figure 4.1: Sampling pattern for auxiliary-fan inlet and duct-outlet velocity measurements

The practical reason for measuring both inlet and outlet conditions is straightforward. If only the outlet is measured, the delivered flow can be estimated but the loss mechanism remains ambiguous. If only the inlet is measured, the fan-side performance can be esti-

mated but the actual delivery to the face or branch remains unknown. Measuring both locations makes it possible to distinguish between fan-side mismatch, duct resistance, and leakage [16, 18, 17].

4.5.4 Processing of the measured velocities

For each circular duct section, the area is

$$A = \frac{\pi D^2}{4} \tag{4.25}$$

where D is the measured diameter. For each repetition i, the measured airflow is

$$Q_i = v_i A \tag{4.26}$$

where v_i is the mean velocity reported by the instrument over the one-minute interval. The accepted mean velocity and accepted mean airflow are then

$$\bar{v} = \frac{v_1 + v_2 + v_3}{3} \tag{4.27}$$

$$\bar{Q} = \bar{v} A \tag{4.28}$$

The repeatability statistics are

$$\sigma_v = \sqrt{\frac{\sum_{i=1}^{3} (v_i - \bar{v})^2}{3 - 1}} \tag{4.29}$$

$$CV = \frac{\sigma_v}{\bar{v}} \times 100 \tag{4.30}$$

In the present thesis, the coefficient of variation (CV) is used as a descriptor of field stability rather than as a strict rejection rule. The auxiliary outlets were frequently deformed, locally turbulent, leaking, or not fully accessible under ideal traverse conditions, and the campaign could not be repeated systematically. For that reason, a single threshold such as $CV < 5\%$ would be too restrictive as a hard calibration gate. The more defensible approach is to classify each point by confidence and then use that confidence in the interpretation of the calibration. The CV confidence classes adopted for this interpretation are summarized in Table 4.8.

No point is disregarded solely because of its coefficient of variation. Instead, the confidence class determines how strongly that point influences the calibration and whether a sensitivity case is needed for interpretation.

The prepared survey notes also contained practical interpretation rules for diagnosing the auxiliary system. A very low v at the fan inlet may indicate that the fan is work-

CV range	Interpretation	Methodological use
0–5%	Excellent repeatability	Strong direct calibration target
5–10%	Good field repeatability	Use normally as a direct calibration target
10–15%	Usable with caution	Retain, but avoid allowing the point to dominate parameter tuning
$> 15\%$	Weak repeatability	Treat as low-confidence supporting evidence or as a sensitivity-check point

Table 4.8: CV confidence classes for auxiliary-measurement repeatability

ing against excessive resistance or is affected by strong inlet system effect [21, 2]. For the duct sizes relevant to the mine, unusually low inlet velocities were treated at this stage only as preliminary warning signs rather than as direct proof of severe resistance or obstruction, because other causes, including section mismatch, disturbed flow, measurement limitations, and modelling inconsistencies, still had to be examined in the later diagnostic stages. At the outlet side, a reading below the practical threshold of approximately 0.08 m/s is treated as effectively dead or near-null delivery for field interpretation. This threshold is used as a practical survey criterion rather than as a replacement for the formal regulatory v limits in the whole network.

4.6 Calibration of the Auxiliary Network in Ventsim

The 30 March 2026 measurements are sufficient to calibrate fan-side flow quantity, delivered-flow behaviour at accessible outlets, branch-level delivery efficiency, local leakage or loss representation, and duty-point plausibility. They are not sufficient to uniquely recalibrate the real fan curves, because fan pressure was not measured in the field. The methodology therefore adopts the existing manufacturer fan curves as the starting representation and calibrates the connected duct and network parameters around them. However, before those fan definitions can be trusted as calibration anchors, the local topology on which the auxiliary fan acts must also be verified. Otherwise, a fan curve error and a local topology error can produce similar flow mismatches and become difficult to distinguish.

4.6.1 Calibration boundary and comparison dataset

The first auxiliary-calibration loop is carried out on the present-day mine only. Short-term development branches are excluded even if they have already been drafted in the scenario model. This is a methodological choice: the present-day network must reproduce

the 30 March 2026 measurements before the more provisional geometry of future branches is allowed to influence the simulated resistance distribution.

For each measured station, a comparison dataset is constructed containing the station identity, measured mean v, measured area or diameter, measured airflow, confidence class from the coefficient of variation, matching Ventsim unique number, simulated baseline airflow, simulated post-calibration airflow, and the corresponding error. The primary comparison variable in the first calibration loop is Q rather than v. This choice is methodological rather than absolute. The calibration problem is centered on how much air the fan section, duct section, or outlet branch is actually carrying or delivering, and Q is the variable that links the field measurements most directly to ventilation duty and branch mass balance [9]. By contrast, v is strongly affected by the local cross-sectional area and by whether the field measurement and Ventsim output refer to the exact same physical location and section geometry. A section-definition mismatch can therefore inflate the apparent velocity error even when the underlying flow mismatch is smaller. For this reason, v is treated first as a diagnostic indicator of section consistency and flow-profile representativeness, whereas direct velocity matching is interpreted only after the comparison geometry has been checked and corrected where necessary. Although Q is also affected by errors in the measured cross-sectional area, it remains the more defensible primary variable for comparing measured and simulated ventilation behaviour in this workflow.

After processing the field measurements and extracting the baseline model outputs, a structured measurement-comparison workbook was created in Microsoft Excel. The initial version compared each measurement station with the baseline Ventsim model, with short-term developments excluded, to quantify the mismatch before any diagnostic or calibration adjustments were applied. The same station-by-station structure was subsequently used throughout the calibration process. The structure and purpose of the initial workbook are summarized in Table 4.9.

The Ventsim unique number served as the stable identifier linking each field station to its corresponding model branch throughout subsequent model revisions. Repeatability indicators, station-specific notes, and model-derived duty pressures were maintained in the same record, providing traceability between the quantitative results and their engineering interpretation.

The role of each branch in the calibration workflow is summarized in Table 4.10. This distinction is important because not all measured points have the same interpretation value. Direct outlet measurements can support leakage or restriction calibration, whereas a return-air station acts primarily as a system-level mass-balance check.

The spatial locations of these measurement stations are shown in Figure 4.2; the numbered labels correspond to the station numbers used throughout the measurement-processing and calibration tables.

The station-level entries from the initial baseline comparison are reproduced in Ap-

Table 4.9: First-version measurement-comparison workbook used before auxiliary-model correction

Workbook section	**Recorded fields**	**Role in calibration workflow**
Station identity and model matching	Station No.; Station Name; Branch/System; Ventsim Unique No.; Point Type; Repeats Used	Match each field station to the correct baseline model branch and classify the point as inlet, outlet, or return check
Field geometry and repeatability	Diameter (mm); Area (m^2); v_1; v_2; v_3; Mean v; Sigma Population; CV Population; CV Confidence Band; Data Quality	Carry the processed measurement data and preserve the confidence level of each station
Measured quantity and notes	Measured Q (m^3/s); Field Note	Retain the derived field airflow and the station-specific caveats needed for later interpretation
Baseline comparison fields	Baseline Sim.* v; Baseline v Error; Baseline Sim. Q; Baseline Q Error; Baseline Duty FTP** (Pa) – Model Derived	Quantify the initial mismatch between the measured network and the uncorrected present-day baseline model
Reserved post-calibration fields	Calibrated Sim. v; Calibrated v Error; Calibrated Sim. Q; Calibrated Q Error; Calibrated Duty FTP (Pa) – Model Derived; Fan Duty / Curve Note; Calibration Action / Parameter Changed; Confidence / Comments	Preserve the same workbook structure for the later diagnosis and correction stages without rebuilding the comparison file
Supplementary section-diagnostic block	Station No.; Model Implied Area; Area error (%); Meaning	Flag cases where disagreement between v and Q may reflect section mismatch or inconsistent geometric representation rather than hydraulic loss alone

* Sim. = simulated value extracted from the Ventsim model.
** FTP = fan total pressure.

Branch	**Fan-side station**	**Downstream station(s)**	**Methodological role**
XS	Station 1	Stations 2–5	Direct inlet-to-outlet comparison, with a sensitivity case because one inlet replicate was taken by a different operator
Sud[1]	Station 6	Stations 7–8	Direct inlet-to-outlet comparison, with Station 8 treated as low-confidence support if its repeatability remains weak
Nord	Station 9	Stations 10–13	Direct inlet-to-outlet comparison, with Station 11 discarded as the measured outlet velocity was below the near-null threshold ($v < 0.08$ m/s)
XN	Station 14	Station 15	Fan-side anchor plus return-air system check; Station 15 is not treated as the outlet of a single duct

[1] In site fan labels, *Sud* denotes South and *Nord* denotes North.

Table 4.10: Measured auxiliary branches and their calibration roles

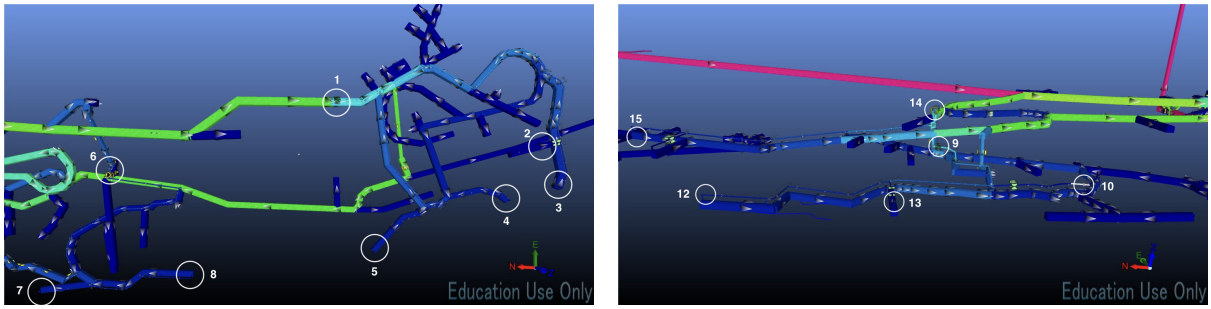

(a) South and South Extension systems (b) North and North Extension systems

Figure 4.2: Auxiliary-ventilation measurement stations; numbered labels correspond to the calibration and results tables

pendix A.1, Tables A.1–A.3. They are placed in the appendix to preserve the audit trail without interrupting the calibration methodology. Fields not applicable at this initial stage are represented by em dashes.

The baseline error indicators in the first version of the workbook were defined as signed percentage errors,

$$e_{v,0} = \frac{v_{\mathrm{sim},0} - \bar{v}}{\bar{v}} \times 100 \tag{4.31}$$

$$e_{Q,0} = \frac{Q_{\mathrm{sim},0} - \bar{Q}}{\bar{Q}} \times 100 \tag{4.32}$$

where the subscript 0 denotes the uncorrected present-day baseline model. A positive value therefore indicates that the baseline model overpredicts the measured quantity, while a negative value indicates underprediction. Because the first workbook was intended as a pre-diagnosis screen, signed errors were preferred over absolute errors so that the direction of mismatch remained visible from the outset.

This first revealed an important limitation of using raw percentage error alone at very weak-flow points. When the measured denominator was smaller than 1, the percentage value became numerically disproportionate even when the absolute flow difference remained in the range of only a few cubic metres per second. For example, Station 2 compared 2.40 m^3/s simulated against 0.303 m^3/s measured, giving an absolute overprediction of 2.097 m^3/s but a raw quantity error of 692.1%. Station 13 compared 3.80 m^3/s against 0.301 m^3/s, giving +3.499 m^3/s and 1162.5%. Station 10, with 6.90 m^3/s simulated against 0.672 m^3/s measured, showed that the same denominator effect could coexist with a genuinely severe physical mismatch. This behaviour is consistent with the known instability of percentage-based error measures when observed values approach zero [28]. The methodological consequence was that raw percentage errors were retained as an audit trail, but weak-flow points were interpreted together with the signed absolute quantity difference, the station classification, and the field note before they were allowed to guide later diagnosis.

For measured quantities below 1 m^3/s, the final workbook therefore introduced a supplementary floored percentage error,

$$e_{Q,\mathrm{floor}} = \frac{Q_{\mathrm{sim}} - Q_{\mathrm{meas}}}{\max(Q_{\mathrm{meas}}, Q_{\mathrm{floor}})} \times 100, \qquad Q_{\mathrm{floor}} = 1 \ m^3/s. \tag{4.33}$$

The floor was applied only when $0 < Q_{\mathrm{meas}} < 1 \ m^3/s$. It changes only the denominator used in this supplementary comparison and does not alter the measured Q, the calibration target, or the retained raw percentage error. Measurements within this range remained eligible for calibration when their CV was within the acceptable band. Station 11 was discarded from the calculations because its measured outlet velocity was below the near-null threshold ($v < 0.08$ m/s).

The initial screening identified possible effective-section mismatches, which motivated the formal geometry-consistency audit described in the following stage. It also documented that Station 15 was a return-tunnel check rather than the outlet of a single duct, so the difference between Fan XN and Station 15 was not interpreted as pure duct leakage.

4.6.2 Stage 1: geometry-consistency correction of comparison sections

Before any fan-side or loss-related diagnosis was accepted, a dedicated geometry-consistency audit was performed using two sequential states of the Excel measurement-comparison workbook. The initial audit used the existing comparison sections, whereas the corrected audit was conducted after the section definitions had been revised. This stage was introduced because the first workbook had already shown that several of the apparent velocity mismatches were dominated by inconsistent comparison sections rather than by aerodynamic behaviour alone. The purpose of the audit was therefore to make the model sections used for comparison geometrically consistent with the duct or airway sections observed underground, so that later velocity and quantity mismatches would be interpreted on a like-for-like basis.

In this dedicated audit, the field section was treated as the reference. The model-implied area was obtained from

$$A_{\mathrm{impl}} = \frac{Q_{\mathrm{sim}}}{v_{\mathrm{sim}}} \tag{4.34}$$

and the corresponding model-implied diameter for circular sections was obtained from

$$D_{\mathrm{impl}} = \sqrt{\frac{4A_{\mathrm{impl}}}{\pi}} \tag{4.35}$$

The geometry-consistency errors were then evaluated as

$$e_A^* = \frac{A_{\text{impl}} - A_{\text{field}}}{A_{\text{field}}} \times 100 \tag{4.36}$$

$$e_D^* = \frac{D_{\text{impl}} - D_{\text{field}}}{D_{\text{field}}} \times 100 \tag{4.37}$$

for the direct duct and fan sections. The classification bands applied to the absolute magnitudes $|e_A^*|$ and $|e_D^*|$ are summarized in Tables 4.11 and 4.12. These thresholds were used as thesis workflow rules for deciding whether a station could already support direct v and Q comparison or whether its geometry or selected comparison section first had to be corrected.

Band (%)	**Interpretation**	**Workflow meaning**
0 to 5	Excellent	Use v and Q directly
5 to 10	Acceptable	Use, but note minor area mismatch
10 to 20	Caution	Check section or diameter; treat velocity mismatch more cautiously
> 20	Not acceptable for v KPI	Correct geometry or selected comparison section before using velocity mismatch diagnostically

Table 4.11: Classification bands used in Stage 1 to interpret the magnitude of area-consistency error, $|e_A^*|$

Band (%)	**Interpretation**	**Workflow meaning**
0 to 2.5	Excellent	Use v and Q directly
2.5 to 5	Acceptable	Use, but note minor diameter mismatch
5 to 10	Caution	Re-check selected Ventsim section, duct size, fan diameter, or airway geometry
> 10	Not acceptable for v KPI	Correct geometry or selected comparison section before using velocity mismatch diagnostically

Table 4.12: Classification bands used in Stage 1 to interpret the magnitude of diameter-consistency error, $|e_D^*|$

The audit showed that some first-pass inlet diameter entries and selected model comparison sections were not yet like-for-like. The selected Ventsim section, represented duct size, and comparison-diameter assignment were therefore revised before hydraulic calibration proceeded. The complete station-by-station before-and-after results are reported in Tables 5.4 and 5.5. This was a prerequisite consistency correction, not a hydraulic calibration of the auxiliary network, and ensured that later error diagnosis reflected ventilation behaviour rather than a geometry mismatch in the comparison itself.

4.6.3 Stage 2: topology verification and auxiliary fan definition setup

After the comparison sections had been made geometrically consistent, the next methodological risk was that the remaining mismatch could still be produced by an incorrect local model topology or by an incorrect fan definition rather than by the real hydraulic behaviour of the auxiliary system. For that reason, a dedicated verification stage was carried out before any fan-side or leakage calibration was accepted.

The first part of this stage was a topology sanity check. The local intake and discharge representation of each auxiliary fan was inspected to confirm that the fan acted on the intended auxiliary branch only, that no duplicate fan support or hidden fixed-flow assistance was present, and that the corrected geometry had not introduced a spurious connectivity error. Particular attention was paid to local reversal or topology sensitivity, because a fan placed on the wrong airway element can artificially disturb the main network or create misleading warnings in the software.

The adopted representation retained the main tunnel as the main airway and placed the auxiliary fan on a short side branch representing the fan casing, followed by the actual outlet duct. In simplified form, the accepted topology is

$$\text{main tunnel} \rightarrow \text{short fan casing branch} \rightarrow \text{outlet duct} \tag{4.38}$$

rather than placing the fan directly on the main tunnel airway. This arrangement follows the Ventsim modelling principle that the fan should act on its intended branch and also matches the physical installation, in which the auxiliary fan draws from the mine heading and delivers into flexible ducting. It therefore prevents the fan from behaving numerically as an inline fan acting on the whole tunnel flow [29, 2].

Once the local topology had been verified, new auxiliary fan definitions were added in Ventsim as clean entries rather than overwriting the inherited ones. This allowed the corrected fan curves to be compared against the previous model state and reduced the risk of losing the earlier database entries during calibration. The extension fans XS and XN were assigned to the Zetal VH1004.4, 2 x 45 kW configuration, while the North and South area fans were assigned to the Zetal VH1004.4, 2 x 30 kW configuration. For ducted auxiliary use, the entered curves were treated on a static-pressure basis. Where the manufacturer information was provided as total pressure, the curve was converted according to

$$FSP = FTP - \frac{1}{2}\rho\left(\frac{Q}{A}\right)^2 \tag{4.39}$$

where FSP is the fan static pressure, FTP is the fan total pressure, ρ is the air density, and Q/A is the mean duct velocity calculated from airflow and cross-sectional

area. This conversion subtracts the velocity-pressure component from the total-pressure curve, so that the software representation remained consistent with ducted-fan practice [9, 29, 30, 31]. Efficiency curves were also entered for duty-point and power reporting.

This stage also included checking whether the observed reversal or instability was caused by the fan curve alone or by the interaction between fan curve and local topology. Controlled tests with previous and corrected local geometries showed that the response depended on the combination of intake topology, local resistance distribution, and selected fan characteristic rather than on the fan curve in isolation. This was an important checkpoint that justified moving forward with fan-side calibration only after the local topological representation had been shown to be defensible.

4.6.4 Stage 3: baseline run and fan-side diagnosis

After the geometry-consistency and topology-verification stages had been completed, the next diagnostic step was to run the model without further auxiliary recalibration and record, for each auxiliary system, the simulated fan quantity, the simulated outlet or return quantity, the model duty point, and any warning state such as stalled, low-pressure, negated, reversed, or fixed-flow conflict. This baseline run established the pre-calibration reference against which all later changes were judged.

If the model did not reproduce the measured fan-inlet quantity, the first response was not to tune leakage. Instead, the methodology first audited the fan-side representation itself. The required checks included the identity and branch assignment of the fan object, the absence of duplicate fan support or hidden fixed-flow conditions, the selected 2 x 30 kW or 2 x 45 kW fan family, the pressure basis and stage representation of the entered curve, the fan direction and operating setting where relevant, and the possibility of strong local inlet system effect caused by the installation geometry.

This sequence was necessary because pressure was not measured during the field campaign. The measurements constrained only the airflow coordinate of the duty point; the corresponding pressure coordinate had to be read from the solved Ventsim model and was therefore treated as model-derived rather than field-measured. Consequently, the methodology did not permit arbitrary reshaping of the fan curve simply to force agreement with one measured flow. Fan-side modifications were accepted only when supported by manufacturer data or by direct evidence that the installed fan model, power version, operating setting, or branch assignment had been represented incorrectly.

4.6.5 Stage 4: local installed-loss calibration by shock-loss representation

After the fan definitions and local topology had been corrected, any remaining fan-side mismatch was no longer attributed automatically to the fan curve itself. The next methodological question was whether the discrepancy could be explained by local installed-system resistance observed during the underground visit or documented in the inherited Howden survey. In practical terms, this meant representing near-wall inlet position, corner placement, asymmetric approach flow, upstream 90° turns in the connected inlet duct, or immediate discharge bends on short local airway segments rather than altering the fan database again [2, 21].

In Ventsim, these local effects were represented with shock-loss factors applied to the short inlet/casing segment or to immediate bend segments. The associated local pressure loss is expressed as

$$\Delta p_{\text{shock}} = X \frac{\rho v^2}{2} \tag{4.40}$$

where X is the dimensionless shock-loss factor. The Ventsim manual provides a useful practical anchor for interpreting this term: $X = 1$ is comparable to a sharp 90° duct corner. This reference was used to judge whether a tested value remained physically interpretable as an installation defect rather than becoming a hidden numerical forcing term [29].

Shock losses were introduced only where a physical defect or sharp turns in the ducts had been observed or reported. The methodological rule was to use the smallest physically defensible correction that moved the duty point in the correct direction, kept the fan on a plausible part of its curve, and did not materially damage the main-network calibration. For that reason, exact matching of the measured fan quantity was not used as the sole criterion at this stage. The inlet measurements were collected in disturbed flow fields, so they may not perfectly represent the full area-average inlet flow, and the downstream duct leakage and delivered-flow losses had not yet been calibrated.

Each candidate installed-loss scenario was therefore evaluated in two gates. The first gate was local fan performance, assessed primarily by absolute quantity error and supported by raw and symmetric percentage descriptors. The second gate was the already calibrated main network, checked using exported Ventsim branch-result tables for airflow reversal, primary-fan changes, and non-local disturbance of high-flow main airways. Once an accepted local-loss package had been identified, it was fixed and carried forward as part of the branch setup for the subsequent downstream calibration stage.

4.6.6 Stage 5: delivered-flow calibration and representation of branch losses

Once a branch has a fan-side quantity that is physically plausible and its local installed losses have been represented, the next calibration stage focuses on the delivered-flow pattern downstream of the fan. The first diagnostic quantities are the apparent delivery efficiency

$$\eta_{\text{delivery}} = \frac{Q_{\text{out}}}{Q_{\text{in}}} \tag{4.41}$$

and the apparent unaccounted fraction

$$\lambda_{\text{app}} = \frac{Q_{\text{in}} - Q_{\text{out}}}{Q_{\text{in}}} \tag{4.42}$$

where Q_{in} is the measured fan-inlet airflow and Q_{out} is the measured delivered outlet flow or the relevant sum of outlet flows. This quantity difference is not interpreted automatically as pure leakage. Depending on the branch, it can also include local restriction, unmeasured discharge points, recirculation, return-air redistribution, or station mismatch. It nevertheless provides the first target for deciding whether the simulated branch behaves as a nearly sealed delivery system or as a strongly lossy one.

If the model matches fan-side flow but overpredicts outlet flow, the downstream system losses are underrepresented. In that case, the branch is calibrated through physically interpretable parameters: distributed leakage for generally worn or holed ducting, localized leakage for dominant tears or poor couplings, increased friction or resistance for rough or deformed duct, and local shock losses or short restriction segments for bends, necked outlets, abrupt geometry changes, or poor fan installation [16, 18, 17, 21]. The site photographs are used as supporting evidence when deciding which representation is most defensible for each branch.

Measured outlet flows may also be imposed temporarily as fixed flows in order to reveal the order of magnitude of the pressure required to achieve them, but fixed-flow conditions are used only diagnostically. They are removed from the final calibrated model, which must reproduce the observed branch behaviour through physical parameters rather than through permanent numerical forcing. The branch-level before-and-after delivery comparison resulting from this stage is reported in Table 5.11, while the final station-level comparison and calibrated leakage-porosity schedule are retained in Appendix A.2.

4.6.7 Branch-specific calibration logic

Although the overall sequence is common to all branches, the four auxiliary systems are not interpreted in exactly the same way.

- **XS**. The inlet measurement is usable but should be accompanied by a sensitivity check because one replicate was taken by a different operator. The preferred sequence is fan-side plausibility first, then local inlet-system-effect correction where justified, and only after that downstream leakage or local loss representation until Stations 2–5 reproduce the measured delivery pattern.

- **Sud**. If the inlet quantity is still too high after the fan-definition correction, the branch must first be treated as an immediate installed-system problem, for example a near-wall inlet or local bend effect, before leakage is tuned. Station 8 should not dominate the calibration if its repeatability remains weak.

- **Nord**. The inlet quantity acts as the primary anchor, but the installation geometry may require a distributed local-loss representation across an upstream turn, inlet disturbance, and downstream bend before the outlet pattern is interpreted as leakage alone.

- **XN**. The downstream measurement is a return-air check rather than the outlet of one duct. The branch is therefore not calibrated as a simple fan-to-outlet leakage path. Instead, the fan-side behaviour and any top-corner or close-wall inlet-system effect are calibrated first and the return station is then used to verify whether the extension-level mass-balance behaviour is reasonable.

4.6.8 Acceptance criteria and methodological limits

The previous Howden calibration provides the practical benchmark for judging model credibility, because the primary model was reportedly brought to a condition in which measured deviations did not exceed about 12% and the total intake-versus-exhaust mass-flow difference was 3.7% [2]. The auxiliary calibration adopts the same spirit, but not an unrealistically strict promise of identical certainty. The following criteria govern acceptance of a calibration stage:

- the fan-side quantity should be physically plausible before outlet losses are tuned;

- accepted local installed-loss corrections should remain physically interpretable and should not create unexplained reversal or excessive main-network disturbance;

- no permanent artificial fixed flows or fixed pressures should remain in the final calibrated model;

- any remaining stalled, low-pressure, negated, or reversed fan warning should be either removed by a physically justified correction or explicitly explained by the calibrated physical state;

- branch-level delivery behaviour should move toward the measured pattern without producing implausible main-network disturbance;
- every major parameter change should have a physical explanation grounded in observed duct or fan condition.

The principal methodological limit is the absence of field pressure measurements. Without measured pressure across the auxiliary fans or along the ducts, the auxiliary calibration cannot claim a unique solution for fan curve, resistance, and leakage simultaneously. The thesis therefore treats the result as the most defensible calibrated scenario consistent with measured airflow, site observations, and the inherited Howden baseline, rather than as a uniquely proven reconstruction of every auxiliary parameter.

4.7 Scenario Construction and Offer Evaluation

After the present-day auxiliary calibration is completed, the calibrated baseline is used as the reference state for scenario construction. The intention is to test the commercial offers under the operating conditions that matter for the real decision while keeping a clear distinction between the validated current network and the more provisional near-term developments.

The scenario set contains two mine states.

- **Pre-2028 layout**. This represents the updated present-day geometry of the existing mine together with the completed auxiliary calibration and acts as the technical baseline for model credibility.
- **Post-2028 layout**. This starts from the calibrated pre-2028 layout and adds the short-term developments and corrections that are sufficiently mature to be modelled for scenario analysis.

At the time of the thesis, the post-2028 development geometry represented the latest planning information made available for assessment rather than a final construction-level development map. The post-2028 model is therefore treated as scenario geometry: suitable for comparing the offered fan arrangements and testing the expected short-term ventilation state, but intended to be refined by the mine when exact coordinates, gradients, elevations, cross-sections, connection points, and auxiliary fan and duct layouts are finalized.

This sequence is deliberate. The auxiliary calibration is not carried out directly on a mixed present-and-future model, because provisional future geometry could mask errors that belong to the current system. The short-term branches are therefore reintroduced

only after the present-day baseline has been brought to a defensible agreement with the field measurements.

Within those mine states, each commercial offer is tested with its proposed arrangement. Each commercial offer was evaluated as a complete proposed installation. The fan type, number of units, and specified parallel or series configuration were therefore retained as defining attributes of each option during the technical comparison.

The methodology also keeps a conservative envelope in mind for short-term uncertainty. A 15% increase in friction factors in future-stage simulations is considered to represent deterioration, roughness uncertainty, and obstructions as a stress mechanism. Where needed, uncertainty is therefore represented through conservative increases in effective resistance rather than through arbitrary geometry changes. This allows the scenario analysis to remain physically interpretable while still acknowledging that the mine layout, duct condition, and local losses are not perfectly static.

4.8 Economic Assessment Procedure

The economic part of the methodology uses four main indicators.

- **CAPEX**. This represents the one-time implementation cost of the option.
- **OPEX**. This represents the recurring annual operating cost, with electricity as the dominant term, which is one of the dominant operating-cost drivers in mine ventilation systems.
- **Payback or discounted payback**. This shows how quickly the additional investment is recovered through savings.
- **NPV**. This aggregates the cash-flow effect over the chosen horizon using a discount rate.

These indicators were selected because together they capture implementation effort, long-term operating burden, and the time value of the savings created by a replacement solution. Maintenance and reliability are also part of the assessment, but in methodological terms they enter through the CAPEX or OPEX structure rather than acting as a completely separate optimisation axis.

The minimum information required for a complete economic comparison includes the fan package price, installation scope, electrical and civil works, control integration, spare parts, internal labour, decommissioning of the old installation, contingency, operating hours, electricity tariff, maintenance expectations, and, where available, financial assumptions such as discount rate and time horizon. This data structure, summarized in

Input category	Typical items required from the company or suppliers
Equipment supply	fan package, motor, VSD, dampers, silencers, sensors, critical spare parts
Installation and construction	lifting, alignment, duct connection works, supports, foundations, plinths, access modifications
Electrical and control works	cables, switchboard or MCC upgrades, transformers, grounding, instrumentation, SCADA integration, commissioning tests
Internal costs	maintenance hours, electrician hours, contractor support, internal rates, engineering or procurement overhead if applicable
Removal and decommissioning	dismantling, transport, disposal, storage, environmental compliance, residual or resale value
Operating data	yearly running hours, electricity tariff, expected maintenance interval, repair assumptions, demand-charge information if relevant
Financial assumptions	contingency, analysis horizon, discount rate, escalation or inflation assumptions if the company uses them

Table 4.13: Economic information structure required for the offer comparison

Table 4.13, is consistent with the way the company itself separates cost components in its planning documents.

The economic comparison is always relative to a baseline. In this thesis, the baseline is the present operating installation represented by the calibrated model. The economic value of a candidate offer therefore comes from the difference between the baseline cost and the option cost, not from the absolute CAPEX value alone. This is why a higher-CAPEX option cannot be rejected automatically. A more expensive option may still be economically preferable if it reduces power demand, maintenance exposure, or the likelihood of further ventilation upgrades.

4.8.1 Implemented discounted-cash-flow procedure

After application of the technical stage gate, annual electricity use for each retained offer is calculated from the modelled electrical input at the selected economic-screening VFD setting. For year y, the energy use and electricity cost are

$$E_y = P_{\mathrm{elec},y} H_y \tag{4.43}$$

$$C_{\mathrm{OPEX},y} = E_y c_e \tag{4.44}$$

where $P_{\text{elec},y}$ is the combined modelled electrical power, H_y is the annual operating time, and c_e is the electricity tariff. Annual saving is then evaluated against the repriced electricity cost of the existing fan installation using the saving expression defined earlier in this chapter.

The implemented calculation uses a 2026–2037 horizon with 12 end-of-year operating cash flows. The pre-2028 fan duty is assigned to 2026 and 2027, and the post-2028 duty is assigned to 2028–2037. CAPEX occurs at time zero. The discount rate is applied annually to the resulting electricity-cost savings.

The discounted payback period is the first point at which cumulative discounted savings recover the initial CAPEX. When recovery occurs within year T, the fractional estimate is

$$\text{DPP} = (T-1) + \frac{C_{\text{CAPEX}} - \sum_{t=1}^{T-1} PV(S_t)}{PV(S_T)} \tag{4.45}$$

where $PV(S_t) = S_t/(1+r)^t$. The present-value life-cycle cost used as a supporting comparison is

$$PV(C_{\text{life}}) = C_{\text{CAPEX}} + \sum_{t=1}^{n} \frac{C_{\text{OPEX},t}}{(1+r)^t} \tag{4.46}$$

The selected reduced-speed duties are used as economic screening points because they satisfy the whole-mine airflow gate in the corresponding model checks. They are not treated as final operational setpoints proving local and regional compliance. Final implementation therefore remains conditional on confirmation of the selected duty after the required auxiliary-network improvement and regional balancing.

The comparison includes the supplied fan-package, VFD-software, and electrical-installation costs and uses electricity as the quantified recurring cost. Maintenance, spare parts, residual value, decommissioning, and auxiliary-network remediation are not assigned numerical values because reliable differentiated costs were not available. Their exclusion is applied consistently to all alternatives and is stated explicitly when interpreting the result.

The resulting economic inputs, annual electricity costs, discounted cash-flow summary, ranking, and sensitivity check are reported in Section 5.6, with the year-by-year discounted cash-flow record provided in Appendix A.4.

4.9 Methodological Boundaries

The methodological boundary of the thesis is defined by the industrial decision it is intended to support. The work evaluates the commercial main-fan replacement offers received for Rodoretto under the current and near-term mine layouts, using the best

model evidence available during the thesis period. It is therefore not a complete redesign of the entire ventilation system, but a staged assessment of whether the offered main-fan arrangements can provide adequate system capacity and whether the retained options are economically justified.

Auxiliary ventilation is therefore not treated as a secondary issue in this methodology. Because the existing model did not contain a field-calibrated representation of the auxiliary network, the field survey, measurement processing, geometry audit, fan-definition correction, local-loss treatment, and downstream branch calibration were used to develop a traceable, flow-consistent auxiliary baseline for the offer assessment. The methodological boundary lies instead at the implementation-design stage. The thesis identifies delivery losses, leakage effects, local restrictions, and remaining distribution constraints, but it does not define or cost the complete set of duct repairs, fan relocations, leakage-reduction measures, or regional control interventions required for construction. Because the auxiliary campaign did not include pressure measurements, the calibrated auxiliary model is also not presented as a unique reconstruction of the real fan curves. It is used as the most defensible calibrated scenario based on measured air quantities, site observations, and the inherited Howden baseline.

Within these boundaries, the methodology is appropriate for the thesis objective. It combines regulation-based KPI definition, traffic-case calculation, field-supported model calibration, model updating, scenario evaluation, staged technical screening, and economic comparison in one decision framework tailored to the Rodoretto main-fan replacement problem.

Chapter 5

Results

This chapter presents the completed sequence of model updating, auxiliary-network measurement and calibration, technical screening of the commercial main-fan offers, and economic comparison of the retained arrangements. The results are reported in the order in which the evidence was developed so that corrections to geometry, comparison sections, fan definitions, topology, and installed losses remain traceable to the final offer assessment.

5.1 Implemented Ventsim model updates

5.1.1 Objective and working approach

The objective of the model-update phase was to implement the developments, branch corrections, duct modifications, and auxiliary-fan additions requested by the mine and to create a revised Ventsim model that can serve as the basis for the next stage of ventilation analysis. After each major group of changes, the simulation was rerun to verify connectivity and identify any new warnings generated by the edits.

The editing strategy followed the logic of a network-based ventilation model. Whenever a requested change affected both geometry and topology, the affected airway or duct section was deleted and redrawn instead of only being reversed or shifted. This approach was adopted because simple movement of an existing airway can leave connected short duct segments in their previous positions, whereas redrawing allows the new geometry to be attached deliberately to the correct nodes and branch points. In addition, where blind headings or stopes were represented, the airway ends were explicitly assigned as closed ends to avoid introducing artificial open connections in the network.

5.1.2 Implemented changes

The completed modifications can be grouped into three categories: correction of existing geometry, addition of new branches and developments, and update of the auxiliary-ventilation layout.

First, airways and duct sections that were incorrectly oriented relative to the requested updated layout were corrected. In locations where the original orientation did not match the intended branch direction, the old tube or airway was removed and recreated with the correct direction and connection points. This was preferred to simple reversal when the geometry itself had to move to the opposite side of a branch or to a different connection node.

Second, new developments were added by branching them from the existing airway network. These additions included straight airways and ramps, as well as more complex branches containing bends. Each new airway was connected in three-dimensional view to ensure that the end nodes were actually snapped to the intended existing airway or junction. Particular care was required in locations where a newly added ramp terminated at a branch from which two additional drifts departed, because in such cases even a small mismatch in node position can lead to disconnected segments or misleading fan warnings.

Third, the auxiliary-ventilation layout was updated in parallel with the new developments. New duct sections were created where required and connected to the revised branches. Additional auxiliary fans were inserted where required, and the branches specified in the update instructions were assigned the same fan configuration as the existing Fan Sud unit.

By the end of this stage, the revised model included the requested corrections to existing geometry, the addition of missing operational branches, and the short-term developments required for the scenario analysis. These updates were based on site observations, underground measurements, company layout information, and follow-up confirmation with the mine engineer. Where no more specific local geometry was available, the new developments were modelled using the mine-indicated dimensions of a 4×4 m gallery and an 800 mm auxiliary duct diameter.

5.1.3 Updated layout and representative geometry revisions

The completed update combined inherited-geometry corrections with the short-term South Intermediate and Far North developments required for the scenario analysis. Figure 5.1 illustrates the correction logic using one inherited network section where an incorrectly oriented airway and an omitted branch were corrected to better match the underground layout.

Additional examples of added development geometry are shown in Figures 5.2 and 5.3. These examples show the Far North upper-level ramp and the South Intermediate ramp-

and-drift additions introduced into the updated model.

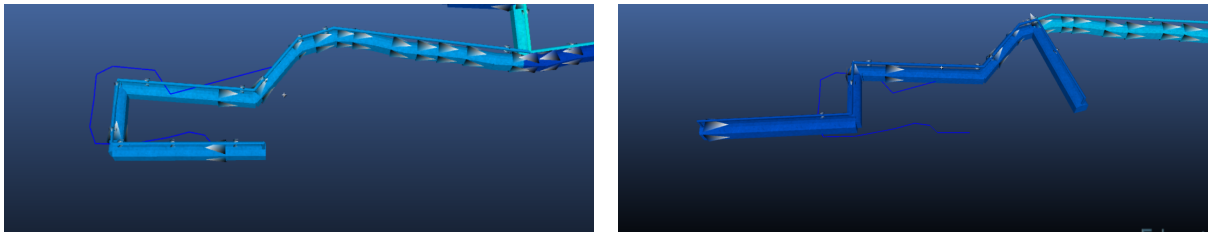

(a) Before correction and addition of the missing airway

(b) After correcting the airway direction and adding the missing airway

Figure 5.1: Representative Rodoretto model geometry revision

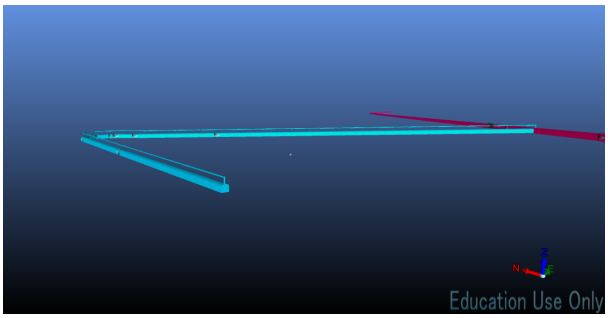

Figure 5.2: Far North upper-level ramp added to the updated Ventsim model.

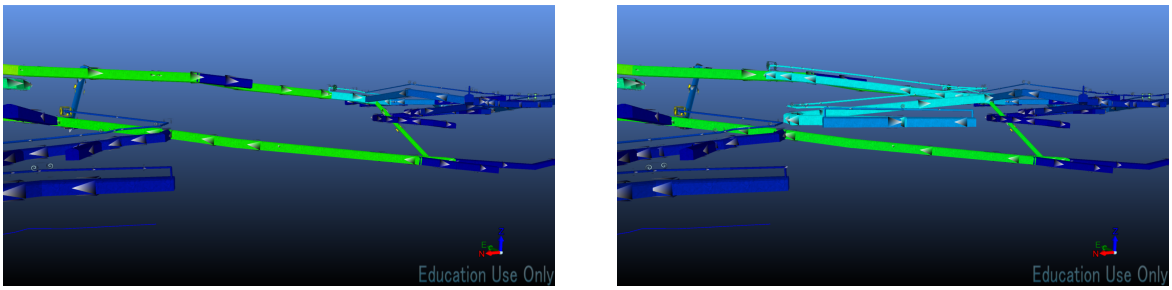

(a) Before adding the South Intermediate ramp and drifts

(b) After adding the South Intermediate ramp and drifts

Figure 5.3: South Intermediate ramp and drift additions in the updated Ventsim model

For the short-term development geometry, the South Intermediate access was represented by adding a ramp with an approximate gradient of 10%, following the mine's indication. The Far North access ramp was extended down to elevation 1020 m following the mine's update request. The resulting ramp geometry remained well below the maximum admissible gradient discussed during the update process, with local values of 1.9% and 3.2% in the final implementation.

5.2 Auxiliary-ventilation measurement campaign

5.2.1 Purpose and relation to the model

A dedicated underground ventilation survey was carried out on 30 March 2026 to obtain the empirical benchmark required for calibration of the auxiliary ventilation network. The primary circuit had already been surveyed and used for model updating in the previous Howden work, but the auxiliary network still contained the greatest uncertainty because actual auxiliary-fan operating behaviour, duct leakage, and local installation effects had not yet been quantified systematically [2]. The purpose of the visit was therefore to test whether the auxiliary-fan duty, duct resistance, and airflow-loss assumptions embedded in the Ventsim model were consistent with the real underground system. In this sense, the measurement campaign provides the field dataset required to convert the overall model from a partially validated design representation into a site-representative baseline for Rodoretto.

5.2.2 Survey coverage and adaptive measurement strategy

The fieldwork focused on the existing auxiliary systems serving the South, South Extension, North, and North Extension areas. Where the branch outlet or duct discharge was active and physically accessible, measurements were taken both at the auxiliary-fan inlet and at the downstream outlet so that the delivered quantity could be compared directly with the quantity drawn by the fan. This paired-measurement logic is essential because a single measurement point cannot distinguish whether poor delivery is caused mainly by fan behaviour, duct resistance, leakage, or a combination of these effects.

In the North Extension, some outlets were inactive or physically inaccessible at the time of the visit. In those cases, an adaptive survey strategy was adopted. The fan inlet was measured directly, while the delivery side was represented by measuring the return airflow in the North Extension main tunnel, which acts as a collection airway for the air distributed within that part of the mine. Although this approach does not provide the same local detail as a direct outlet measurement, it still offers a useful mass-balance check for the corresponding extension and preserves the possibility of calibrating that sector at system level.

5.2.3 Executed measurement procedure

All velocity measurements were taken with the available Testo 425 thermal anemometer, whose timed-averaging function was suitable for the low and locally fluctuating velocities encountered in the auxiliary system.

At each station, three one-minute readings were recorded following the sampling logic

described in Subsection 4.5.3. At fan inlets and accessible duct outlets, the probe was moved slowly across the active flow area so that the recorded value represented the cross-sectional mean velocity rather than a single local jet. Where geometry, outlet deformation, or access conditions prevented a full traverse, the measurement was taken in the most stable accessible part of the duct opening or jet, including slightly inside the duct mouth where this was physically possible and safer. At Station 15, the instrument was positioned to capture the return-air profile representative of the North Extension main-tunnel cross-section.

(a) Station 5

(b) Station 12

Figure 5.4: Representative outlet stations included in the executed auxiliary-ventilation measurement procedure at Station 5 and Station 12.

5.2.4 Observed physical condition of the auxiliary installations

The visit also provided direct evidence of why calibration of the auxiliary system cannot be based on nominal fan data alone. The same issue was observed at the fan installations themselves, where several auxiliary fans were positioned close to the wall or airway corner, or were connected so that the discharge entered the duct through an abrupt bend rather than through a clean straight section. Several outlet sections were not fully circular in operation. Because the actual delivered flow was often small relative to the nominal duct diameter, some duct mouths were partially collapsed or deformed, so the effective discharge area was smaller and less regular than the nominal geometry would suggest. In some locations, ropes or improvised restraints had been tied around the duct to redirect or reduce the outlet flow toward a specific working area, which further distorted the outlet section. Additional local irregularities were observed near certain outlets and duct sections, including holes or damaged portions close to the discharge. These conditions produced highly non-uniform exit jets and made it necessary to position the probe only in the open or aerodynamically stable parts of the outlet. From a modelling perspective,

these observations are important because they point directly to local losses, deformation effects, and leakage mechanisms that an idealized duct representation does not capture automatically.

(a) Fan Sud close-wall position

(b) Fan Nord outlet bend

(c) Fan XN close-wall position

Figure 5.5: Field-observed auxiliary-fan installation constraints affecting local system losses.

(a) Local duct holes

(b) Large duct tear

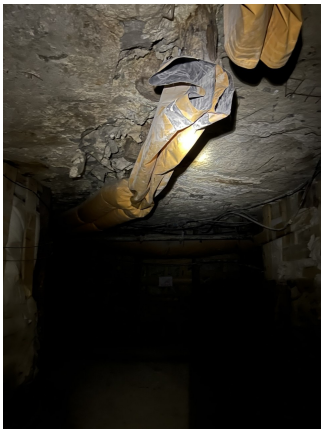

(c) Deformed outlet section

(d) Deformed outlet section

Figure 5.6: Auxiliary-duct defects observed during the field survey.

5.2.5 Immediate outcome of the campaign

The campaign produced the processed field dataset used for auxiliary-network calibration. Each station was reduced to mean velocity, airflow quantity, standard deviation, and coefficient of variation, with repeatability used to assign confidence to each measurement point. The first-version measurement-comparison record derived from the campaign is reproduced in Appendix A.1, Tables A.1–A.3. The survey did not constitute a calibrated model by itself. Instead, it provided the measured benchmark against which the auxiliary network could be corrected.

The paired fan-inlet and outlet measurements confirmed that fan-side behaviour and downstream delivery losses had to be interpreted separately. Together with the observed installation defects, duct leakage, and outlet deformation, this established the calibration sequence followed in the next sections, beginning with fan-definition and local installed-loss correction and continuing with branch-level treatment of leakage, restriction, and effective resistance.

5.3 Initial baseline comparison before auxiliary calibration

After the measurement campaign, the processed field data and the corresponding present-day baseline Ventsim outputs were organized in a station-by-station workbook for direct comparison. The short-term development branches were still excluded at this stage, so the comparison represented only the existing auxiliary network. This first pass was used to quantify the initial mismatch between measured and simulated values before any diagnostic correction, fan-definition adjustment, leakage treatment, or local-loss calibration was applied.

The first baseline pass showed that the uncorrected auxiliary model generally overpredicted both v and Q relative to the field measurements. Because the workbook used signed percentage error, the predominance of positive values means that the baseline simulated values were mostly higher than the corresponding measured values. The mismatch was especially severe at several outlet stations, whereas the fan inlets, although still substantially mismatched, provided the most useful anchors for the next stages of calibration.

The first comparison also showed that v and Q did not always tell the same story. The clearest example was Fan Sud. In the first workbook, the baseline quantity error at Station 6 was only 8.6%, but the corresponding velocity error was 159.1%. The supplementary model-implied area block indicated that the model was behaving like an effective section of approximately 777 mm rather than the 1200 mm diameter recorded in the field. This result was important methodologically because it confirmed that Q had to remain the primary comparison variable, while v and the area-consistency diagnostic were needed to identify section mismatch or geometric representation problems rather than being interpreted in isolation.

Representative examples from the first baseline comparison are listed in Table 5.1. The table is not intended to provide a final diagnosis yet. Its role is to show the spread of mismatch that the first workbook revealed before any fan-curve correction, shock-loss adjustment, leakage tuning, or other calibration adjustment was carried out.

Two further observations from the first template were important for the continuation of the work. First, the workbook itself showed that not every abnormally high percentage error had the same meaning. At weak-flow points, the denominator of the percentage formula was so small that the percentage value became numerically extreme even when the absolute quantity difference was much smaller in engineering terms. The first examples are shown in Table 5.2. Stations 2 and 13 were especially important because they combined measured quantities of only 0.303 and 0.301 m^3/s with baseline simulations of 2.40 and 3.80 m^3/s, producing raw percentage errors of 692.1% and 1162.5%, respectively. These were still real overpredictions, but their numerical size was amplified by the

Station	Name	Point type	Baseline v err. (%)	Baseline Q err. (%)	First-pass interpretation
6	Fan Sud	Fan inlet	159.1	8.6	Small Q error but large v error indicated section-representation mismatch rather than fan-flow mismatch.
9	Fan Nord	Fan inlet	93.4	90.3	Substantial fan-side overprediction confirmed that the baseline model required correction before interpretation.
3	Station 3	Outlet / branch end	66.1	177.6	Outlet delivery was strongly overpredicted despite a smaller velocity error, indicating downstream distribution mismatch.
10	Station 10	Outlet / branch end	969.6	926.8	Very large outlet overprediction indicated severe downstream mismatch in this branch.
13	Station 13	Outlet / branch end	1336.6	1162.5	Extreme weak-flow outlet mismatch, combined with poor duct condition, made this a high-priority diagnostic case.

Table 5.1: Representative first-pass baseline mismatches before auxiliary calibration

near-zero denominator, which is a known limitation of percentage-based error measures [28]. The practical alternative adopted from this point onward was therefore to retain the raw percentage values as an audit trail, while interpreting weak-flow points through the signed absolute quantity difference and the physical station class before allowing them to drive the diagnosis.

The final comparison workbook also reported the supplementary floored percentage defined in Chapter 4 whenever $0 < Q_{\text{meas}} < 1$ m^3/s. Using 1 m^3/s as the denominator floor reduced the corresponding indicators for Stations 2 and 13 to 209.7% and 349.9%, while their raw values remained unchanged. The floored indicator therefore stabilized the numerical scale without concealing the underlying overprediction or changing the measured airflow.

Second, the supplementary model-implied-area block showed that some of the most extreme velocity discrepancies were not only hydraulic mismatches; they were also section-consistency warnings. Table 5.3 reproduces the key values that triggered this realization. The strongest pattern appeared at Stations 3 to 7, where the implied model section corresponded to diameters substantially different from the measured duct sizes. This was the point at which it became clear that the diameters, or at least the effective comparison sections used to extract Ventsim values, had to be checked before fan-side or leakage diagnosis could be trusted.

Station	Q_{meas} (m^3/s)	$Q_{\text{sim},0}$ (m^3/s)	ΔQ (m^3/s)	**Raw Q err. (%)**	**First-pass interpretation**
2	0.303	2.40	+2.097	692.1	Weak outlet flow; raw percentage was amplified by the small measured denominator.
10	0.672	6.90	+6.228	926.8	Severe outlet mismatch; the large absolute difference confirmed a physically excessive baseline branch response.
13	0.301	3.80	+3.499	1162.5	Weak damaged outlet; near-zero measured delivery made the raw percentage extreme.
15	2.000	13.10	+11.100	555.0	Return-tunnel check, not a direct duct outlet; percentage error could not be interpreted as a leakage indicator.

Table 5.2: First-pass examples showing denominator effects in raw quantity-error interpretation

In practical terms, the first workbook therefore led to two immediate pre-correction conclusions. The first was that weak-flow or special stations had to be interpreted through absolute quantity difference and point classification, not through raw percentage error alone. The second was that part of the apparent velocity mismatch was caused by inconsistent diameter or section representation, so diameter and section matching had to be audited before the later stages of fan, leakage, and local-loss diagnosis were attempted.

5.3.1 Geometry-consistency correction of diameters and comparison sections

The first baseline screen showed that some apparent airflow mismatch could not be interpreted reliably until the measured and modelled comparison sections were made geometrically consistent. This correction was carried out as a controlled geometry-consistency step based on two sequential comparison tables, the initial geometry diagnosis and the corrected-section audit. In this stage, the measured duct or airway section observed underground was used as the reference, and the model-implied area and diameter at each selected comparison location were checked directly against it. Where the selected Ventsim

Station	Measured dia. (mm)	Field area (m^2)	Implied model area (m^2)	Implied dia. (mm)	Area err. (%)	First-pass interpretation
1	800	0.503	0.497	796	-1.10	Control case; inlet section was already represented consistently.
3	600	0.283	0.473	776	40.2	Model behaved like a larger section than the measured outlet.
4	600	0.283	0.520	814	45.6	Velocity mismatch was consistent with an oversized effective model section.
5	600	0.283	0.482	784	41.4	Repeated the same oversized-section pattern, confirming a systematic representation issue.
6	1200	1.131	0.474	777	-138.5	Similar Q but mismatched v exposed a major fan-inlet section inconsistency.
7	600	0.283	0.212	520	-33.3	Model behaved like a smaller section than the measured outlet.
9	800	0.503	0.495	794	-1.63	Second control case; inlet section consistency was acceptable.

Table 5.3: First-pass model-implied-area checks used to identify section-representation mismatches

section or assigned comparison diameter was not like-for-like, it was corrected before any hydraulic interpretation was attempted.

This step materially changed the reliability of the comparison basis. In the initial geometry audit, several stations were still being compared against model sections that behaved like much larger or smaller diameters than the observed ducts. After correction, the direct duct and fan stations were brought into near-equality with the measured sections. The maximum absolute area error fell from 83.94% to 1.18%, and the maximum absolute diameter error fell from 35.61% to 0.59%. Particularly strong improvements were observed at Stations 3, 4, 5, 6, and 8, while the already good matches at Stations 1 and 9 remained good. In other words, this intermediate step did not solve the airflow calibration, but it removed a major source of artificial error from the measurement-to-model

comparison itself.

Tables 5.4 and 5.5 report the complete station-by-station geometry audit before and after correction. Station 11 is absent because no direct section comparison was available there, and Station 15 is excluded because it was a return-tunnel check rather than a circular duct section.

The corrected audit also clarified the interpretation of the first-pass Fan Sud inconsistency. Initially, Station 6 appeared to compare a 1200 mm field inlet against a model section behaving like about 777 mm. After the comparison section was revised, the residual mismatch fell to 0.10% in area and 0.05% in diameter. Similar corrections occurred for Stations 3, 4, 5, and 8, whose apparent section errors dropped from the range of roughly 71 to 84% in area to values between about -1.18% and 1.05%. This is why the later calibration stages could treat the remaining v and Q mismatches as predominantly hydraulic rather than as artifacts of comparing dissimilar sections.

At this point, the dataset provided a geometrically consistent comparison basis. Only after this step did it become meaningful to proceed to the later diagnosis of fan definition, local installed losses, leakage, and downstream resistance. The fan-definition and local shock-loss stage reported below followed this correction, after which downstream duct losses were treated in the branch-level calibration.

Station	Measured dia.* (mm)	Field area (m^2)	Implied model dia.* (mm)	Implied model area (m^2)	Area error (%)	Diameter error (%)
1 (Fan XS)	800.00	0.50	800.07	0.50	0.01	0.01
2	565.00	0.25	567.58	0.25	0.92	0.46
3	600.00	0.28	797.88	0.50	76.87	32.98
4	600.00	0.28	813.69	0.52	83.94	35.61
5	600.00	0.28	783.76	0.48	70.66	30.63
6 (Fan Sud)	1200.00	1.13	776.98	0.47	-58.08	-35.25
7	600.00	0.28	519.69	0.21	-24.97	-13.38
8	600.00	0.28	811.07	0.52	82.76	35.18
9 (Fan Nord)	800.00	0.50	793.58	0.49	-1.61	-0.80
10	800.00	0.50	783.81	0.48	-4.01	-2.02
12	600.00	0.28	669.13	0.35	24.39	11.52
13	600.00	0.28	562.34	0.25	-12.15	-6.28
14 (Fan XN)	800.00	0.50	791.58	0.49	-2.10	-1.05

Table 5.4: Station-by-station geometry-consistency diagnosis before correction

Station	Corrected dia.* (mm)	Reference area (m^2)	Implied model dia.* (mm)	Implied model area (m^2)	Area error (%)	Diameter error (%)
1 (Fan XS)	1000.00	0.79	1000.41	0.79	0.08	0.04
2	565.00	0.25	562.56	0.25	-0.86	-0.43
3	600.00	0.28	600.09	0.28	0.03	0.02
4	600.00	0.28	596.72	0.28	-1.09	-0.55
5	600.00	0.28	596.45	0.28	-1.18	-0.59
6 (Fan Sud)	1000.00	0.79	1000.49	0.79	0.10	0.05
7	600.00	0.28	599.46	0.28	-0.18	-0.09
8	600.00	0.28	603.14	0.29	1.05	0.52
9 (Fan Nord)	1000.00	0.79	1002.22	0.79	0.44	0.22
10	800.00	0.50	797.88	0.50	-0.53	-0.26
12	600.00	0.28	598.41	0.28	-0.53	-0.26
13	600.00	0.28	599.73	0.28	-0.09	-0.05
14 (Fan XN)	1000.00	0.79	1000.44	0.79	0.09	0.04

Table 5.5: Station-by-station geometry-consistency diagnosis after correction

* dia. = diameter.

5.3.2 Topology verification and auxiliary fan definition setup

After the duct and airway sections used to compare measured and modelled values had been corrected, the next task was to ensure that the remaining mismatch was not being generated by a local topology problem in the Ventsim model itself. Before moving to fan-side calibration, the local auxiliary-fan representation was therefore checked to confirm that the fan acted on the intended auxiliary branch, that the main tunnel topology was preserved, and that no hidden modelling artifact such as an inappropriate inline placement or wrong legacy fan assignment was driving the result.

The accepted Ventsim representation retained the main tunnel as the main airway and placed the auxiliary fan on a short side branch representing the fan casing, followed by the actual outlet duct. This distinction was important because the real auxiliary fans draw air from the mine heading and discharge into flexible ducting; they do not act as inline fans on the entire main tunnel flow. The topology check therefore established the local modelling basis required before the remaining fan-side mismatch could be interpreted as a calibration problem.

Once this local representation had been verified, new auxiliary fan definitions were added as clean database entries and assigned by area. Table 5.6 summarises the accepted mapping used in the calibrated model. The extension branches XS and XN were assigned the larger Zetal VH1004.4, 2 x 45 kW configuration, whereas the North and South area fans were assigned the 2 x 30 kW configuration. For these ducted auxiliary installations, the entered curves were expressed on a static-pressure basis because the calibration required the pressure available to overcome duct and branch resistance rather than the total pressure including the outlet velocity-pressure component.

The manufacturer characteristic sheets used to construct these entries are shown in Figure 5.7. These catalogue curves provided the original power, pressure, and efficiency information for the two auxiliary-fan families subsequently digitised and entered into the Ventsim fan database [30, 31]. They document that the adopted definitions were based on supplied manufacturer data rather than on arbitrary curve selection.

Figure 5.8 documents the XS–XN 2 x 45 kW auxiliary-fan definition entered in the Ventsim fan database. The digitised total-pressure points were checked against the imported manufacturer source image for the selected variation used at this stage of the work. Table 5.7 provides a representative database-entry verification using the duty-point values reported by Ventsim.

The same database-entry verification was retained for the Nord–Sud 2 x 30 kW auxiliary-fan definition used for the North and South area fans. Figure 5.9 shows the fan entry as stored in the Ventsim database, while Table 5.8 summarises a representative duty-point check for the same entered definition.

In practical terms, this stage completed the preconditions for fan-side calibration.

Model area	Added fan definition	Curve variation	Pressure basis
XS	Zetal VH1004.4, 2 x 45 kW	25°	Static
XN	Zetal VH1004.4, 2 x 45 kW	25°	Static
N	Zetal VH1004.4, 2 x 30 kW	20°	Static
S	Zetal VH1004.4, 2 x 30 kW	20°	Static

Table 5.6: Auxiliary-fan definitions assigned during the fan-definition stage

Software-reported parameter	Value	Unit
Fan efficiency at duty point	80.6	%
Operating speed	1450	rpm
Air density	1.06	kg/m^3
Fan static pressure at duty point	1903.4	Pa
Flow quantity at duty point	17.1	m^3/s
Equivalent air velocity, v	21.6	m/s

Table 5.7: Representative duty-point values reported by Ventsim for the entered XS–XN Zetal VH1004.4, 2 x 45 kW fan definition

Software-reported parameter	Value	Unit
Fan efficiency at duty point	89.2	%
Operating speed	1450	rpm
Air density	1.07	kg/m^3
Fan static pressure at duty point	2106.4	Pa
Flow quantity at duty point	12.5	m^3/s
Equivalent air velocity, v	15.9	m/s

Table 5.8: Representative duty-point values reported by Ventsim for the entered Nord–Sud Zetal VH1004.4, 2 x 30 kW fan definition

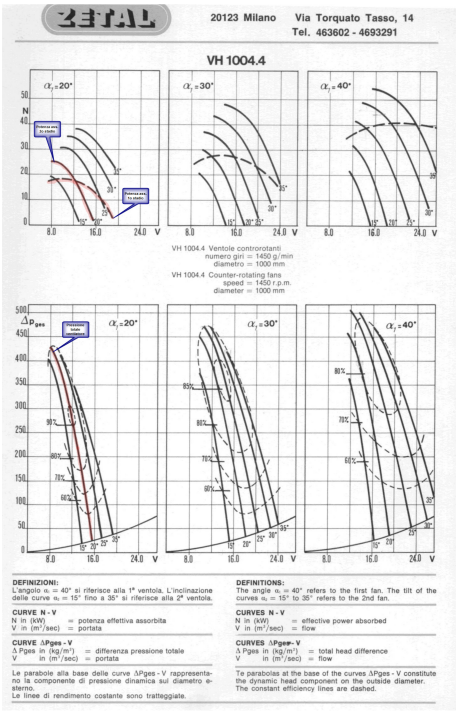

(a) Zetal VH1004.4 characteristic sheet for the 2 x 30 kW configuration used for the North and South area fans.

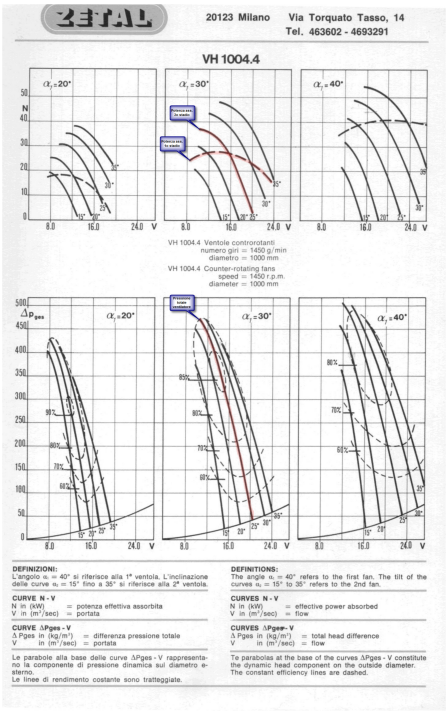

(b) Zetal VH1004.4 characteristic sheet for the 2 x 45 kW configuration used for the South and North extensions.

Figure 5.7: Zetal VH1004.4 catalogue curves used for the baseline auxiliary-fan definitions [30, 31]

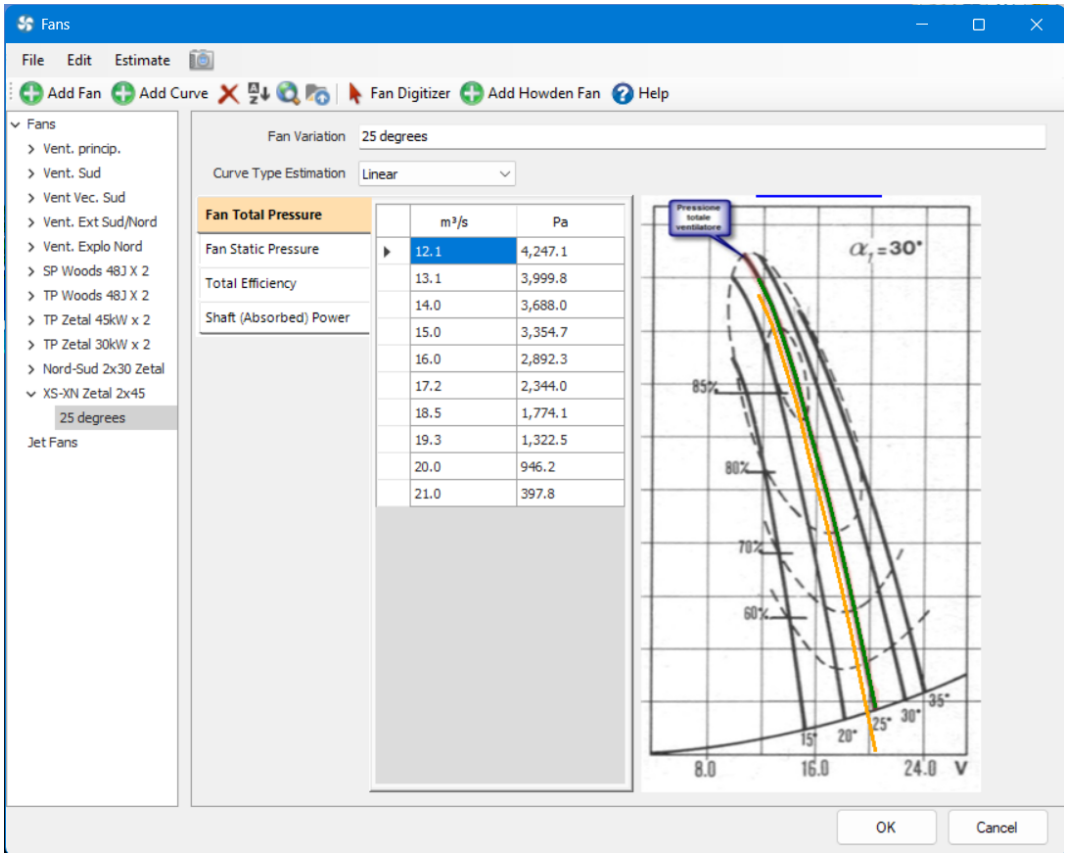

Figure 5.8: XS–XN Zetal VH1004.4, 2 x 45 kW fan definition entered in Ventsim

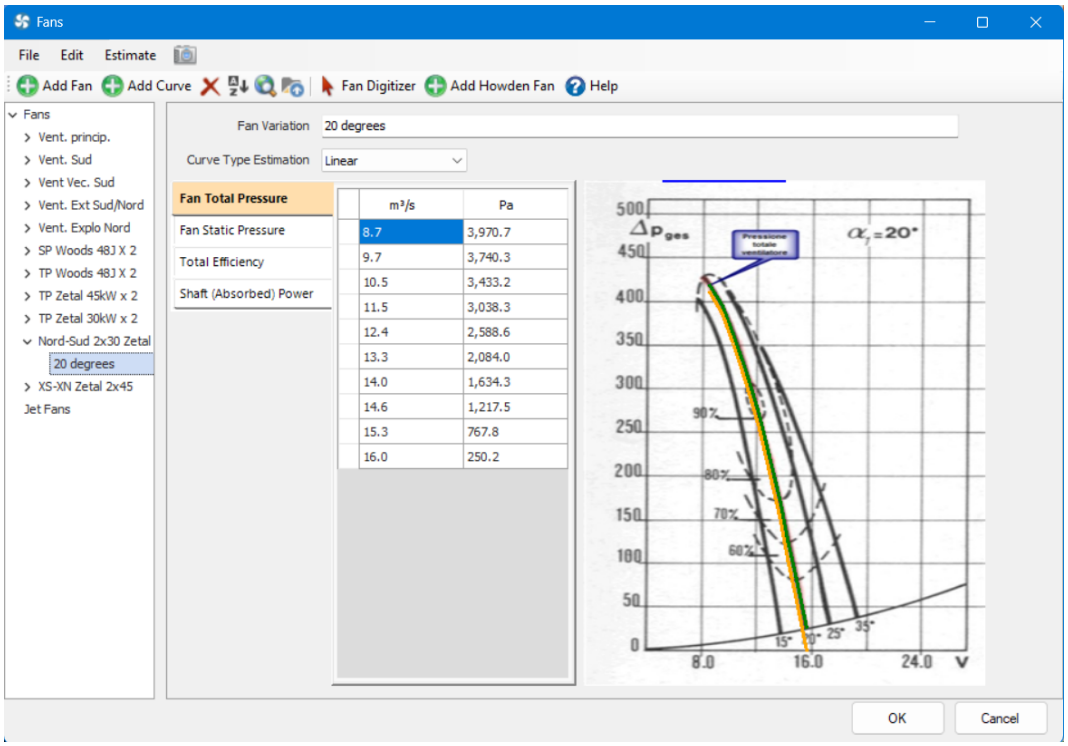

Figure 5.9: N–S Zetal VH1004.4, 2 x 30 kW fan definition entered in Ventsim

The duct and airway sections used for measured-model comparison had already been corrected, the auxiliary fans had been added and assigned to the appropriate branches, the static-pressure basis had been established for ducted use, and the local topology had been checked so that the auxiliary fans were not acting through a misleading network representation. Only after these steps did it become scientifically meaningful to interpret the remaining inlet mismatch as a true fan-side calibration issue rather than as a geometry or topology artifact.

5.4 Auxiliary-network loss calibration

5.4.1 Calibration basis and evaluation logic

After the fan definitions and local topology had been verified, the remaining inlet mismatch was no longer attributed directly to the fan curves. The next step was to examine whether the discrepancy was consistent with installed-system effects observed during the underground survey. These effects, documented in Section 5.2 and illustrated in Figures 5.5 and 5.6, included near-wall or corner fan positions, non-centred inlets, asymmetric approach flow, upstream 90° turns, and immediate duct bends that were not represented by an ideal catalogue fan alone [21]. Similar installation issues had also been noted in the Howden survey report and were used as supporting context for the field observations [2].

In this stage, local shock losses were introduced only on the short inlet/casing segments or immediate bend segments where a physical defect had been observed or reported. The modelling principle was not to force the measured quantity numerically at any cost. Instead, each candidate scenario had to satisfy three conditions: it had to move the duty point in the correct direction, remain physically interpretable in relation to the observed installation, and avoid creating unacceptable disturbance of the already calibrated main network. The Ventsim interpretation of shock loss, including the practical anchor that $X = 1$ is comparable to a sharp 90° duct corner, provided the reference scale for judging whether a tested value remained defensible [29].

Fan Sud was treated first because it showed the largest fan-side mismatch while its inlet measurement was internally repeatable. The three inlet velocities of 4.64, 4.27, and 4.52 m/s yielded a mean flow of 3.516 m^3/s and a coefficient of variation of 3.443%, so the discrepancy with the simulated quantity could not reasonably be dismissed as random measurement scatter alone. This made Fan Sud the clearest diagnostic case for establishing the installed-loss calibration logic before applying the same reasoning to the other auxiliary fans.

The remaining fans were then treated in a diagnostic sequence rather than in a geographical order. Once the accepted Fan Sud correction had been fixed, Fan XS was as-

sessed as a mainly local inlet-position correction, Fan Nord as a distributed inlet-and-bend correction, and Fan XN as the final case because it produced the broadest main-network response and therefore required a caution flag for later re-checking. Each accepted local-loss package was followed by a main-network check using exported Ventsim branch-result tables for reversal, primary-fan change, and broader disturbance of high-flow non-fan airways.

5.4.2 Accepted fan-by-fan shock-loss scenarios

Table 5.9 summarises the accepted installed-loss scenarios selected from the shock-loss calibration work. The chosen state was Fan Sud inlet $X = 5$ with duct-bend $X = 1$; Fan XS inlet $X = 10$; Fan Nord represented by a distributed $(1, 2, 2)$ package for the upstream bend, inlet, and downstream bend; and Fan XN inlet $X = 10$, accepted with caution. Exact matching of the measured fan quantity was not used as the only criterion, especially for Fan Sud and Fan XN, because downstream duct leakage and delivered-flow loss had not yet been calibrated and the inlet measurements were taken in disturbed flow fields.

Before these values were retained, the tested candidate sets were Fan Sud inlet $X = 0, 1, 2, 5, 20, 30$ with the duct-bend term fixed at $X = 1$, Fan XS inlet $X = 0, 5, 10, 20$, Fan Nord packages $(0, 0, 0)$ and $(1, 2, 2)$, and Fan XN inlet $X = 0, 5, 10$.

The resulting interpretation is physically differentiated by fan. For Fan Sud, the accepted scenario reduced the simulated quantity in the correct direction without forcing the duty point out of the fan curve, but a large residual mismatch remained, confirming that downstream losses were still missing from the model. For Fan XS and Fan Nord, the accepted local-loss packages brought the simulated fan quantities close to the measured values while remaining physically consistent with the observed inlet and bend conditions. For Fan XN, the $X = 10$ inlet case provided the best tested local correction among the candidate scenarios, but it was retained only provisionally because of the broader response it caused elsewhere in the network.

5.4.3 Main-network gate and transition to downstream calibration

After each accepted local-loss package had been selected at fan level, the resulting model state was checked against the already calibrated main network. Table 5.10 summarises these gate results. No accepted scenario generated airflow reversal or a main-network disturbance.

Fan	Fan curve	Observed local defect	Accepted shock values	Q_{sim}	Q_{meas}	Status
Sud	2 x 30 kW, 20°, static	Near-wall or off-centre inlet plus immediate duct-bend effect	Inlet $X = 5$; bend $X = 1$	11.3	3.516	Accepted as local-loss starting point
XS	2 x 45 kW, 25°, static	Incorrect corner or wall-close inlet; asymmetric approach flow	Inlet $X = 10$	14.0	13.569	Accepted
Nord	2 x 30 kW, 20°, static	Upstream 90° turn, disturbed inlet, downstream bend due to orientation	Upstream $X = 1$; inlet $X = 2$; downstream $X = 2$	12.6	11.328	Accepted
XN	2 x 45 kW, 25°, static	Incorrect top-corner inlet; close-wall inlet-system effect	Inlet $X = 10$	12.6	8.446	Accepted with caution

Table 5.9: Accepted auxiliary-fan installed-loss scenarios selected from the local shock-loss calibration stage. Airflow quantities are in m^3/s

Fan	Primary-fan response	High-flow non-fan main-airway response	Reversal	Gate decision
Sud	Flow changed only from about 29.7 to 29.6 m^3/s, with small pressure change	43 rows changed by at least 0.1 m^3/s; none by 1.0 m^3/s; maximum change about 0.4 m^3/s	No	Accepted
XS	No material change in primary-fan operating state	No high-flow non-fan main airway changed by 0.1 m^3/s or more	No	Accepted; local only
Nord	No material change in primary-fan operating state	No high-flow non-fan main airway changed by 0.1 m^3/s or more	No	Accepted; local only
XN	Primary-fan flow remained about 29.6 m^3/s; pressure increased slightly from about 250 to 255 Pa	48 rows changed by at least 0.1 m^3/s; 28 by at least 1.0 m^3/s; maximum change about 1.4 m^3/s	No	Accepted with caution

Table 5.10: Stage-gate main-network check applied after each accepted local shock-loss scenario

5.4.4 Downstream branch-loss and leakage calibration

After the accepted local installed-loss packages had been fixed, the remaining mismatch was treated as a downstream branch-delivery problem. The calibration used the measured outlet or return quantities together with the observed duct condition to represent distributed duct leakage, local tears or poor couplings, restrictions, deformation, and remaining local losses. Leakage porosity was treated as a branch- and condition-dependent calibration parameter rather than as a universal duct-material constant. Higher porosity was assigned only where the duct condition and delivery pattern supported it, while better-condition sections were assigned lower values.

Table 5.11 shows the change from the fan-side calibrated state to the final downstream-calibrated state. The final model reproduced the four measured fan-inlet quantities within 5.93%, and the four branch outlet or return totals within 7.02%. The maximum difference between measured and simulated delivery ratio was 2.29 percentage points. The full final station-level comparison and calibrated leakage-porosity schedule are provided in Appendix A.2.

Auxiliary system	**Measured**			**Model after fan-side calibration**			**Model after downstream calibration**		
	Q_{in}	Q_{out}	**Delivery %**	Q_{in}	Q_{out}	**Delivery %**	Q_{in}	Q_{out}	**Delivery %**
XS	13.57	4.61	33.9	16.90	17.00	100.6	13.90	4.40	31.7
Sud	3.52	2.05	58.2	12.50	12.30	98.4	3.60	2.10	58.3
Nord	11.33	2.15	19.0	14.20	14.40	101.4	12.00	2.30	19.2
XN	8.45	2.00	23.7	14.70	14.90	101.4	8.60	2.00	23.3

Table 5.11: Downstream airflow-delivery comparison before and after branch-level downstream calibration. Airflow quantities are in m^3/s; delivery percentage is $100Q_{\text{out}}/Q_{\text{in}}$

The fan-side state is after the accepted local shock-loss package and before downstream duct leakage and loss representation; the downstream state is after those branch-level losses were added. For XN, Q_{out} refers to the Station 15 return-air check rather than a direct duct outlet.

For Sud and North Extension, physically observed leakage, bends, obstructions, and sealing conditions did not by themselves reduce the simulated fan-inlet airflow to the measured values without using losses that were no longer defensible from the field evidence. Equivalent airflow-control resistances were therefore introduced immediately downstream of those fans to represent the remaining aggregate resistance required by the measured hydraulic state (Table 5.12). These elements are calibration resistances, not installed regulators.

5.4.5 Final calibrated auxiliary-network state

The downstream calibration completed the auxiliary-network state used for the offer assessment. The model was not tuned to remove all remaining local deficiencies. Instead, residual leakage, duct damage, coupling losses, restrictions, and weak delivered-flow be-

Branch	Unique no.	Target Q (m^3/s)	Model Q	Opening (%)	Control R ($N\,s^2/m^8$)	Total R
Sud	14255	3.50	3.60	14.10	284.68	293.78
XN	14568	8.40	8.60	35.70	35.86	36.97

Table 5.12: Equivalent downstream airflow-control resistance used in the final auxiliary calibration

haviour were retained where they were supported by field observations and measurement-to-model comparison. This preserved the distinction between the capacity of the offered main fans and the ability of the existing auxiliary system to distribute that capacity to the active areas.

In the final calibrated state, Fan XS and Fan Nord remained within their represented auxiliary-fan curves, whereas Fan Sud and Fan XN remained in the stall region of their entered characteristic curves. This result is consistent with the Howden survey observation that some auxiliary fans operated in stalled or unfavourable conditions [2]. For Fan Sud and Fan XN, the stall condition is interpreted together with the observed duct damage, leakage, high local resistance, and unfavourable installation geometry, rather than as evidence that the fan curves should be reshaped to force agreement.

The calibrated model was therefore carried forward as a defensible representation of the existing auxiliary-distribution problem, not as an idealized repaired network. This final state provides the basis for the following offer assessment, where the main-fan packages are evaluated against a network that still contains the local and regional distribution constraints observed during the thesis work.

5.5 Comparative technical assessment of the offered main-fan arrangements

Following completion of the calibrated pre-2028 baseline, the commercial main-fan offers were evaluated in two operating layouts. The pre-2028 layout represents the existing operating network, while the post-2028 layout represents the planned short-term state in which the North and South production areas are closed, South Intermediate and Far North are active, and the South ramp remains part of the circulation network. These labels correspond directly to the assessed Ventsim models and are used throughout the comparison. Each offered arrangement was simulated at 100% fan speed using the same designated intake, exhaust, active-face, access-airway, and regional controls. The classifications were based on the exported numerical results, while the map colours were used to visually check and illustrate the airflow pattern.

The technical assessment followed the stage-gate formulation established in Section 4.3.

The whole-mine requirement at the designated exhaust was evaluated first. Offers satisfying this requirement in both layouts were then assessed against the local Q requirements, the accepted v range, and the regional inflow criterion. This sequence prevented an arrangement with insufficient fundamental capacity from being retained on the basis of isolated local results.

5.5.1 Representation and operating points of the offered fans

The manufacturer characteristics supplied with the CFT, Aero/Systemair, and Howden offers were digitized and entered in Ventsim as total-pressure curves with their associated efficiency and absorbed-power data, because the supplier curves and Ventsim duty-point reporting for these main-fan arrangements were expressed on that basis [3, 4, 5]. The CFT and Aero arrangements each use one fan in each of the two parallel main-fan airways. The Howden arrangement uses two stages in series in one installation. Provisional inlet and outlet resistances were included to represent the accessory losses documented during model construction.

Offer	**Name**	**Arrangement**	**Rated motor power**	**Model representation**
CFT	AIR-A-U/1250-6-28/55-4-50Hz	Parallel	2×55 kW	One fan per main-fan airway; total provisional accessory resistance of 0.18366 $\mathrm{Ns^2/m^8}$ per branch
Aero	Systemair AXC 1250-8/34°-4-P	Parallel	2×75 kW	One fan per main-fan airway; total provisional accessory resistance of 0.20408 $\mathrm{Ns^2/m^8}$ per branch
Howden	AXN 1200/708A-100	Series	2×55 kW	Two-stage series panel; total provisional accessory resistance of 0.34602 $\mathrm{Ns^2/m^8}$

Table 5.13: Main-fan definitions and arrangements represented in the comparative Ventsim models

The CFT accessory resistance in Table 5.13 was derived from the installation components included in the supplier offer. The quoted package included inlet and outlet cones, wire guards, and silencers, but did not provide individual component pressure-drop curves or a certified complete-assembly loss. To avoid representing these accessories as zero loss, while also avoiding an unsupported large penalty, a transparent screening allowance of 100 Pa at the supplier reference flow of 33 $\mathrm{m^3/s}$ was assigned to the inlet side and the

same value to the outlet side of each CFT fan branch. The symmetric allowance reflects the absence of separate certified inlet- and outlet-component loss data.

The Ventsim quadratic resistance relation is

$$\Delta P = RQ^2. \tag{5.1}$$

Using Equation 5.1, the resistance assigned to each side of each CFT fan was

$$R_{\text{in}} = R_{\text{out}} = \frac{100}{33^2} = 0.09183 \text{ Ns}^2/\text{m}^8. \tag{5.2}$$

The total manually assigned accessory resistance per CFT fan branch was therefore

$$R_{\text{inst}} = R_{\text{in}} + R_{\text{out}} = 0.18366 \text{ Ns}^2/\text{m}^8. \tag{5.3}$$

At the modelled branch flow of approximately 35.1 m^3/s, this corresponds to an installation pressure loss of about

$$\Delta P_{\text{inst}} = 0.18366(35.1)^2 \approx 226 \text{ Pa}, \tag{5.4}$$

which is consistent with the fan-loss values reported by Ventsim for the CFT branches. The resulting pressure, efficiency, and power values should therefore be interpreted as conditional on this documented accessory-loss assumption until component-level or complete-assembly loss data are supplied by the manufacturer.

The Aero accessory resistance in Table 5.13 was derived using the same screening logic. The Aero/Systemair offer included inlet silencing and connection accessories, and the mine confirmed one shutter and one VFD per fan, but supplier-certified component or complete-assembly pressure-drop data were not available. Because the documented inlet and outlet accessory scopes were different, a transparent screening allowance of 150 Pa at 35 m^3/s was assigned to the inlet side and 100 Pa at 35 m^3/s to the outlet side of each Aero fan branch.

Using the same quadratic relation, the assigned Aero accessory resistances were

$$R_{\text{in}} = \frac{150}{35^2} = 0.12245 \text{ Ns}^2/\text{m}^8, \tag{5.5}$$

and

$$R_{\text{out}} = \frac{100}{35^2} = 0.08163 \text{ Ns}^2/\text{m}^8. \tag{5.6}$$

The total manually assigned accessory resistance per Aero fan branch was therefore

$$R_{\text{inst}} = R_{\text{in}} + R_{\text{out}} = 0.20408 \text{ Ns}^2/\text{m}^8. \tag{5.7}$$

At the modelled Aero branch flows of approximately 42 m^3/s, this corresponds to an installation pressure loss of about

$$\Delta P_{\text{inst}} = 0.20408 Q^2 \approx 360\text{–}365 \text{ Pa} \tag{5.8}$$

per fan over the reported duty range. The Aero pressure, efficiency, and power values should therefore also be interpreted as conditional on this documented accessory-loss assumption until certified component-level or complete-assembly loss data are supplied.

The resulting operating points are reported in Table 5.14, with the corresponding CFT and Aero duty panels shown in Figures 5.10–5.13. Both parallel arrangements produced closely balanced branch duties and remained on their entered curves in both layouts. This contrasts with the two existing main fans, which were identified as operating in a low-pressure region outside their represented characteristic curves [2]. The CFT fans operated at approximately 35 m^3/s per branch and required a combined electrical input of 78.3–78.8 kW. The Aero fans operated at approximately 42 m^3/s per branch and required 134.3–134.5 kW. The Howden series panel operated near the low-pressure edge of its represented curve at approximately 34 m^3/s.

Offer	**Layout**	**Branch Q (m^3/s)**	**FTP (Pa)**	η (%)	**Electrical input (kW)**	**Interpretation**
CFT	Pre-2028	34.997–35.096	660.2–664.9	64.6–64.7	78.3	Stable operation
	Post-2028	34.811–34.911	672.3–677.1	64.9–65.0	78.8	Stable operation
Aero	Pre-2028	42.151–42.311	1009.2–1016.2	67.2–67.3	134.3	Stable operation
	Post-2028	41.965–42.122	1019.3–1026.1	67.4–67.6	134.5	Stable operation
Howden	Pre-2028	34.0	542.7	38.6	50.3	Low-pressure edge
	Post-2028	34.0	548.5	39.0	50.3	Low-pressure edge

Table 5.14: Modelled duty points of the offered arrangements at 100% fan speed

5.5.2 Whole-mine capacity gate

The mandatory whole-mine airflow requirement, derived from the main-gallery high-traffic sizing case in Table 4.2 using Equation 4.4, is 47.97 m^3/s at the exhaust shaft. The exhaust shaft was used instead of the sum of the fan-airway flows because it provides a consistent control across arrangements and avoids interpreting internal or recirculating flow as useful mine delivery. The resulting capacity check is presented in Table 5.15.

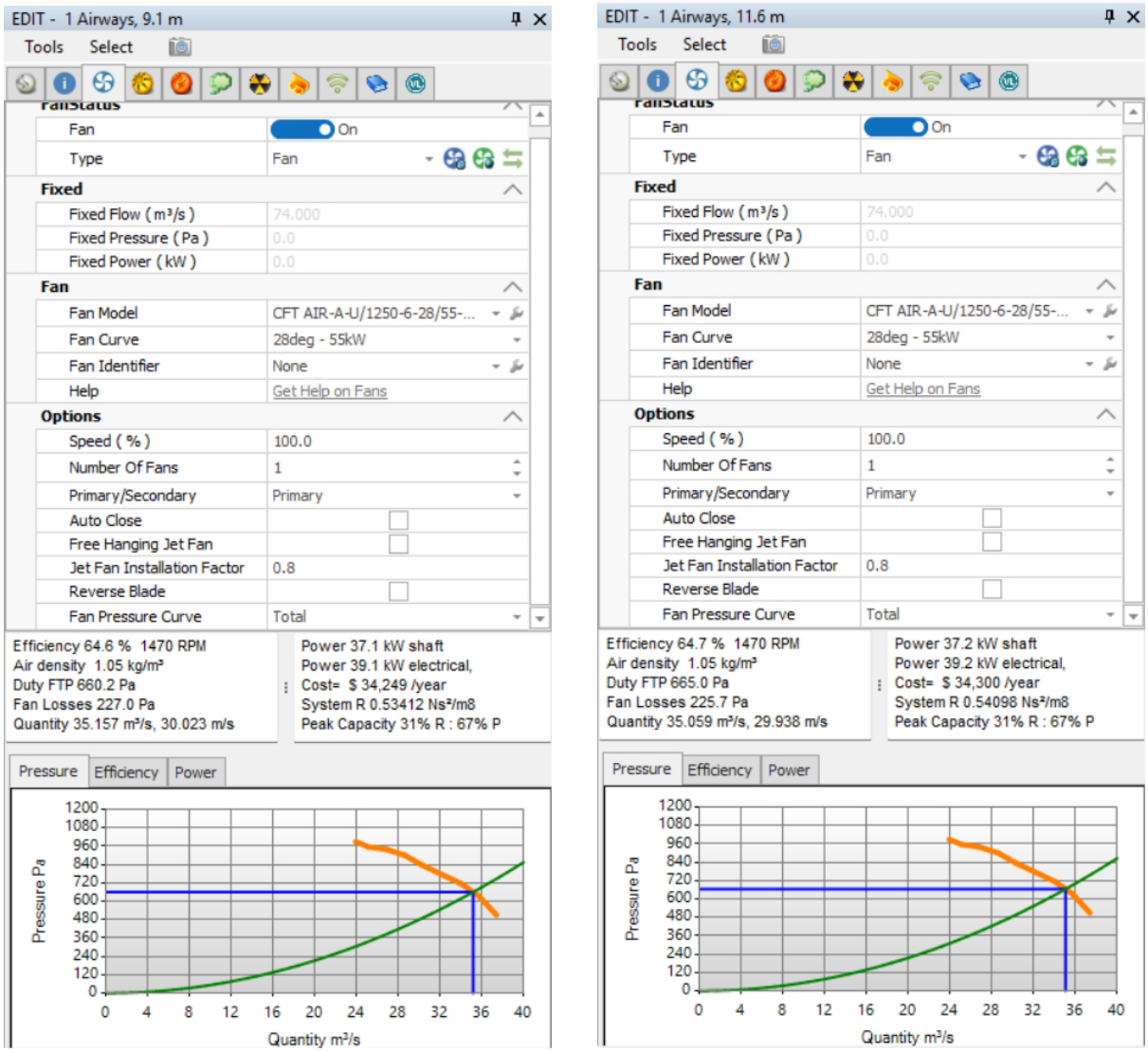

(a) Main-fan airway, 9.1 m. (b) Main-fan airway, 11.6 m.

Figure 5.10: CFT pre-2028 duty panels at 100% fan speed.

Offer	Layout	Exhaust Q (m^3/s)	Margin (m^3/s)	Relative margin (%)	Result
CFT	Pre-2028	69.606	+21.636	+45.1	Pass
	Post-2028	69.193	+21.223	+44.2	Pass
Aero	Pre-2028	83.864	+35.894	+74.8	Pass
	Post-2028	83.473	+35.503	+74.0	Pass
Howden	Pre-2028	33.1	-14.87	-31.0	Fail
	Post-2028	33.1	-14.87	-31.0	Fail

Table 5.15: Whole-mine capacity screening at the designated exhaust

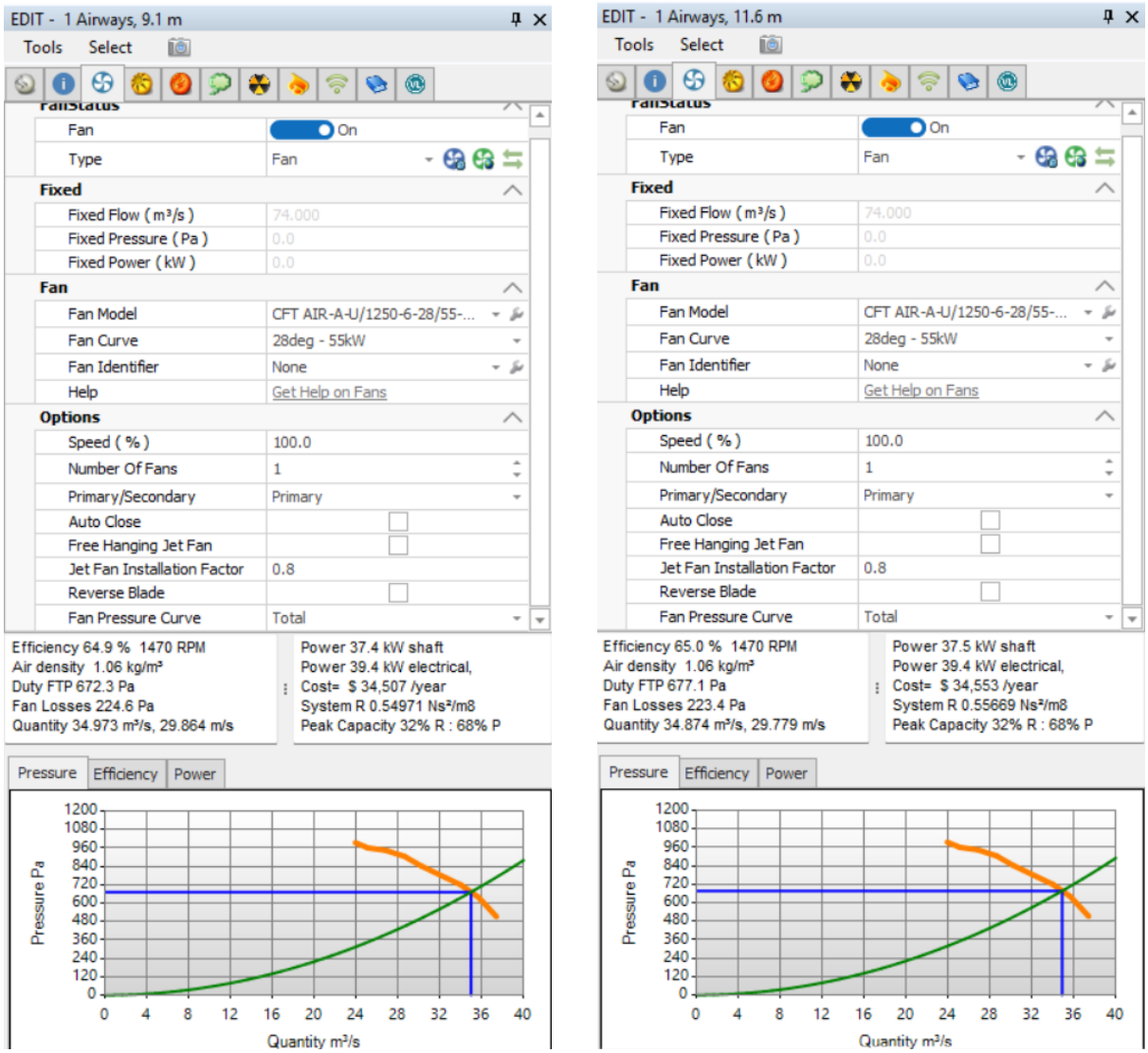

(a) Main-fan airway, 9.1 m. (b) Main-fan airway, 11.6 m.

Figure 5.11: CFT post-2028 duty panels at 100% fan speed.

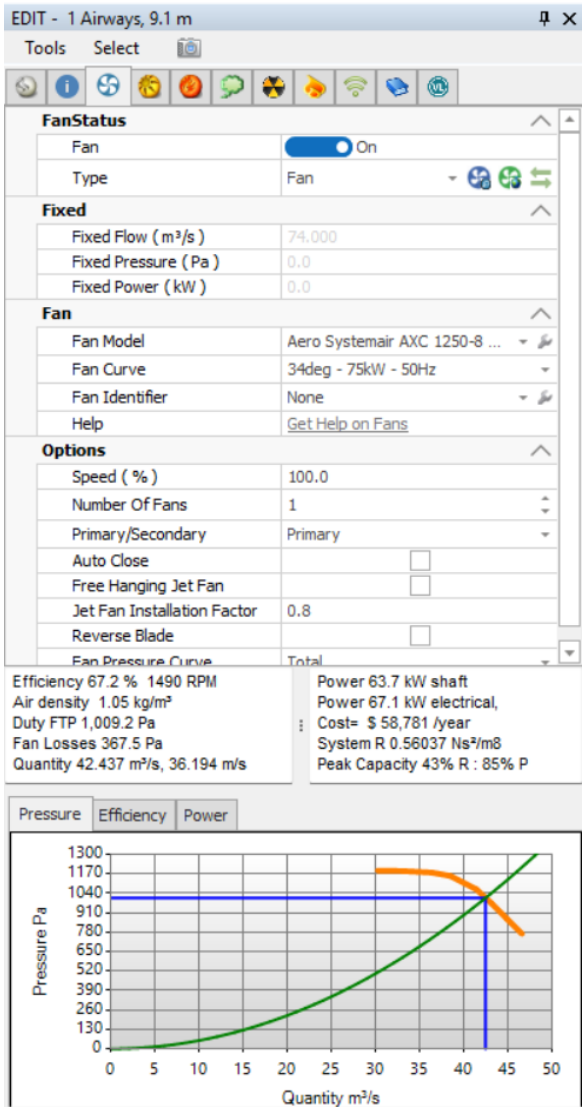

(a) Main-fan airway, 9.1 m.

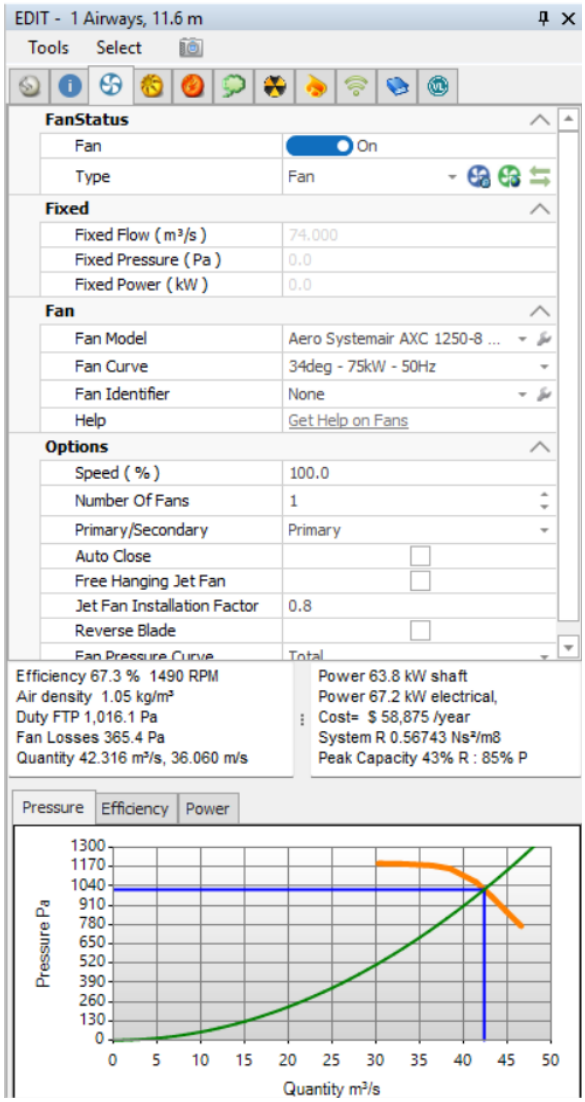

(b) Main-fan airway, 11.6 m.

Figure 5.12: Aero pre-2028 duty panels at 100% fan speed.

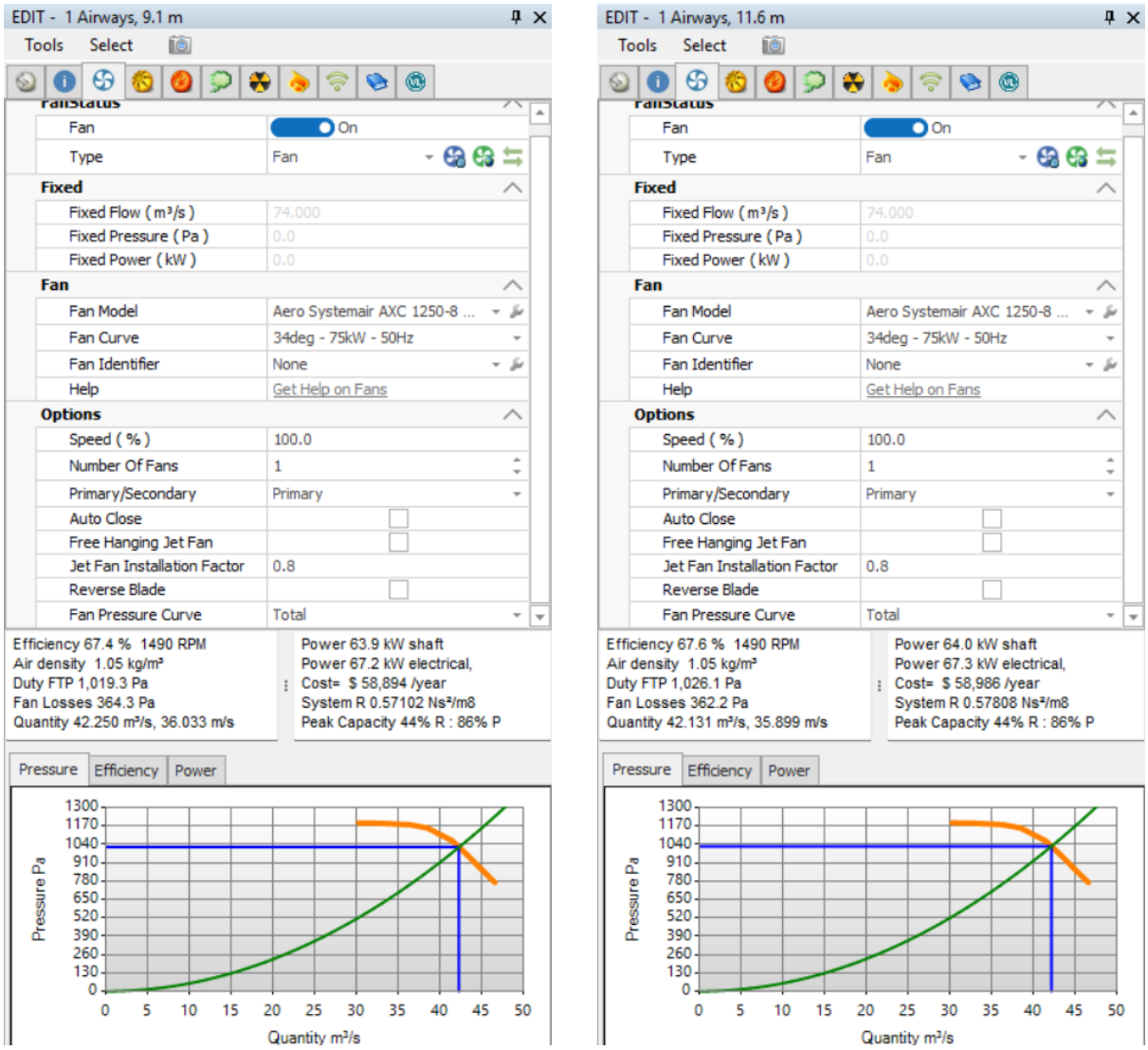

(a) Main-fan airway, 9.1 m. (b) Main-fan airway, 11.6 m.

Figure 5.13: Aero post-2028 duty panels at 100% fan speed.

CFT and Aero pass the whole-mine gate in both layouts. Aero provides the larger capacity margin, while CFT satisfies the requirement with substantially lower electrical input. The Howden series arrangement supplies only 33.1 m^3/s and has a deficit of 14.87 m^3/s, or 31.0%, in both layouts. It is therefore excluded from detailed local assessment and from the subsequent economic comparison. This conclusion applies to the offered series arrangement and does not constitute a general assessment of other Howden fan selections.

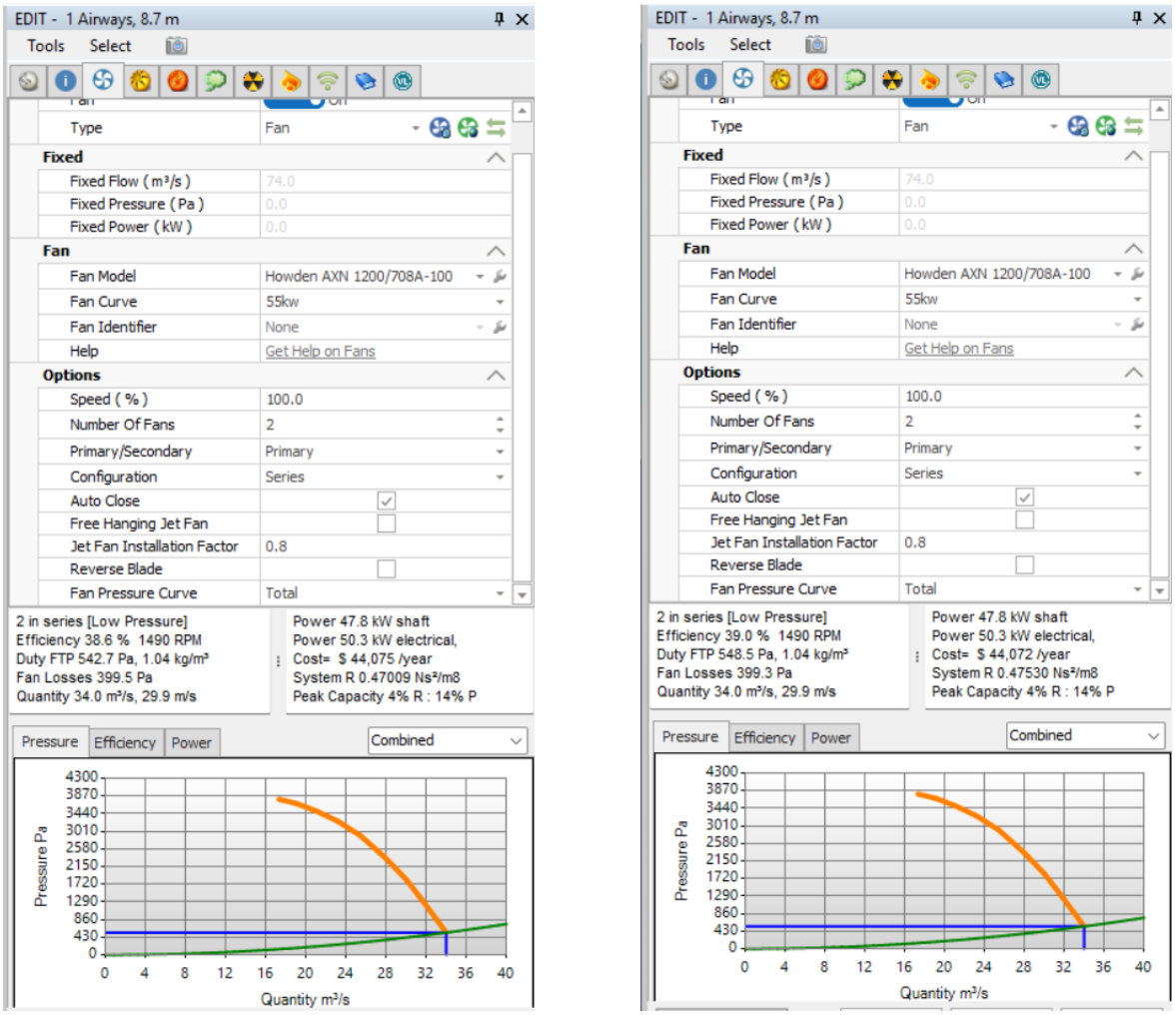

(a) Pre-2028 layout.

(b) Post-2028 layout.

Figure 5.14: Modelled duty panels for the offered Howden series arrangement at 100% speed. Both cases remain near 34 m^3/s and operate at the low-pressure edge of the represented curve

5.5.3 Local and regional performance of the retained offers

CFT and Aero were assessed at the same nine active-face controls in each layout. The local activity classes used the Q thresholds reported in Table 4.4, derived from Equation 4.4, with 2.26 m^3/s for supporting, 6.52 m^3/s for mucking, and 8.78 m^3/s for simultaneous supporting and mucking. Named passageways, ramps, and stair inclines were screened against the velocity range in Table 4.1, $0.100 \leq v \leq 6.000$ m/s, and one non-overlapping inflow boundary was used for each active region to prevent double counting.

For the post-2028 Aero case, equivalent KPI control locations were retained. The affected Far North upper level regional-boundary control is documented in Table A.10.

KPI	**CFT pre-2028**	**CFT post-2028**	**Aero pre-2028**	**Aero post-2028**
Designated exhaust (m^3/s)	69.606	69.193	83.864	83.473
Whole-mine margin (%)	45.1	44.2	74.8	74.0
Combined electrical input (kW)	78.3	78.8	134.3	134.5
Fan efficiency range (%)	64.6–64.7	64.9–65.0	67.2–67.3	67.4–67.6
Faces failing supporting flow	9 of 9	5 of 9	9 of 9	5 of 9
Faces supporting supporting-only work	0	3	0	3
Faces supporting mucking-only work	0	1	0	1
Faces supporting simultaneous work	0	0	0	0
Face velocity failures	7 of 9	3 of 9	7 of 9	3 of 9
Access velocity failures	29 of 212	9 of 243	23 of 212	12 of 243
Regions satisfying 13.366 m^3/s	1 of 4	1 of 5	1 of 4	1 of 5

Table 5.16: Comparative KPI results for the retained CFT and Aero arrangements before auxiliary-network improvement

The two retained offers produce nearly identical active-face classifications despite their markedly different whole-mine quantities. In the pre-2028 layout, all nine face controls fail the supporting threshold for both offers and seven also fail the minimum velocity criterion. In the post-2028 layout, three controls support supporting-only work, one South Intermediate control supports mucking-only work, and five controls remain below the supporting threshold. No assessed close end supports simultaneous supporting and mucking. Only the XS regional control passes in either layout, consistent with the airflow and velocity distributions shown in Figures 5.15, 5.16, 5.17, and 5.18; the detailed CFT and Aero regional-boundary records are provided in Tables A.8 and A.10, respectively. The additional capacity provided by Aero therefore increases the main-circuit margin but does not correct the represented local distribution deficiencies.

The detailed face-control exports for the retained CFT and Aero arrangements are provided in Tables A.7 and A.9, respectively. These records confirm the same active-face activity classifications for both offers. Small numerical differences between individual CFT and Aero controls do not change the interpretation: the post-2028 layout improves

local delivery to the newly active areas, while the persistent XS and XN deficits continue to govern the local result.

This limited local response is consistent with hydraulic control by the auxiliary network. Damaged or leaking ducting, high local resistance, and unfavourable auxiliary-fan positioning introduce pressure losses and can promote recirculation, as observed during the fieldwork and also noted in the Howden survey. Additional main-fan capacity is therefore redistributed mainly through lower-resistance routes in the primary circuit rather than producing a proportional increase at the active faces [2, 21].

Table 5.17 gives the colour interpretation used for the offer-assessment maps. Figures 5.15, 5.16, 5.17, and 5.18 show the corresponding airflow and velocity distributions. The maps document the network-wide response, while the classifications in Table 5.16 remain based on the exact numerical exports.

Airflow map		
Colour	**Range (m^3/s)**	**Interpretation**
	$Q < 2.26$	Below supporting-only threshold
	$2.26 \leq Q < 6.52$	Supporting-only range
	$6.52 \leq Q < 8.78$	Mucking-only range
	$8.78 \leq Q < 13.366$	Simultaneous local activity range
	$13.366 \leq Q < 47.97$	Regional quantity range
	$Q \geq 47.97$	Whole-mine benchmark range

Velocity map		
Colour	**Range (m/s)**	**Interpretation**
	$v < 0.099$ m/s	Clear minimum-velocity failure
	$0.099 < v \leq 0.100$	Boundary band
	$0.100 < v \leq 1.962$	Above the minimum
	$1.962 < v \leq 3.940$	Within accepted range
	$3.940 < v \leq 5.920$	Approaching upper limit
	$5.920 < v \leq 6.000$	Upper-limit boundary
	$v > 6.000$	Above passageway upper limit

Table 5.17: Colour-map interpretation used for the offer-assessment airflow and velocity figures

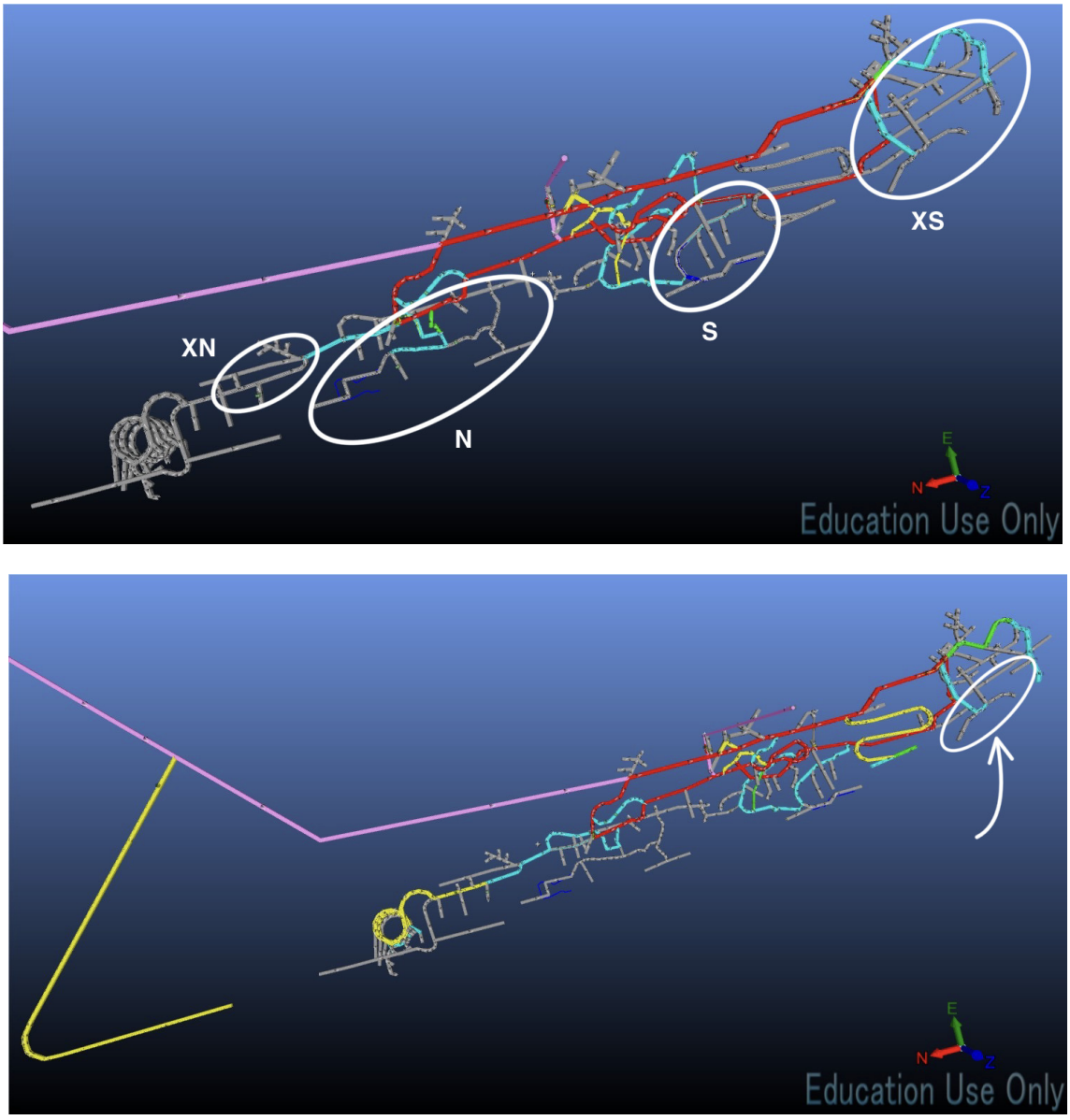

Figure 5.15: CFT airflow distribution at 100% speed in the pre-2028 layout (top) and post-2028 layout (bottom)

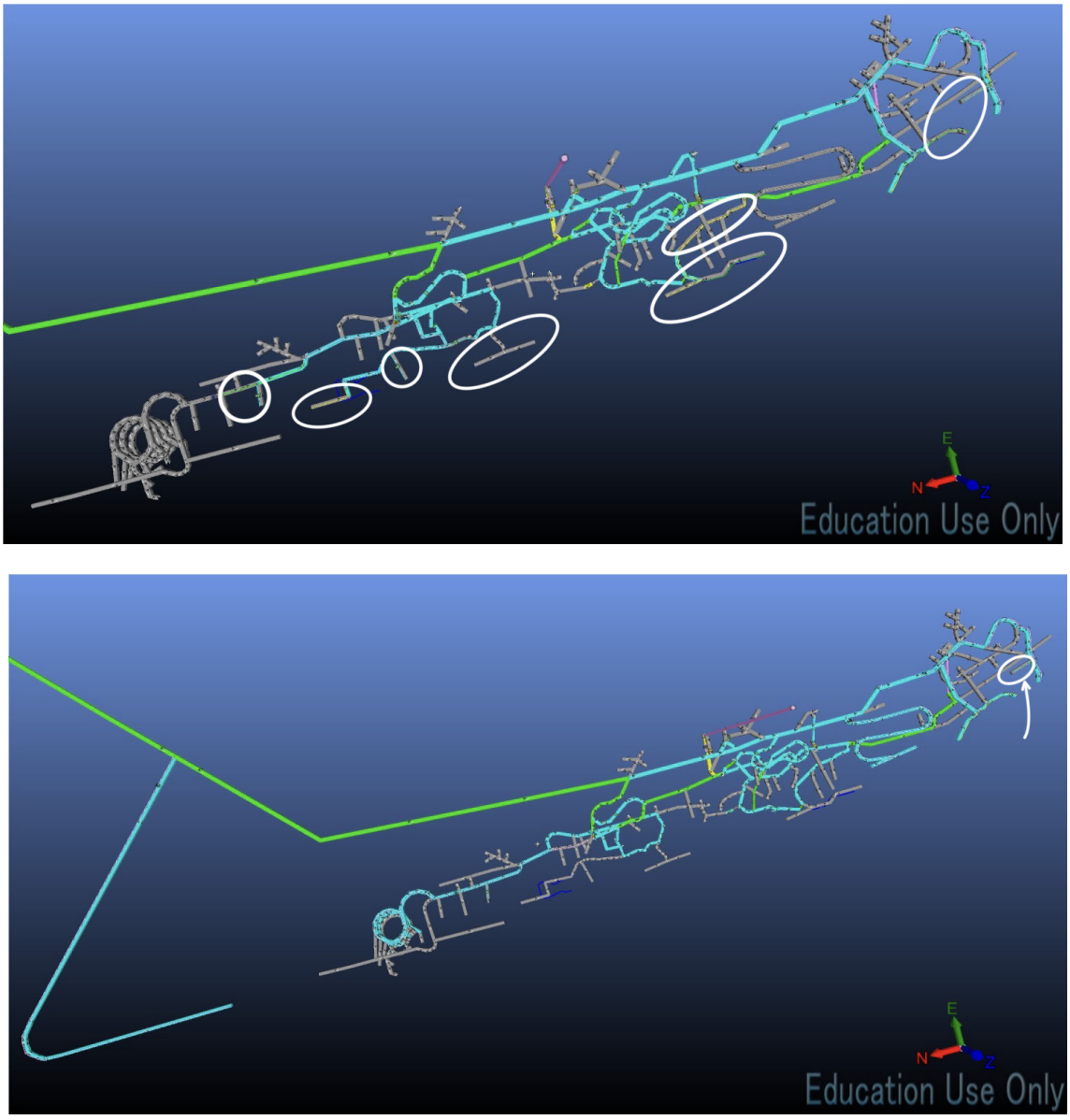

Figure 5.16: CFT velocity distribution at 100% speed in the pre-2028 layout (top) and post-2028 layout (bottom)

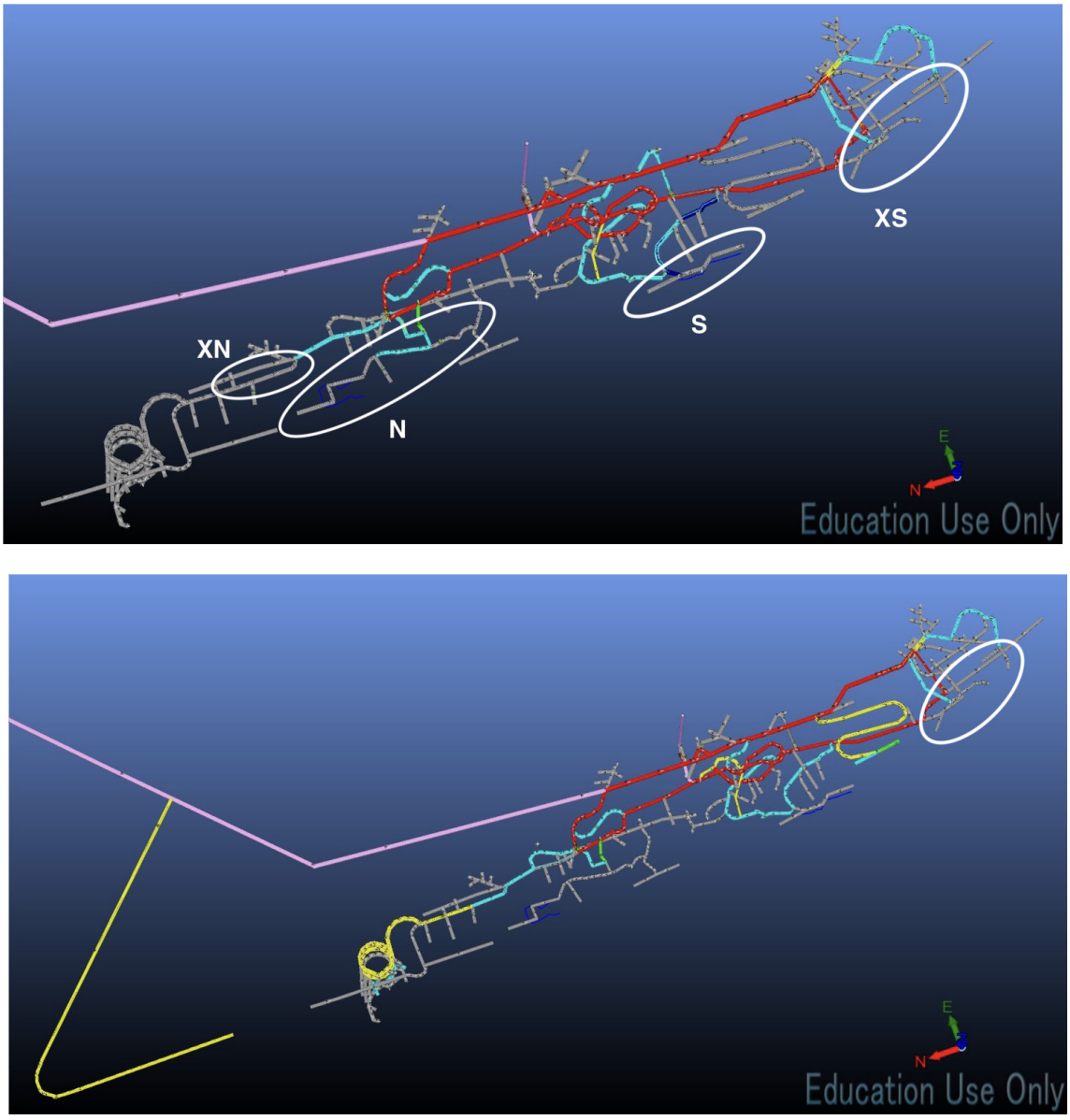

Figure 5.17: Aero airflow distribution at 100% speed in the pre-2028 layout (top) and post-2028 layout (bottom)

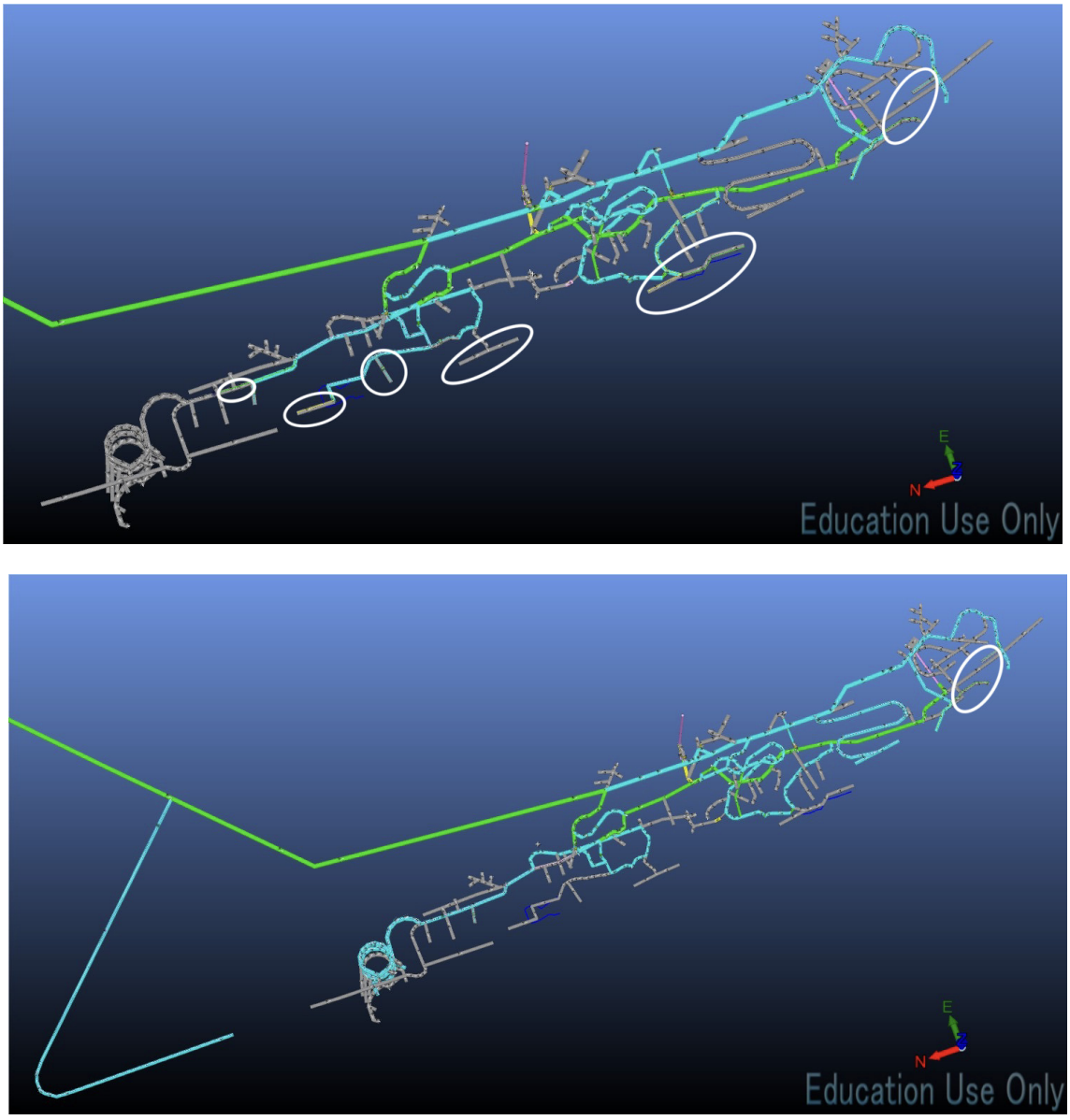

Figure 5.18: Aero velocity distribution at 100% speed in the pre-2028 layout (top) and post-2028 layout (bottom)

5.5.4 Auxiliary-network improvement sensitivity

A diagnostic sensitivity, summarized in Table 5.18, was used to test whether the local KPI failures arose primarily from insufficient main-fan capacity or from the represented auxiliary network. The accepted main-fan definitions and speeds were retained. The represented auxiliary-fan inlet and shock losses were removed, and active ducts were assigned a leakage area of 25 mm^2/m^2, consistent with the new duct condition represented in South Intermediate and Far North. This case represents an idealized network-improvement condition and is used to identify hydraulic control; it is not a construction specification.

Offer	Layout	Network state	Exhaust Q (m^3/s)	Face failures	Access failures	Regions passing
CFT	Pre-2028	Represented	69.606	9 of 9	29 of 212	1 of 4
		Improved	70.804	1 of 9	12 of 212	0 of 4
Aero	Pre-2028	Represented	83.864	9 of 9	23 of 212	1 of 4
		Improved	85.194	1 of 9	9 of 211	1 of 4
CFT	Post-2028	Represented	69.193	5 of 9	9 of 243	1 of 5
		Improved	69.685	0 of 9	4 of 243	1 of 5
Aero	Post-2028	Represented	83.473	5 of 9	12 of 243	1 of 5
		Improved	69.683	0 of 9	4 of 243	1 of 5

Table 5.18: Effect of the idealized auxiliary-network improvement on the principal KPI outcomes

The detailed improved-network active-face and regional-boundary records supporting this summary are provided in Appendix A.3.3.

The pre-2028 sensitivity improves eight of the nine face controls to supporting-only capability for both offers; North Station 12 remains below both the supporting-flow threshold and the strict minimum velocity. In the post-2028 layout, all nine assessed controls meet the supporting-flow and face-velocity criteria. Eight support supporting-only work and the South Intermediate control with unique ID 13365 supports mucking-only work. No control reaches the simultaneous-work threshold.

The improvement in face delivery is not accompanied by complete regional compliance. In the post-2028 layout, XS remains the only passing region, XN reaches 13.098 m^3/s and remains 2.0% below the regional criterion, and South Intermediate and the two Far North controls retain larger deficits. The pre-2028 CFT sensitivity also illustrates the effect of redistribution, since the number of passing regional controls decreases even though local face delivery improves. The result demonstrates that renewal of auxiliary ducts and reduction of installation losses can improve close-end delivery substantially, but regional balancing remains a separate engineering requirement. It also explains why the larger Aero whole-mine flow does not produce better local activity classes than CFT.

5.5.5 Stress-scenario and variable-speed decision

The methodology defines a stress scenario by increasing the relevant network resistance by 15%. This test was not applied as an acceptance test to the represented CFT and Aero layouts because both already fail mandatory local, access, or regional criteria at 100% speed. Increasing resistance cannot convert a failing baseline into an acceptable case, so proceeding to the stress scenario would not alter the stage-gate decision.

Both retained arrangements can be operated with variable-speed control. The whole-mine margins indicate potential for reduced-speed operation, but those margins alone do not establish a safe setpoint because local controls remain deficient at full speed. A defensible VFD setpoint must therefore be determined only after a defined auxiliary-network improvement and regional-balancing case satisfies the mandatory baseline KPIs. The 15% resistance stress scenario can then be applied to that feasible configuration to test whether its compliance remains robust.

5.5.6 Technical screening outcome

The offered Howden two-stage series arrangement is technically rejected because it fails the mandatory whole-mine airflow gate in both layouts. CFT and Aero are retained as feasible main-fan arrangements for economic comparison because both satisfy the whole-mine requirement and operate at stable points on their entered curves. At 100% fan speed, CFT provides adequate whole-mine capacity at approximately 78–79 kW combined electrical input. Aero provides greater pressure and airflow headroom with slightly higher fan efficiency, but requires approximately 134–135 kW.

This screening distinguishes main-fan feasibility from complete ventilation-system adequacy. Neither retained offer, when applied to the represented auxiliary network, satisfies every local and regional KPI. The common local classifications and the auxiliary-network sensitivity show that the controlling issue is the distribution of air through the auxiliary fans, ducts, leakage paths, and branch resistances rather than a shortage of main-fan capacity. CFT and Aero can therefore proceed to the economic stage, while any final operational recommendation must preserve the requirement for auxiliary-network improvement and regional balancing.

5.6 Economic evaluation of the retained main-fan offers

The economic evaluation was applied only to CFT and Aero because these arrangements passed the preceding whole-mine technical gate. The comparison follows the lexicographic decision model defined in Subsection 4.3.1, with incremental NPV as the governing eco-

nomic criterion and discounted payback, CAPEX, and OPEX used in that order only if the preceding criterion does not separate the alternatives.

The evaluation concerns the main-fan replacement packages. Costs for redesigning or improving the auxiliary network are not included because no sufficiently defined scope or associated CAPEX was available. This does not remove the auxiliary-network requirement established by the technical assessment; it keeps an uncosted common system intervention from being assigned arbitrarily to either main-fan offer.

5.6.1 Economic inputs and operating basis

The CAPEX values were assembled from the retained supplier offers and the common costs supplied by the mine for the VFD software and electrical installation [3, 4, 32]. The resulting comparison is shown in Table 5.19. Aero has the lower initial cost by EUR 520, equivalent to approximately 0.4% of total CAPEX.

Offer	**Fan offer**	**Softime**	**Microl**	**Total CAPEX**
CFT	42,900	56,000	26,610	125,510
Aero/Systemair	42,380	56,000	26,610	124,990

Table 5.19: Candidate CAPEX used in the economic comparison. All values are in EUR; Softime and Microl are common to both alternatives

The mine-provided electricity consumption, tariff, and fan OPEX values used to define the baseline electricity cost are summarized in Table 5.20.

Economic input	**Year**	**Value**
Electricity consumption	2026 (Jan-May)	218,590 kWh
	2025	608,310 kWh
Electricity tariff	2026	EUR 0.203/kWh
	2025	EUR 0.256/kWh
Fan OPEX	2026 (Jan-May)	EUR 44,374
	2025 recorded	EUR 155,727

Table 5.20: Mine-provided electricity consumption, tariff, and fan OPEX values used to define the baseline electricity cost

The existing installation, which had no VFD control and therefore operated at full speed, consumed 608,310 kWh in the complete 2025 operating year. Its recorded 2025 tariff was EUR 0.256/kWh. For the primary comparison, the complete-year energy quantity was repriced at the 2026 tariff of EUR 0.203/kWh so that the baseline and candidate costs use the same electricity-price basis. The resulting baseline is

$$C_{\text{base}} = 608{,}310 \times 0.203 = 123{,}486.93 \text{ EUR/year}. \tag{5.9}$$

The January–May 2026 record of 218,590 kWh was not used as the primary baseline because it covers only five months. It was retained for the sensitivity analysis in Subsection 5.6.5.

Candidate electricity use was calculated from the Ventsim electrical-power outputs at the lowest tested VFD settings retained for economic screening while satisfying the whole-mine airflow gate. CFT was evaluated at 70% speed and Aero at 60% speed. These different settings allow each offer to be compared at its lowest retained main-circuit screening duty rather than at an arbitrary common percentage of nominal speed. As established in Subsection 5.5, they are not final operational setpoints demonstrating complete local and regional compliance.

Offer	**Layout**	**Fan 1 (kW)**	**Fan 2 (kW)**	**Combined (kW)**	**Screening basis**
CFT	Pre-2028	13.4	13.4	26.8	70% speed
	Post-2028	13.5	13.5	27.0	70% speed
Aero	Pre-2028	14.5	14.5	29.0	60% speed
	Post-2028	14.6	14.5	29.1	60% speed

Table 5.21: Modelled electrical-power inputs used in the economic calculation

The calculation covers 2026–2037, corresponding to the mine-life horizon supplied for the assessment. The pre-2028 duty is applied in 2026 and 2027, and the post-2028 duty is applied in 2028–2037. A continuous operating schedule of 8,760 hours per year is used, CAPEX occurs at time zero, and annual savings are credited at each year end. The remaining financial assumptions are summarized in Table 5.22.

Parameter	**Assumption**
Analysis horizon	2026–2037, 12 operating years
Discount rate	10.87% per year, supplied by the mine
Base-case electricity tariff	EUR 0.203/kWh, held constant in the base case
Running time	8,760 h/year
Maintenance and spare parts	Excluded because reliable offer-specific values were unavailable
Residual value and decommissioning	Excluded because no defensible differentiated values were supplied
Auxiliary-network improvement	Excluded because a dedicated auxiliary-network improvement study is required to define the intervention scope and associated costs

Table 5.22: Financial assumptions applied consistently to the retained offers

5.6.2 Annual energy use and operating cost

Table 5.23 reports the annual energy and electricity costs obtained from the power inputs in Table 5.21. At the selected screening settings, CFT uses 19,272 kWh less than Aero in each pre-2028 year and 18,396 kWh less in each post-2028 year. At the adopted tariff, these differences correspond to annual CFT OPEX advantages of EUR 3,912.22 and EUR 3,734.39, respectively.

Offer	**Layout**	**Power (kW)**	**Energy (kWh/y)**	**OPEX (EUR/y)**	**Saving (EUR/y)**
CFT	Pre-2028	26.8	234,768	47,657.90	75,829.03
	Post-2028	27.0	236,520	48,013.56	75,473.37
Aero	Pre-2028	29.0	254,040	51,570.12	71,916.81
	Post-2028	29.1	254,916	51,747.95	71,738.98

Table 5.23: Annual candidate energy use, electricity OPEX, and saving relative to the existing-fan baseline

Over the undiscounted 12-year horizon, candidate electricity OPEX is EUR 575,451.41 for CFT and EUR 620,619.72 for Aero. CFT therefore reduces undiscounted electricity expenditure by EUR 45,168.31 relative to Aero over the evaluated period.

5.6.3 Discounted cash-flow results

Baseline electricity OPEX has a present value of EUR 806,710.70 over the analysis horizon. Applying the 10.87% discount rate to each candidate's annual savings produces the results in Table 5.24. The full year-by-year discounted record is provided in Appendix A.4.

Metric	**CFT**	**Aero**	**Difference favouring CFT**
CAPEX (EUR)	125,510.00	124,990.00	-520.00
Undiscounted 12-year OPEX (EUR)	575,451.41	620,619.72	45,168.31
PV of candidate OPEX (EUR)	313,051.03	337,751.96	24,700.93
PV of savings against baseline (EUR)	493,659.67	468,958.74	24,700.93
Incremental NPV (EUR)	**368,149.67**	343,968.74	**24,180.93**
PV life-cycle cost (EUR)	**438,561.03**	462,741.96	**24,180.93**
Simple payback (years)	1.655	1.738	0.083
Discounted payback (years)	**1.926**	2.031	**0.105**
Completed-year payback point	Year 2	Year 3	CFT earlier

Table 5.24: Economic results over the 2026–2037 analysis horizon

Both candidates produce positive incremental NPVs and satisfy the mine's approximate three-year payback preference under the primary assumptions. CFT has an incremental NPV of EUR 368,149.67, exceeding Aero by EUR 24,180.93. Its fractional

discounted payback is 1.926 years compared with 2.031 years for Aero, corresponding to recovery approximately 0.105 years, or 38 days, earlier.

5.6.4 Lexicographic economic ranking

The ranking is resolved by the first economic criterion. As shown in Table 5.25, CFT has the higher NPV, so the lower-order criteria cannot reverse the decision. Discounted payback and present-value OPEX nevertheless support the same choice. Aero's only quantitative advantage is its EUR 520 lower CAPEX.

Order	Criterion	CFT	Aero	Decision
1	Maximize incremental NPV (EUR)	368,149.67	343,968.74	CFT preferred; ranking stops
2	Minimize discounted payback (years)	1.926	2.031	Also favours CFT
3	Minimize CAPEX (EUR)	125,510	124,990	Favours Aero by EUR 520
4	Minimize PV OPEX (EUR)	313,051.03	337,751.96	Favours CFT

Table 5.25: Sequential lexicographic comparison of the retained offers

The direct difference between the candidates provides the same result without dependence on the existing-fan baseline.

$$\Delta\mathrm{NPV}_{\mathrm{CFT-Aero}} = PV(C_{\mathrm{OPEX,Aero}} - C_{\mathrm{OPEX,CFT}}) - (C_{\mathrm{CAPEX,CFT}} - C_{\mathrm{CAPEX,Aero}}) \quad (5.10)$$

$$\Delta\mathrm{NPV}_{\mathrm{CFT-Aero}} = 24{,}700.93 - 520.00 = 24{,}180.93 \text{ EUR}. \quad (5.11)$$

CFT's additional EUR 520 CAPEX is therefore more than recovered by its lower electricity demand. The common baseline cancels in this direct comparison, which shows that the preference is produced by the candidate power and CAPEX differences rather than by the selected representation of existing-fan consumption.

5.6.5 Sensitivity and robustness

The January–May 2026 consumption was annualized as a sensitivity case.

$$E_{\mathrm{base,2026ann}} = 218{,}590 \times \frac{12}{5} = 524{,}616 \text{ kWh/year}. \quad (5.12)$$

At the 2026 tariff, this gives a lower baseline cost of EUR 106,497.05/year. The resulting comparison is reported in Table 5.26.

Metric	CFT	Aero
PV of savings (EUR)	382,668.82	357,967.89
Incremental NPV (EUR)	257,158.82	232,977.89
Discounted payback (years)	2.573	2.766

Table 5.26: Sensitivity to annualized January–May 2026 baseline consumption

The lower baseline reduces both absolute NPVs. CFT nevertheless remains ahead by EUR 24,180.93, and both candidates remain within the approximate three-year payback preference. The unchanged difference is expected because the candidate-to-candidate energy and CAPEX terms are unaffected by the common baseline.

The present-value energy advantage of CFT over Aero is approximately 121,679 kWh over the analysis horizon. CFT's EUR 520 CAPEX premium is recovered whenever the electricity tariff exceeds

$$c_{e,\text{break-even}} = \frac{520}{121{,}679} = 0.0043 \text{ EUR/kWh}. \tag{5.13}$$

This value is substantially below the adopted tariff of EUR 0.203/kWh. The candidate ranking is therefore robust to any plausible electricity-price reduction, provided that the relative modelled electrical powers remain representative.

5.6.6 Economic recommendation

CFT is the economically preferred retained main-fan offer under the thesis decision rule. It wins at the governing NPV criterion and is also supported by its lower present-value OPEX, life-cycle cost, and discounted payback. Aero remains technically feasible at the main-fan level and has marginally lower CAPEX, but its greater capacity does not compensate economically for its higher modelled electricity demand under the evaluated schedule.

The recommendation is conditional on confirmation of the complete installed scope and supplier accessory losses and on rechecking the selected 70% CFT duty after the required auxiliary-network improvement and regional balancing. The economic result supports selection among the retained main-fan packages; it does not alter the technical conclusion that main-fan replacement alone does not establish complete local and regional ventilation adequacy.

Chapter 6

Discussion

This chapter interprets the technical and economic results and examines their implications for ventilation management and the main-fan replacement strategy at Rodoretto.

6.1 Future research on auxiliary-network improvement

The comparative assessment shows that main-fan replacement cannot be considered independently from the condition of the auxiliary network. CFT and Aero both provide sufficient whole-mine main-fan capacity, yet neither arrangement satisfies every local and regional KPI when applied to the represented auxiliary system. The diagnostic improvement sensitivity strengthens this interpretation. Improving the assumed duct condition and removing the represented installation losses substantially increases delivery to the close ends, but regional compliance is still not achieved. In the post-2028 sensitivity, all nine assessed face controls meet the supporting-flow and face-velocity criteria, while XS remains the only region satisfying the regional airflow requirement and XN remains 2.0% below it. These results confirm the influence of auxiliary-network condition without defining a complete improvement design.

The field measurements, calibration work, fan-characteristic checks, and scenario analyses undertaken in this thesis provide an appropriate basis for evaluating the commercial main-fan offers and identifying the interaction between the main and auxiliary systems. However, determining how the auxiliary network should be improved requires a separate and more detailed engineering study. This is necessary because possible interventions may involve different combinations of duct repair or replacement, leakage reduction, routing and diameter changes, fan relocation or replacement, and regional airflow control. Their effectiveness and cost depend on local installation conditions and on their combined influence on face delivery, regional airflow, recirculation risk, and the main ventilation circuit.

Consequently, the present economic comparison is intentionally limited to the retained

main-fan packages. A reliable cost for auxiliary-network improvement cannot be included until a defined technical solution and implementation scope are available. This separate assessment would determine and cost the auxiliary-network measures required to deliver the necessary airflow to all active areas.

Chapter 7

Conclusions

This thesis developed and applied a technical-economic decision framework for selecting a replacement main-fan arrangement for the Rodoretto underground mine. The industrial question was addressed as a system-level ventilation problem rather than as a comparison of nominal fan power. Regulatory and operational requirements were first translated into measurable airflow and velocity KPIs. The mine model was then updated and assessed against field evidence before the commercial offers were screened for technical feasibility and compared economically. This sequence ensured that economic preference could not compensate for inadequate ventilation performance.

7.1 Principal findings

The model-preparation work established a traceable basis for the offer assessment. Existing geometry was corrected, missing and recently developed workings were incorporated, and the planned short-term layout was represented as the post-2028 case. The auxiliary measurement campaign supplied the field evidence needed to examine the distribution of air beyond the primary circuit. Auditing the measurement and model comparison sections reduced the maximum absolute area inconsistency from 83.94% to 1.18%, after which auxiliary-fan definitions, local topology, and installed losses could be interpreted on a consistent hydraulic basis. The remaining auxiliary-network distribution deficiencies were kept in the assessed model rather than removed by artificial model tuning. The resulting model therefore distinguished the capacity of the offered main fans from the ability of the auxiliary network to deliver that capacity to the active areas.

The mandatory whole-mine airflow requirement was established as 47.97 m^3/s at the designated exhaust. Both parallel arrangements passed this gate in the pre-2028 and post-2028 layouts. CFT produced 69.606 and 69.193 m^3/s, respectively, while Aero produced 83.864 and 83.473 m^3/s. Their modelled operating points remained stable on the entered manufacturer curves, unlike the existing main fans, which were identified in the

available survey information as operating in a low-pressure region outside their represented curves. The offered Howden two-stage series arrangement supplied approximately 33.1 m^3/s in both layouts and therefore failed the whole-mine requirement by 14.87 m^3/s, or 31.0%. It was consequently excluded from the economic comparison. This finding applies specifically to the offered arrangement and does not constitute a general judgement on other fan selections from the same manufacturer.

Passing the whole-mine gate did not establish complete ventilation-system adequacy. Neither CFT nor Aero satisfied every local and regional KPI when connected to the represented auxiliary network. The auxiliary-network improvement sensitivity substantially increased airflow delivery to the close ends. In the post-2028 case, all nine assessed face controls then satisfied the supporting-flow and face-velocity criteria. Regional airflow remained incomplete, however, with XS as the only passing region and XN remaining 2.0% below its requirement. The comparison therefore showed that the principal constraint is not insufficient main-fan capacity, but the distribution of air through the auxiliary fans, ducts, leakage paths, and regional branches. It also demonstrated why the greater whole-mine capacity of Aero did not produce a corresponding improvement in local activity classifications.

The 15% resistance stress scenario was not used as an acceptance test for the represented CFT and Aero cases because the baseline results already showed non-compliance with mandatory local or regional criteria. Applying additional resistance could not change that stage-gate outcome. Similarly, the 70% CFT and 60% Aero speeds used in the economic screening are not final operational setpoints. They represent comparable reduced-speed duties that satisfy the main-circuit capacity gate and are suitable for evaluating the relative energy performance of the retained offers.

The economic comparison was resolved by the governing criterion in the lexicographic model. Over the 12-year evaluation horizon, CFT achieved an incremental NPV of EUR 368,149.67, compared with EUR 343,968.74 for Aero. The resulting advantage of EUR 24,180.93 outweighed CFT's additional CAPEX of EUR 520. CFT also had the lower present-value OPEX and life-cycle cost, together with a discounted payback of 1.926 years compared with 2.031 years for Aero. Both offers remained within the mine's approximate three-year payback preference, but the lower modelled electricity demand of CFT made it the stronger economic option. The sensitivity assessment preserved the same ranking when the lower annualized 2026 baseline consumption was used.

7.2 Final recommendation

Among the commercial offers assessed in this thesis, the CFT parallel arrangement is the recommended main-fan replacement solution. It satisfies the whole-mine airflow requirement in both assessed layouts, operates at stable points on its entered curves, and

provides sufficient main-circuit capacity with substantially lower electrical input than Aero. It is also preferred by the governing NPV criterion, with the other principal economic indicators supporting the same decision. Aero remains technically feasible at the main-fan level and provides greater airflow and pressure headroom, but that additional capacity does not offset its higher modelled energy cost under the evaluated operating schedule. The offered Howden series arrangement is not recommended because it fails the mandatory whole-mine capacity gate.

This recommendation concerns selection among the assessed main-fan packages and can support the planned procurement decision. Confirmation of the complete installed scope and supplier accessory losses remains appropriate during detailed procurement and commissioning. The 70% CFT speed used for economic comparison should be treated as a screening duty rather than as the final operating setting.

7.3 Further work

Main-fan replacement alone does not resolve the local and regional airflow deficiencies identified in the represented network. As discussed in Chapter 6, the auxiliary network therefore requires a separate engineering study to define and cost the improvements needed to deliver the required airflow to all active areas. This work complements the main-fan selection established by the thesis and should provide the basis for confirming the final operating setpoint and demonstrating complete system-level ventilation adequacy.

The thesis therefore answers the central research question through a staged and evidence-based decision process. A technically acceptable replacement cannot be identified from fan power or whole-mine airflow alone. It must be selected by combining regulation-based requirements, field-informed network modelling, duty-point assessment, local and regional KPI checks, and economic ranking. Applied to Rodoretto, this process identifies CFT as the preferred main-fan offer while locating the remaining ventilation requirement within the auxiliary distribution system.

References

[1] Imerys Talc Italy S.p.A. *Annual Technical Report 2024 for Talc Mineral Resources and Ore Reserves Assessment: Rodoretto Mine*. Unpublished internal technical report, February 2025.

[2] Howden. *Rodoretto Mine: Ventilation Model Calibration*. Report M073584, Version 01. Unpublished report prepared for Imerys Talc Italy S.p.A., 25 July 2025.

[3] CFT GmbH. *Quotation No. 220-IT-25-13116 / Offer No. 25-13116, AIR-A-U/1250-6-28/55-4-50Hz*. Unpublished commercial and technical offer prepared for Imerys Talc Italy S.p.A., 5 November 2025.

[4] Aero S.r.l. *Offer No. 26013, Revision 1: Potenziamento ventilazione primaria*. Includes Systemair AXC 1250-8 34° characteristic data. Unpublished commercial and technical offer prepared for Imerys Talc Italy S.p.A., 5 April 2026.

[5] Howden. *Proposal EP00467, Revision 0: Scope of Supply and AXN 1200/708A Performance Data*. Unpublished commercial and technical proposal prepared for Imerys Talc Italy S.p.A., September 2025.

[6] Swiss Society of Engineers and Architects. *SIA 196:1998, Ventilation des chantiers souterrains*. Zurich: SIA, 1998.

[7] President of the Italian Republic. *Decree of the President of the Republic 9 April 1959, No. 128: Norme di polizia delle miniere e delle cave*. *Gazzetta Ufficiale della Repubblica Italiana*, No. 87, Ordinary Supplement, 11 April 1959. https://www.normattiva.it/uri-res/N2Ls?urn:nir:presidente.repubblica:decreto:1959-04-09;128

[8] President of the Italian Republic. *Decree of the President of the Republic 20 March 1956, No. 320: Norme per la prevenzione degli infortuni e l'igiene del lavoro in sotterraneo*. *Gazzetta Ufficiale della Repubblica Italiana*, No. 109, Ordinary Supplement, 5 May 1956. https://www.gazzettaufficiale.it/eli/id/1956/05/05/056U0320/sg

[9] McPherson, M. J. *Subsurface Ventilation and Environmental Engineering*. 1st ed. Dordrecht: Springer, 1993. https://doi.org/10.1007/978-94-011-1550-6

[10] Wallace, K., Prosser, B., and Stinnette, J. D. "The practice of mine ventilation engineering." *International Journal of Mining Science and Technology*, 25(2), 2015, pp. 165–169. https://doi.org/10.1016/j.ijmst.2015.02.001

[11] de Souza, E. "Improving the energy efficiency of mine fan assemblages." *Applied Thermal Engineering*, 90, 2015, pp. 1092–1097. https://doi.org/10.1016/j.applthermaleng.2015.04.048

[12] Dziurzynski, W., Krach, A., and Palka, T. "Airflow sensitivity assessment based on underground mine ventilation systems modeling." *Energies*, 10(10), 2017, 1451. https://doi.org/10.3390/en10101451

[13] El-Nagdy, K. A. "Stability of multiple fans in mine ventilation networks." *International Journal of Mining Science and Technology*, 23(4), 2013, pp. 569–571. https://doi.org/10.1016/j.ijmst.2013.07.016

[14] Kursunoglu, N., and Onder, M. "Selection of an appropriate fan for an underground coal mine using the Analytic Hierarchy Process." *Tunnelling and Underground Space Technology*, 48, 2015, pp. 101–109. https://doi.org/10.1016/j.tust.2015.02.005

[15] Chatterjee, A., Zhang, L., and Xia, X. "Optimization of mine ventilation fan speeds according to ventilation on demand and time of use tariff." *Applied Energy*, 146, 2015, pp. 65–73. https://doi.org/10.1016/j.apenergy.2015.01.134

[16] Duckworth, I. J., and Lowndes, I. S. "Modelling of auxiliary ventilation systems." *Mining Technology*, 112(2), 2003, pp. 105–113. https://doi.org/10.1179/037178403225001665

[17] Menendez, J., Fernandez-Oro, J. M., Merle Hevia, N., Galdo Vega, M., Alvarez de Prado, L., Lopez Fanjul, C., and Bernardo-Sanchez, A. "Auxiliary ventilation systems in mining and tunnelling: Air leakage prediction and system design to optimize the energy efficiency and operation costs." *Tunnelling and Underground Space Technology*, 140, 2023, 105298. https://doi.org/10.1016/j.tust.2023.105298

[18] Millar, D., Levesque, M., and Hardcastle, S. "Leakage and air flow resistance in mine auxiliary ventilation ducts: Effects on system performance and cost." *Mining Technology*, 126(1), 2017, pp. 10–21. https://doi.org/10.1080/14749009.2016.1199182

[19] ASHRAE. "Mine Ventilation and Air Conditioning." In *ASHRAE Handbook–HVAC Applications*, Chapter 29. Atlanta, GA: ASHRAE, 2015. https://handbook.ashrae.org/Handbooks/A15/IP/A15_CH29/a15_ch29_ip.aspx

[20] Morla, R., Karekal, S., Godbole, A., Bandyopadhyay, A., Mishra, D. P., and Bhattacharjee, R. "Optimum auxiliary fan location to control air recirculation." *Mining, Metallurgy & Exploration*, 39, 2022, pp. 2291–2299. https://doi.org/10.1007/s42461-022-00690-1

[21] Humann, M. "Mitigating system effect to optimize fan performance and efficiency." *AMCA inmotion*, 2020. Air Movement and Control Association International. Online edition published 4 June 2024. https://www.amca.org/educate/articles-and-technical-papers/amca-inmotion-articles/mitigating-system-effect-to-optimize-fan-performance-efficiency.html

[22] Xu, G., Huang, J., Nie, B., Chalmers, D., and Yang, Z. "Calibration of mine ventilation network models using the non-linear optimization algorithm." *Energies*, 11(1), 2018, 31. https://doi.org/10.3390/en11010031

[23] Karagianni, M., and Benardos, A. "Ventilation design modeling and optimization for an underground bauxite mine." *Materials Proceedings*, 5(1), 2021, 29. https://doi.org/10.3390/materproc2021005029

[24] Maleki, S., Sotoudeh, F., and Sereshki, F. "Application of VENTSIM 3D and mathematical programming to optimize underground mine ventilation network: A case study." *Journal of Mining and Environment*, 9(3), 2018, pp. 741–752. https://doi.org/10.22044/jme.2018.6793.1503

[25] Sjostrom, S., Klintenas, E., Johansson, P., and Nyqvist, J. "Optimized model-based control of main mine ventilation air flows with minimized energy consumption." *International Journal of Mining Science and Technology*, 30(4), 2020, pp. 533–539. https://doi.org/10.1016/j.ijmst.2020.05.016

[26] Wen, L., Zhong, D., Bi, L., Wang, L., and Liu, Y. "Optimization method of mine ventilation network regulation based on mixed-integer nonlinear programming." *Mathematics*, 12(17), 2024, 2632. https://doi.org/10.3390/math12172632

[27] Saleem, H. A. "Energy consumption reduction in underground mine ventilation system: An integrated approach using mathematical and machine learning models toward sustainable mining." *Sustainability*, 17(3), 2025, 1038. https://doi.org/10.3390/su17031038

[28] Hyndman, R. J., and Koehler, A. B. "Another look at measures of forecast accuracy." *International Journal of Forecasting*, 22(4), 2006, pp. 679–688. https://doi.org/10.1016/j.ijforecast.2006.03.001

[29] Howden. *Ventsim DESIGN Training Manual*. Unpublished training manual, n.d.

[30] Zetal. *VH1004.4 Auxiliary Fan Characteristic Curve,* 2×30 *kW Configuration*. Unpublished manufacturer curve sheet supplied to the thesis project, n.d.

[31] Zetal. *VH1004.4 Auxiliary Fan Characteristic Curve,* 2×45 *kW Configuration*. Unpublished manufacturer curve sheet supplied to the thesis project, n.d.

[32] Imerys Talc Italy S.p.A. *Main-Fan Replacement Economic Input Dataset*. Unpublished internal dataset supplied to the thesis project, July 2026.

Appendix A

Supplementary Calculations and Supporting Material

A.1 Auxiliary-Ventilation Measurement-Comparison Records

The first-version measurement-comparison workbook used after the auxiliary-ventilation campaign is reproduced in Tables A.1–A.3. Because all entries refer to the 30 March 2026 campaign, the campaign date is reported in the captions rather than repeated as a separate table column.

Initial field and measured-airflow comparison block																
Station No.	Station Name	Branch	Ventsim Unique No.	Point Type	Repeats Used	Diameter (mm)	Area (m^2)	v_1 (m/s)	v_2 (m/s)	v_3 (m/s)	$\bar{v}$ (m/s)	σ_{pop} (m/s)	CV (%)	CV Band	Data Quality	Measured Q (m^3/s)
1	Fan XS	XS	8712	Fan inlet	3	800	0.5027	20.07	16.39	15.37	17.277	2.019	11.7	10–15%	Caution – use with lower weight	8.684
2	Station 2	XS	13725	Outlet / branch end	3	565	0.2507	1.24	1.12	1.26	1.207	0.062	5.1	5–10%	Good – direct target	0.303
3	Station 3	XS	13049	Outlet / branch end	3	600	0.2827	6.48	6.70	6.69	6.623	0.101	1.5	0–5%	Excellent – direct target	1.873
4	Station 4	XS	8705	Outlet / branch end	3	600	0.2827	3.66	3.33	3.48	3.490	0.135	3.9	0–5%	Excellent – direct target	0.987
5	Station 5	XS	8690	Outlet / branch end	3	600	0.2827	5.26	4.98	5.08	5.107	0.116	2.3	0–5%	Excellent – direct target	1.444
6	Fan Sud	Sud	8610	Fan inlet	3	1200	1.1310	4.64	4.27	4.52	4.477	0.154	3.4	0–5%	Excellent – direct target	5.063
7	Station 7	Sud	13209	Outlet / branch end	3	600	0.2827	4.18	3.99	3.81	3.993	0.151	3.8	0–5%	Excellent – direct target	1.129
8	Station 8	Sud	12651	Outlet / branch end	3	600	0.2827	4.01	3.22	2.51	3.247	0.613	18.9	> 15%	Weak – low-confidence support	0.918

Table A.1: First-version auxiliary-ventilation measurement-comparison record for the 30 March 2026 campaign, Part I-A: field, repeatability, and measured-airflow columns for Stations 1–8

Field notes: Station 1 replicate 1 was taken by a different operator and may be tested in sensitivity by exclusion; Station 8 showed high repeat variability and should be used cautiously or remeasured.

Initial field and measured-airflow comparison block																
Station No.	Station Name	Branch	Ventsim Unique No.	Point Type	Repeats Used	Diameter (mm)	Area (m^2)	v_1 (m/s)	v_2 (m/s)	v_3 (m/s)	$\bar{v}$ (m/s)	σ_{pop} (m/s)	CV (%)	CV Band	Data Quality	Measured Q (m^3/s)
9	Fan Nord	Nord	8619	Fan inlet	3	800	0.5027	14.37	13.85	15.05	14.423	0.491	3.4	0–5%	Excellent – direct target	7.250
10	Station 10	Nord	8629	Outlet / branch end	3	800	0.5027	1.50	1.17	1.34	1.337	0.135	10.1	10–15%	Caution – use with lower weight	0.672
12	Station 12	Nord	13726	Outlet / branch end	3	600	0.2827	4.24	4.08	4.16	4.160	0.065	1.6	0–5%	Excellent – direct target	1.176
13	Station 13	Nord	13193	Outlet / branch end	2	600	0.2827	1.06	1.07	—	1.065	0.005	0.5	0–5%	Good CV; caveat: 2 samples / poor duct	0.301
14	Fan XN	XN	8649	Fan inlet	3	800	0.5027	10.96	11.22	10.08	10.753	0.488	4.5	0–5%	Excellent – direct target	5.405
15	Station 15	XN	8537	Return tunnel check	3	—	15.0000	0.13	0.13	0.14	0.133	0.005	3.5	Return check	Return check only	2.000

Table A.2: First-version auxiliary-ventilation measurement-comparison record for the 30 March 2026 campaign, Part I-B: field, repeatability, and measured-airflow columns for Stations 9–15

Field notes: Station 10 showed high repeat variability and should be used cautiously or remeasured; Station 13 used only two samples and had very poor duct condition with a narrow outlet; Fan XN had acceptable workbook CV, but the sample-CV criterion flagged it for review; Station 15 is a return-tunnel check rather than a duct outlet.

Initial model-comparison and calibration-tracking block												
Station No.	Baseline Sim. v (m/s)	Baseline v Error (%)	Calibrated Sim. v (m/s)	Calibrated v Error (%)	Baseline Sim. Q (m^3/s)	Baseline Q Error (%)	Calibrated Sim. Q (m^3/s)	Calibrated Q Error (%)	Baseline Duty FTP (Pa)	Calibrated Duty FTP (Pa)	Fan Duty / Curve Note	Calibration Action
1	36.4	110.7	—	—	18.1	108.4	—	—	1819.5	—	—	—
2	8.3	587.7	—	—	2.4	692.1	—	—	—	—	—	—
3	11.0	66.1	—	—	5.2	177.6	—	—	—	—	—	—
4	10.0	186.5	—	—	5.2	426.8	—	—	—	—	—	—
5	11.4	123.2	—	—	5.5	280.9	—	—	—	—	—	—
6	11.6	159.1	—	—	5.5	8.6	—	—	379.4	—	—	—
7	9.9	147.9	—	—	2.1	86.0	—	—	—	—	—	—
8	6.0	84.8	—	—	3.1	237.7	—	—	—	—	—	—
9	27.9	93.4	—	—	13.8	90.3	—	—	1450.8	—	—	—
10	14.3	969.6	—	—	6.9	926.8	—	—	—	—	—	—
12	9.1	118.8	—	—	3.2	172.1	—	—	—	—	—	—
13	15.3	1336.6	—	—	3.8	1162.5	—	—	—	—	—	—
14	25.4	136.2	—	—	12.5	131.3	—	—	2350.4	—	—	—
15	0.9	576.7	—	—	13.1	555.0	—	—	—	—	—	—

Table A.3: First-version auxiliary-ventilation measurement-comparison record for the 30 March 2026 campaign, Part II: model-comparison and reserved post-calibration columns

A.2 Final Auxiliary-Calibration Records

The following tables provide the final station-level comparison and leakage-porosity record supporting the downstream auxiliary calibration reported in Section 5.4.4. Tables A.4 and A.5 reproduce the final calibrated velocity and airflow comparison from the `Measurement Comparison v4` worksheet. Table A.6 records the leakage-porosity assignments used in the final calibrated model.

Station No.	Station name	Point type	Measured $\bar{v}$ (m/s)	Final model $\bar{v}$ (m/s)	Raw v error (%)	Floored v error (%)	Absolute v error (m/s)
1	Fan XS	Fan inlet	17.28	17.70	2.45	Not needed	0.42
2	Station 2	Outlet / branch end	1.21	1.10	-8.84	Not needed	0.11
3	Station 3	Outlet / branch end	6.62	6.30	-4.88	Not needed	0.32
4	Station 4	Outlet / branch end	3.49	3.40	-2.58	Not needed	0.09
5	Station 5	Outlet / branch end	5.11	4.50	-11.88	Not needed	0.61
6	Fan Sud	Fan inlet	4.48	4.60	2.76	Not needed	0.12
7	Station 7	Outlet / branch end	3.99	4.40	10.18	Not needed	0.41
8	Station 8	Outlet / branch end	3.25	2.90	-10.68	Not needed	0.35
9	Fan Nord	Fan inlet	14.42	15.20	5.38	Not needed	0.78
10	Station 10	Outlet / branch end	1.34	1.10	-17.71	Not needed	0.24
12	Station 12	Outlet / branch end	4.16	4.50	8.17	Not needed	0.34
13	Station 13	Outlet / branch end	1.07	1.40	31.46	Not needed	0.33
14	Fan XN	Fan inlet	10.75	10.90	1.36	Not needed	0.15
15	Station 15	Return tunnel check	0.13	0.10	-25.00	-3.33%	0.03

Table A.4: Final calibrated station-level velocity comparison used to assess the auxiliary-ventilation calibration for the 30 March 2026 campaign

Station No.	Station name	Point type	Measured Q (m^3/s)	Final model Q (m^3/s)	Raw Q error (%)	Floored Q error (%)	Absolute Q error (m^3/s)
1	Fan XS	Fan inlet	13.57	13.90	2.44	Not needed	0.33
2	Station 2	Outlet / branch end	0.30	0.30	-0.84	-0.25%	0.00
3	Station 3	Outlet / branch end	1.87	1.80	-3.88	Not needed	0.07
4	Station 4	Outlet / branch end	0.99	1.00	1.34	1.32%	0.01
5	Station 5	Outlet / branch end	1.44	1.30	-9.96	Not needed	0.14
6	Fan Sud	Fan inlet	3.52	3.60	2.39	Not needed	0.08
7	Station 7	Outlet / branch end	1.13	1.30	15.14	Not needed	0.17
8	Station 8	Outlet / branch end	0.92	0.80	-12.85	-11.80%	0.12
9	Fan Nord	Fan inlet	11.33	12.00	5.93	Not needed	0.67
10	Station 10	Outlet / branch end	0.67	0.60	-10.70	-7.19%	0.07
12	Station 12	Outlet / branch end	1.18	1.30	10.52	Not needed	0.12
13	Station 13	Outlet / branch end	0.30	0.40	32.84	9.89%	0.10
14	Fan XN	Fan inlet	8.45	8.60	1.83	Not needed	0.15
15	Station 15	Return tunnel check	2.00	2.00	0.00	Not needed	0.00

Table A.5: Final calibrated station-level airflow comparison used to assess the auxiliary-ventilation calibration for the 30 March 2026 campaign

Branch	Assigned model extent	Treated length (m)	Porosity (mm^2/m^2)
XS	Spiral-duct sections 8715 and 14243, downstream of Fan XS and immediately before flexible-duct section 8711	–	0.00
XS	Flexible-duct trunk from 8711 to 13237, ending immediately before the junction serving Station 2	199.90	1500.00
XS	Branches from 13237 to Stations 2 and 3, continuing to the ends of both drifts	64.50	1000.00
XS	Ducts beginning at the 8669/8711 junction and continuing toward Stations 4 and 5	–	750.00
Sud (S)	Flexible-duct trunk from 8419 to 8504, ending immediately before the split to Stations 7 and 8	176.90	100.00
Sud (S)	Branches from 8504 to Stations 7 and 8, continuing to the ends of both drifts	91.80	200.00
Nord (N)	Ducting from 8619 to 13338, including the route to Station 10 and the end of its drift	139.30	2500.00
Nord (N)	Ducting beginning at the 8621/8626 junction and continuing toward Stations 12 and 13	168.40	2000.00
XN	Ducting immediately downstream of the initial XN duct connection to segment 14545, delivering airflow as far as airway 8491	227.60	2500.00

Table A.6: Final calibrated duct leakage porosity assignments used in the downstream auxiliary calibration

A dash indicates that a separate aggregate length was not supplied for that extent. Porosity is reported in the Ventsim unit of leakage opening area per duct surface area.

A.3 Detailed Offer KPI Records

A.3.1 CFT Local and Regional KPI Records

Tables A.7 and A.8 provide the detailed CFT local and regional KPI records supporting the classifications reported in Section 5.5. The supporting-only threshold is 2.26 m^3/s, the regional airflow requirement is 13.366 m^3/s, and the velocity criterion is $0.100 \leq v \leq 6.000$ m/s.

Layout	Region	Face control	Unique ID	Q (m^3/s)	v (m/s)	Support margin	Classification
Pre-2028	XS	Station 2	13217	0.251	0.017	-88.9%	Fails supporting, mucking, and combined; low velocity
Pre-2028	XS	Station 3	10147	1.778	0.119	-21.3%	Fails supporting, mucking, and combined; velocity passes
Pre-2028	XS	Station 4	8523	0.958	0.083	-57.6%	Fails supporting, mucking, and combined; low velocity
Pre-2028	XS	Station 5	8520	1.260	0.110	-44.2%	Fails supporting, mucking, and combined; velocity passes
Pre-2028	XN	Active face	8538	0.090	0.006	-96.0%	Fails supporting, mucking, and combined; low velocity
Pre-2028	S	Station 7	13201	1.256	0.084	-44.4%	Fails supporting, mucking, and combined; low velocity
Pre-2028	S	Station 8	12635	0.854	0.057	-62.2%	Fails supporting, mucking, and combined; low velocity
Pre-2028	N	Station 12	12658	1.270	0.085	-43.8%	Fails supporting, mucking, and combined; low velocity
Pre-2028	N	Station 13	13084	0.390	0.034	-82.7%	Fails supporting, mucking, and combined; low velocity
Post-2028	XS	Station 2	13217	0.251	0.017	-88.9%	Fails supporting, mucking, and combined; low velocity
Post-2028	XS	Station 3	10147	1.778	0.119	-21.3%	Fails supporting, mucking, and combined; velocity passes
Post-2028	XS	Station 4	8523	0.958	0.083	-57.6%	Fails supporting, mucking, and combined; low velocity
Post-2028	XS	Station 5	8520	1.260	0.110	-44.2%	Fails supporting, mucking, and combined; velocity passes
Post-2028	XN	Face	8538	0.644	0.043	-71.5%	Fails supporting, mucking, and combined; low velocity
Post-2028	South Intermediate	Control A	13867	4.489	0.299	+98.6%	Supporting only
Post-2028	South Intermediate	Southern control	13365	6.811	0.454	+201.4%	Mucking only; below the 8.78 m^3/s combined threshold
Post-2028	Far North Lower	Control A	12579	5.578	0.372	+146.8%	Supporting only
Post-2028	Far North Lower	Control B	12625	4.114	0.274	+82.0%	Supporting only

Table A.7: Detailed CFT active-face control results at 100% fan speed in the pre-2028 and post-2028 layouts

Support margin is calculated relative to the 2.26 m^3/s supporting-only threshold. The post-2028 layout excludes closed North and South production-face records from the active face-control count.

Layout	Region	Boundary ID	Q (m^3/s)	Margin	Result
Pre-2028	XS	8410	16.619	+24.3%	Pass
Pre-2028	S	8354	1.285	-90.4%	Fail
Pre-2028	N	8384	3.604	-73.0%	Fail
Pre-2028	XN	8459	3.159	-76.4%	Fail
Post-2028	XS	8410	18.732	+40.1%	Pass
Post-2028	XN	8459	4.098	-69.3%	Fail
Post-2028	South Intermediate	13581	11.831	-11.5%	Fail
Post-2028	Far North Upper	14876	9.624	-28.0%	Fail
Post-2028	Far North Lower	8400	10.284	-23.1%	Fail

Table A.8: Detailed CFT regional-boundary results at 100% fan speed in the pre-2028 and post-2028 layouts

Each boundary is a non-overlapping regional inflow control assessed directly against the 13.366 m^3/s regional requirement.

A.3.2 Aero Local and Regional KPI Records

Tables A.9 and A.10 provide the detailed Aero local and regional KPI records supporting the classifications reported in Section 5.5. The supporting-only threshold is 2.26 m^3/s, the regional airflow requirement is 13.366 m^3/s, and the velocity criterion is $0.100 \leq v \leq 6.000$ m/s.

Layout	Region	Face control	Unique ID	Q (m^3/s)	v (m/s)	Support margin	Classification
Pre-2028	XS	Station 2	13217	0.251	0.017	-88.9%	Fails supporting, mucking, and combined; low velocity
Pre-2028	XS	Station 3	10147	1.778	0.119	-21.3%	Fails supporting, mucking, and combined; velocity passes
Pre-2028	XS	Station 4	8523	0.958	0.083	-57.6%	Fails supporting, mucking, and combined; low velocity
Pre-2028	XS	Station 5	8520	1.260	0.110	-44.2%	Fails supporting, mucking, and combined; velocity passes
Pre-2028	XN	Active face	8538	0.090	0.006	-96.0%	Fails supporting, mucking, and combined; low velocity
Pre-2028	S	Station 7	13201	1.255	0.084	-44.5%	Fails supporting, mucking, and combined; low velocity
Pre-2028	S	Station 8	12635	0.854	0.057	-62.2%	Fails supporting, mucking, and combined; low velocity
Pre-2028	N	Station 12	12658	1.270	0.085	-43.8%	Fails supporting, mucking, and combined; low velocity
Pre-2028	N	Station 13	13084	0.390	0.034	-82.7%	Fails supporting, mucking, and combined; low velocity
Post-2028	Far North Lower	Control 1	12579	5.569	0.371	+146.4%	Supporting only
Post-2028	Far North Lower	Control 2	12625	4.109	0.274	+81.8%	Supporting only
Post-2028	South Intermediate	Control 13365	13365	6.801	0.453	+200.9%	Mucking only; below the 8.78 m^3/s combined threshold
Post-2028	South Intermediate	Control 13867	13867	4.482	0.299	+98.3%	Supporting only
Post-2028	XN	Face	8538	0.655	0.044	-71.0%	Fails supporting, mucking, and combined; low velocity
Post-2028	XS	Station 2	13217	0.251	0.017	-88.9%	Fails supporting, mucking, and combined; low velocity
Post-2028	XS	Station 3	10147	1.778	0.119	-21.3%	Fails supporting, mucking, and combined; velocity passes
Post-2028	XS	Station 4	8523	0.958	0.083	-57.6%	Fails supporting, mucking, and combined; low velocity
Post-2028	XS	Station 5	8520	1.260	0.110	-44.2%	Fails supporting, mucking, and combined; velocity passes

Table A.9: Detailed Aero active-face control results at 100% fan speed in the pre-2028 and post-2028 layouts

Support margin is calculated relative to the 2.26 m^3/s supporting-only threshold. The post-2028 layout excludes closed North and South production-face records from the active face-control count.

Layout	Region	Boundary ID	Q (m^3/s)	Margin	Result
Pre-2028	XS	8410	24.173	+80.9%	Pass
Pre-2028	S	8354	2.137	-84.0%	Fail
Pre-2028	N	8384	2.936	-78.0%	Fail
Pre-2028	XN	8459	3.162	-76.3%	Fail
Post-2028	XS	8410	26.061	+95.0%	Pass
Post-2028	XN	8459	4.125	-69.1%	Fail
Post-2028	South Intermediate	13581	11.816	-11.6%	Fail
Post-2028	Far North Lower	8400	10.324	-22.8%	Fail
Post-2028	Far North Upper	13639*	9.687	-27.5%	Fail

Table A.10: Detailed Aero regional-boundary results at 100% fan speed in the pre-2028 and post-2028 layouts

Each boundary is a non-overlapping regional inflow control assessed directly against the 13.366 m^3/s regional requirement.
*Aero airway 13639 is the topology-equivalent control for CFT regional segment 14876; the Aero model retains this approach as one unsplit airway.

A.3.3 Auxiliary-Network Improvement Sensitivity Records

Tables A.11 and A.12 provide the detailed active-face records supporting the auxiliary-network improvement sensitivity reported in Section 5.5, while Table A.13 provides the corresponding regional-boundary records. The improved-network case retained the accepted main-fan definitions and removed the represented auxiliary-fan inlet and shock-loss additions while assigning active ducts a leakage area of 25 mm^2/m^2. The supporting-only threshold is 2.26 m^3/s, the regional airflow requirement is 13.366 m^3/s, and the velocity criterion is $0.100 \leq v \leq 6.000$ m/s.

Layout	Region	Face control	ID	Rep. Q (m^3/s)	Imp. Q (m^3/s)	Imp. v (m/s)	Support margin	Classification
Pre-2028	XS	Station 2	13217	0.251	4.550	0.303	+101.3%	Supporting only
Pre-2028	XS	Station 3	10147	1.778	4.304	0.287	+90.4%	Supporting only
Pre-2028	XS	Station 4	8523	0.958	2.589	0.225	+14.6%	Supporting only
Pre-2028	XS	Station 5	8520	1.260	3.370	0.293	+49.1%	Supporting only
Pre-2028	XN	Active face	8538	0.090	5.684	0.379	+151.5%	Supporting only
Pre-2028	S	Station 7	13201	1.256	4.803	0.320	+112.5%	Supporting only
Pre-2028	S	Station 8	12635	0.854	3.364	0.224	+48.8%	Supporting only
Pre-2028	N	Station 12	12658	1.270	1.491	0.099	-34.0%	Fails supporting; low velocity
Pre-2028	N	Station 13	13084	0.390	3.189	0.278	+41.1%	Supporting only
Post-2028	XS	Station 2	13217	0.251	3.456	0.230	+52.9%	Supporting only
Post-2028	XS	Station 3	10147	1.778	3.268	0.218	+44.6%	Supporting only
Post-2028	XS	Station 4	8523	0.958	2.523	0.220	+11.6%	Supporting only
Post-2028	XS	Station 5	8520	1.260	3.285	0.286	+45.4%	Supporting only
Post-2028	XN	Face	8538	0.644	2.507	0.167	+10.9%	Supporting only
Post-2028	South Intermediate	Control A	13867	4.489	4.489	0.299	+98.6%	Supporting only
Post-2028	South Intermediate	Southern control	13365	6.811	6.811	0.454	+201.4%	Mucking only
Post-2028	Far North Lower	Control A	12579	5.578	5.717	0.381	+153.0%	Supporting only
Post-2028	Far North Lower	Control B	12625	4.114	4.217	0.281	+86.6%	Supporting only

Table A.11: CFT improved-network active-face control records for the auxiliary-network sensitivity

Rep. Q is the represented-network value from the retained-offer assessment; Imp. Q and Imp. v are the corresponding improved-network sensitivity values. Support margin is calculated relative to 2.26 m^3/s.

Layout	Region	Face control	ID	Rep. Q (m^3/s)	Imp. Q (m^3/s)	Imp. v (m/s)	Support margin	Classification
Pre-2028	XS	Station 2	13217	0.251	4.544	0.303	+101.1%	Supporting only
Pre-2028	XS	Station 3	10147	1.778	4.309	0.287	+90.7%	Supporting only
Pre-2028	XS	Station 4	8523	0.958	2.592	0.226	+14.7%	Supporting only
Pre-2028	XS	Station 5	8520	1.260	3.372	0.294	+49.2%	Supporting only
Pre-2028	XN	Active face	8538	0.090	5.693	0.380	+151.9%	Supporting only
Pre-2028	S	Station 7	13201	1.255	4.909	0.327	+117.2%	Supporting only
Pre-2028	S	Station 8	12635	0.854	3.437	0.229	+52.1%	Supporting only
Pre-2028	N	Station 12	12658	1.270	1.491	0.099	-34.0%	Fails supporting; low velocity
Pre-2028	N	Station 13	13084	0.390	3.192	0.278	+41.2%	Supporting only
Post-2028	XS	Station 2	13217	0.251	3.456	0.230	+52.9%	Supporting only
Post-2028	XS	Station 3	10147	1.778	3.268	0.218	+44.6%	Supporting only
Post-2028	XS	Station 4	8523	0.958	2.523	0.220	+11.6%	Supporting only
Post-2028	XS	Station 5	8520	1.260	3.285	0.286	+45.4%	Supporting only
Post-2028	XN	Face	8538	0.655	2.507	0.167	+10.9%	Supporting only
Post-2028	South Intermediate	Control 13867	13867	4.482	4.489	0.299	+98.6%	Supporting only
Post-2028	South Intermediate	Control 13365	13365	6.801	6.811	0.454	+201.4%	Mucking only
Post-2028	Far North Lower	Control 1	12579	5.569	5.717	0.381	+153.0%	Supporting only
Post-2028	Far North Lower	Control 2	12625	4.109	4.217	0.281	+86.6%	Supporting only

Table A.12: Aero improved-network active-face control records for the auxiliary-network sensitivity

Rep. Q is the represented-network value from the retained-offer assessment; Imp. Q and Imp. v are the corresponding improved-network sensitivity values. Support margin is calculated relative to 2.26 m^3/s.

Offer	Layout	Region	Boundary ID	Rep. Q (m^3/s)	Imp. Q (m^3/s)	Imp. margin	Result
CFT	Pre-2028	XS	8410	16.619	8.565	-35.9%	Fail
CFT	Pre-2028	S	8354	1.285	4.581	-65.7%	Fail
CFT	Pre-2028	N	8384	3.604	0.803	-94.0%	Fail
CFT	Pre-2028	XN	8459	3.159	12.888	-3.6%	Fail
CFT	Post-2028	XS	8410	18.732	15.220	+13.9%	Pass
CFT	Post-2028	XN	8459	4.098	13.098	-2.0%	Fail
CFT	Post-2028	South Intermediate	13581	11.831	11.831	-11.5%	Fail
CFT	Post-2028	Far North Upper	14876	9.624	9.602	-28.2%	Fail
CFT	Post-2028	Far North Lower	8400	10.284	10.539	-21.2%	Fail
Aero	Pre-2028	XS	8410	24.173	16.043	+20.0%	Pass
Aero	Pre-2028	S	8354	2.137	3.871	-71.0%	Fail
Aero	Pre-2028	N	8384	2.936	1.528	-88.6%	Fail
Aero	Pre-2028	XN	8459	3.162	12.964	-3.0%	Fail
Aero	Post-2028	XS	8410	26.061	15.219	+13.9%	Pass
Aero	Post-2028	XN	8459	4.125	13.098	-2.0%	Fail
Aero	Post-2028	South Intermediate	13581	11.816	11.831	-11.5%	Fail
Aero	Post-2028	Far North Upper	13639/14876*	9.687	9.602	-28.2%	Fail
Aero	Post-2028	Far North Lower	8400	10.324	10.539	-21.2%	Fail

Table A.13: Improved-network regional-boundary records for the auxiliary-network sensitivity

Each boundary is assessed against the 13.366 m^3/s regional requirement. *For the Aero post-2028 Far North Upper control, the represented-network boundary uses airway 13639 and the improved-network export uses the topology-equivalent split boundary segment 14876.

A.4 Year-by-year discounted cash-flow record

Tables A.14 and A.15 provide the annual calculation record supporting the discounted results reported in Section 5.6. Savings are measured relative to the existing-fan baseline of EUR 123,486.93 per year, and each annual saving is discounted at 10.87% from the end of the corresponding operating year.

Year	Layout	OPEX (EUR)	Saving (EUR)	Discounted saving (EUR)	Cumulative discounted (EUR)
2026	Pre-2028	47,657.90	75,829.03	68,394.54	68,394.54
2027	Pre-2028	47,657.90	75,829.03	61,688.95	130,083.49
2028	Post-2028	48,013.56	75,473.37	55,379.83	185,463.32
2029	Post-2028	48,013.56	75,473.37	49,950.24	235,413.55
2030	Post-2028	48,013.56	75,473.37	45,052.98	280,466.53
2031	Post-2028	48,013.56	75,473.37	40,635.86	321,102.39
2032	Post-2028	48,013.56	75,473.37	36,651.81	357,754.20
2033	Post-2028	48,013.56	75,473.37	33,058.36	390,812.57
2034	Post-2028	48,013.56	75,473.37	29,817.23	420,629.80
2035	Post-2028	48,013.56	75,473.37	26,893.87	447,523.67
2036	Post-2028	48,013.56	75,473.37	24,257.12	471,780.78
2037	Post-2028	48,013.56	75,473.37	21,878.88	493,659.67

Table A.14: CFT discounted savings relative to the existing-fan baseline

Year	Layout	OPEX (EUR)	Saving (EUR)	Discounted saving (EUR)	Cumulative discounted (EUR)
2026	Pre-2028	51,570.12	71,916.81	64,865.89	64,865.89
2027	Pre-2028	51,570.12	71,916.81	58,506.26	123,372.15
2028	Post-2028	51,747.95	71,738.98	52,639.66	176,011.80
2029	Post-2028	51,747.95	71,738.98	47,478.72	223,490.53
2030	Post-2028	51,747.95	71,738.98	42,823.78	266,314.30
2031	Post-2028	51,747.95	71,738.98	38,625.22	304,939.52
2032	Post-2028	51,747.95	71,738.98	34,838.29	339,777.81
2033	Post-2028	51,747.95	71,738.98	31,422.65	371,200.47
2034	Post-2028	51,747.95	71,738.98	28,341.89	399,542.35
2035	Post-2028	51,747.95	71,738.98	25,563.17	425,105.53
2036	Post-2028	51,747.95	71,738.98	23,056.89	448,162.41
2037	Post-2028	51,747.95	71,738.98	20,796.33	468,958.74

Table A.15: Aero discounted savings relative to the existing-fan baseline